GNS

Safety Analyses Report

Type B(U)F Transport Package CASTOR® geo69

Docket No.: 71-9383

Non-Proprietary Version

Dokumententyp Document Type	SR
Dokumenten-Nr. Document No.	1014-SR-00001
Revision Revision	1

	Name, Funktion Name, Function	**Datum** Date	**Unterschrift** Signature
Ersteller Prepared			
Fachprüfer Reviewed			
Freigabe Approved			

0.2 Revision Status of this Document

	Name, Function	Date	Signature
Prepared	[redacted]		
Reviewed			

Revision	Date	Author	Revised section
0	22.12.2020	T. Fischer-Wasels	- First issue
1	30.08.2021	I. Eichmann	Revised / new Sections: - 0.2, 0.3, 0.4, 0.5 - 1.2 - 2.0, 2.1, 2.2, 2.12 - 3.1, 3.2, 3.4, 3.5, 3.6, 3.7 - 5.1, 5.2, 5.3, 5.4 - 6.3 - 7.0, 7.1, 7.2 - 8.1, 8.2, 8.3

Changes in relation to the previous revision are be marked with a vertical bar on the left side

0.3 Revision Status of Sections

	Name, Function	Date	Signature
Prepared	[redacted]		
Reviewed			

Section	Rev.	Date	Summary description of change
0			
0.1	0	18.12.2020	First issue
0.2	1	25.08.2021	Addition of Revision 1 incl. list of revised sections
0.3	1	25.08.2021	Description of Revision of sections
0.4	1	25.08.2021	Update of Table of Contents
0.5	1	25.08.2021	Addition of new Definitions
1			
1.0	0	18.12.2020	First issue
1.1	0	18.12.2020	First issue
1.2	1	18.08.2021	Correction of Table 1.2-11
1.3	0	18.12.2020	First issue
2			
2.0	1	12.08.2021	Editorial Changes
2.1	1	17.08.2021	Editorial Changes
2.2	1	13.08.2021	Revision of Section 2.2.1 (Material Properties)
2.3	0	18.12.2020	First issue
2.4	0	21.12.2020	First issue
2.5	0	21.12.2020	First issue
2.6	0	21.12.2020	First issue
2.7	0	21.12.2020	First issue
2.8	0	21.12.2020	First issue
2.9	0	21.12.2020	First issue
2.10	0	21.12.2020	First issue
2.11	0	21.12.2020	First issue
2.12	1	18.08.2021	Revision of Appendix 2-2 Addition of Appendices 2-4 to 2-10
3			
3.0	0	17.12.2020	First issue

3.1	1	18.08.2021	Editorial Changes
3.2	1	18.08.2021	Editorial Changes Corrections Table 3.2-9
3.3	0	17.12.2020	First issue
3.4	1	18.08.2021	Editorial Changes
3.5	1	18.08.2021	Implementation of chapter for thermal evaluation of fuel rod failure
3.6	0	25.08.2021	Implementation of chapter for thermal evaluation of short-term operations
3.7	0	18.08.2021	Relocation due to issue of new chapters 3.5 and 3.6
4			
4.0	0	11.12.2020	First issue
4.1	0	11.12.2020	First issue
4.2	0	11.12.2020	First issue
4.3	0	11.12.2020	First issue
4.4	0	11.12.2020	First issue
4.5	0	11.12.2020	First issue
5			
5.0	0	10.12.2020	First issue
5.1	1	11.08.2021	Editorial changes
5.2	1	11.08.2021	Taking into account grid spacers and longer cooling times
5.3	1	11.08.2021	Editorial changes
5.4	1	11.08.2021	Plots for the axial ends of the package
5.5	0	10.12.2020	First issue
6			
6.0	0	10.12.2020	First issue
6.1	0	10.12.2020	First issue
6.2	0	10.12.2020	First issue

6.3	1	11.08.2021	Editorial changes (Figure 6.3-3, Table 6.3-5 and Figure 6.3-11) Evaluation of fuel basket deformations
6.4	0	10.12.2020	First issue
6.5	0	10.12.2020	First issue
6.6	0	10.12.2020	First issue
6.7	0	10.12.2020	First issue
6.8	0	10.12.2020	First issue
6.9	0	10.12.2020	First issue
7			
7.0	1	12.08.2021	Editorial changes
7.1	1	12.08.2021	Adjustments regarding time constraints and He-filling Deletion of usage of a transport hood Mention of canister drying criteria (vacuum pressure, residual moisture/pressure rise, hold time)
7.2	1	12.08.2021	Distinction between direct FA removal or FA removal via transfer cask Deletion of usage of a transport hood Discussion on drying procedure Thermal constraints on loading operation
7.3	0	18.12.2020	First issue
7.4	0	18.12.2020	First issue
7.5	1	12.08.2021	Editorial changes
8			
8.0	0	18.12.2020	First issue
8.1	1	12.08.2021	Editorial changes More precise description of acceptance tests and criteria with regard to codes and standards Pneumatic test corrected into hydrostatic test Consideration of material tests on non-ASME BPVC materials
8.2	1	12.08.2021	Editorial changes More precise description of maintenance program

8.3	1	12.08.2021	Editorial changes

0.4 Table of Contents

	Name, Function	Date	Signature
Prepared	[redacted]		
Reviewed			

CASTOR® is a registered trade mark.

0 GENERAL AND ORGANISATION

0.1 Document Organisation

0.2 Revision Status of this Document

0.3 Revision Status of Sections

0.4 Table of Contents

0.5 Glossary

1 GENERAL INFORMATION

1.0 Overview

1.1 Introduction

1.2 Package Description

1.3 Appendix

2 Structural Evaluation

2.0 Overview

2.1 Description of the Structural Design

2.2 Materials

2.3 Fabrication and Examination

2.4 General Requirements for all Packages

2.5 Lifting and Tie Standards for all Packages

2.6 Normal Conditions of Transport

2.7 Hypothetical Accident Conditions

2.8 Accident Conditions for Air Transport of Plutonium

2.9 Accident Conditions for Fissile Material Packages for Air Transport

2.10 Special Form

2.11 Fuel Rods

2.12 Appendix

3 Thermal Evaluation

3.0 Overview

3.1 Description of Thermal Design

3.2 Material Properties and Component Specifications

3.3 Thermal Evaluation under Normal Conditions of Transport

3.4 Thermal Evaluation und Hypothetical Accident Conditions

3.5 Thermal Evaluation of Fuel Rod Failure

3.6 Thermal Evaluation of Short-Term Operations

3.7 Appendix

4 Containment
4.0 Overview
4.1 Description of the Containment System
4.2 Containment under Normal Conditions of Transport
4.3 Containment und Hypothetical Accident Conditions
4.4 Leakage Rate Tests for Type B Packages
4.5 Appendix

5 Shielding Evaluation
5.0 Overview
5.1 Description of Shielding Design
5.2 Source Specification
5.3 Shielding Model
5.4 Shielding Evaluation
5.5 Appendix

6 Criticality Evaluation
6.0 Overview
6.1 Description of Criticality Design
6.2 Fissile Material Content
6.3 General Considerations
6.4 Single Package Evaluation
6.5 Evaluation of Package Arrays und Normal Conditions of Transport
6.6 Package Arrays und Hypothetical Accident Conditions
6.7 Fissile Material Packages for Air Transport
6.8 Benchmark Evaluation
6.9 Appendix

7 Package Operations
7.0 Overview
7.1 Package Loading
7.2 Package Unloading
7.3 Preparation of Empty Package for Transport
7.4 Other Operations
7.5 Appendix

8 Acceptance Tests and Maintenance Program
8.0 Overview

8.1 Acceptance Tests

8.2 Maintenance Program

8.3 Appendix

0.5 Glossary

	Name, Function	Date	Signature
Prepared	[redacted]		
Reviewed			

10CFR71	Title 10, Code of Federal Regulations Part 71: Packaging and transportation of radioactive material
ASME	American Society of Mechanical Engineers
BPVC	2017 Edition of the ASME Boiler & Pressure Vessel Code
BWR	Boiling Water Reactor
Cask	CASTOR® geo69
CASTOR®	Registered trade mark for a dual purpose cask providing sufficient neutron and gamma shielding, heat dissipation, activity retention, criticality safety and mechanical integrity for transport and storage of spent nuclear fuel and radioactive waste
CASTOR® geo69	Manufacturer's designation for the specified package design
DCI	Ductile Cast Iron
CLU	Cask Loading Unit
CoC	Certificate of Compliance
Confinement	Assembly of fissile material and packaging components intended to preserve criticality safety
Containment	Assembly of components of the packaging intended to retain the radioactive material during transport
Design Drawing	Engineering drawing as required by the NRC Regulatory Guide 7.9
Design Parts List	Supporting design document containing further information as e.g. references on materials, codes and standards or applicable design drawings
Division 3	Applicable division of the BPVC Section III for containment systems for transportation and storage of spent nuclear fuel and high-level radioactive material
DPC	Dual Purpose Cask
FA	Fuel Assembly
FEA, FEM	Finite Element Analysis, Finite Element Method
GNS	GNS Gesellschaft für Nuklear-Service mbH - Headquarters: Frohnhauser Straße 67, D-45127 Essen - Shop: Kranbahnallee 3, D-45473 Mülheim / Ruhr
GUR®	Product name of UHMW PE
HAC	Hypothetical Accident Conditions
HC	Handling Conditions
Item	Parts, components or subcomponents of the overall package system, especially when used in context with the parts list
LAP	Load Attachment Point
LT	Leak Testing
Manual	Document defining the applicable underlying quality assurance system

MNOP	Maximum Normal Operating Pressure
MT	Magnetic Particle Testing
NCT	Normal Conditions of Transport, i.e. minor mishaps
NDE	Non-Destructive Examination or Evaluation, respectively
NPP	Nuclear Power Plant
NRC	U. S. Nuclear Regulatory Commission
OM	Operation & Maintenance
Package	The packaging together with its radioactive contents as presented for transport
Packaging	The assembly of components necessary to ensure compliance with the packaging requirements of 10 CFR Part 71
PE	Polyethylene
PT	Liquid Penetrant Examination
PU	Polyurethane
QA	Quality Assurance
RG	U.S. NRC Regulatory Guide
RT	Radiographic Testing
SAR	Safety Analysis Report
Section III	Applicable Section of the BPVC containing rules for construction of nuclear facility components
SNF	Spent Nuclear Fuel
UHMW PE	Ultra-High Molecular Weight PE
Undamaged Fuel	is according to ISG-11 [1] fuel, that can meet all fuel-specific and system-related functions. Undamaged fuel may be breached. Fuel assembly classified as undamaged may have assembly defects.
UT	Ultrasonic Testing
VT	Visual Testing

List of References

[1] Interim Staff Guidance - 11, Revision 3
Cladding Considerations for the Transportation and Storage of Spent Fuel
Spent Fuel Project Office

1.2 Package Description

	Name, Function	Date	Signature
Prepared	[redacted]		
Reviewed			
Reviewed 1.2.2 only			

The packaging and its components are specified by the parts lists and drawings listed in Table 1.2-1, which are also included in section 1.3.

Table 1.2-1 Documents for packaging specification

Document type	Content	Component	Document no.
Design Parts list	Information about the single parts of the components: e.g. item no., quantity, designation, material, material specifications required certificate, safety classification	Cask	1014-DPL-30934
		Canister	1014-DPL-36855
		Fuel Basket	1014-DPL-30984
		Shielding elements	1014-DPL-33604
		Impact limiters	1014-DPL-38772
Design Drawing	Design and dimensions of the packaging and its components	Cask	1014-DD-30934
		Canister	1014-DD-36855
		Fuel Basket	1014-DD-30984
		Shielding elements	1014-DD-33604
		Impact limiters	1014-DD-38772

The design and dimensions of the packaging are defined by the set of parts lists and drawings. These documents provide all design related information required for the safety assessment of the package. Furthermore, the design drawings contain the dimensions of the interfaces needed for cask assembly and operation.

1.2.1 Packaging

The packaging consists of the cask with the cask body and the cask lid enclosing the canister and the fuel basket (Figure 1.2-1) intended for the accommodation of up to 69 FA. Furthermore, the packaging includes two impact limiters fastened to the face ends of the cask in order to protect the cask and its content especially under hypothetical accident conditions.

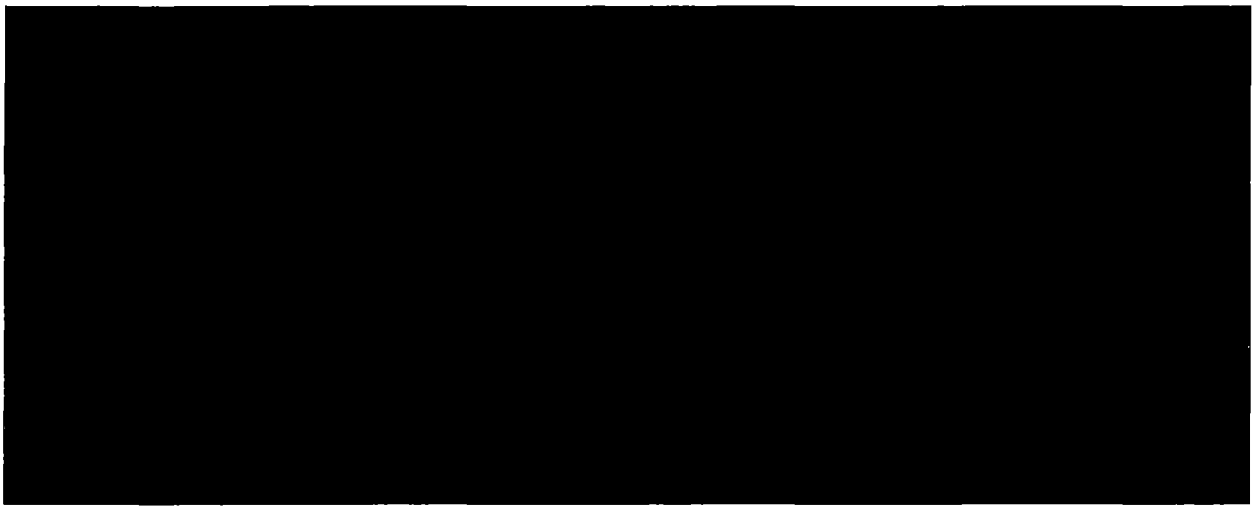

Figure 1.2-1 Main components of the packaging (exploded view)

Hereinafter the main components of the packaging are described in detail. The item numbers used in the following chapters of this SAR correspond to the ones in the parts list of the respective component acc. to Table 1.2-1.

1.2.1.1 Cask body

The basic structure of the cask body (Item 2) made of DCI is a hollow cylinder with a closed bottom end, cast in one piece. Subsequently to the casting process, every surface of the cask body is machined. This process includes machining of the radial cooling fins into the outer cask surface and the axial drilling of two circumferential rows of each ■ deep-holes from the bottom side into the cask wall. Each borehole houses a column of moderator rods (Item 4, 54, 141) completed by steel bars (Item 8, 53), which are kept in place by compression springs (Item 6, 31) and the stainless steel closure plate (Item 7) bolted to the cask bottom. At the two angular positions of the trunnions, each three outer boreholes and the six moderator rods (Item 54) are slightly shortened. A bottom moderator plate (Item 5) made of polyethylene is placed in a recess at the bottom end and screwed to the bottom of the cask body via three cap screws (Item 52) and bushes (Item 57).

The closure plate covers the bottom moderator plate (Item 5), closes the deep-boreholes and serves as a seating for the compression springs (Item 6, 31). An elastomer sealing ring (Item 47) is inserted into a groove in the closure plate and each of the 28 hexagon head screw (Item 9) is equipped with a bonded seal (Item 49). Eight circular openings close to the edge of the closure plate give access to threaded blind holes ■ in the cask body for fastening the bottom impact limiter. The openings are sealed by O-rings (Item 66). When the bottom impact limiter is not assembled e.g. during loading, the threaded blind holes are closed by seal plugs (Item 93) equipped with an O-ring (Item 94). For leak-testing of the complete closure plate a test port is added. Chan-

nels in the closure plate connect all seals with the test port. During underwater loading, the test port is closed leak-tight by a sealing screw (Item 26) and an O-ring (Item 74). After loading, the sealing screw is replaced by a sealing screw with valve (Item 155) (with a factory-fitted seal) which limits the gas overpressure in the volume enclosed by the closure plate to a maximum of [redacted]. Accordingly, the channel system of the closure plate also interconnects the deep boreholes for the moderator rods and the recess for the bottom moderator disc.

For fastening the lid impact limiter, [redacted] threaded blind holes [redacted] on an outer diameter of the lid-end face of the cask body are used. The unused blind holes are closed during operation and transport.

For handling, the cask is equipped with one pair of lid side trunnions (Item 12) and one pair of tilting studs at the bottom end. The stainless steel trunnions are form-fitted in recesses that are machined into the cask body and are each fastened by 16 stainless steel cap screws (Item 13). The cap screws may be applied in a way [redacted]. The trunnions are intended as load attachment points and allow vertical handling as well as tilting of the cask. The tilting studs are [redacted] to support the cask during tilting operations but are not intended for the attachment of load lifting devices. They are covered against wear and corrosion by corresponding wear protection (Item 183) made of stainless steel, which are sealed with an O-ring (Item 184). The wear protections are shrink fitted on the tilting studs and additionally secured against twisting by 2 hexagon screws (Item 185) with bonded seals (Item 49) each.

The package is marked with a type plate (Item 105), which is mounted on the cooling fin area of the cask body (see Figure 1.2-1). The type plate is mounted via grooved pins with round head (Item 107), distance bolts (Item 108) and discs (Item 87).

1.2.1.2 Cask lid system

The cask lid (Item 55) closes the cask body (Item 2) and thus the outer containment. The cask lid has two service orifices that are separately covered by the blind flange (Item 89) and the protection cap (Item 113) which are each sealed via metal gaskets (Item 44, 71). The two service orifices are used for vacuum drying of the cask interior, if necessary and helium filling. Their centres are located above the circumferential gap between moderator plate (Item 56) and retention ring (Item 21). One service orifice is equipped with a quick-connect (Item 60) and a bonded seal (Item 77), which provides pressure-resistant access to the free gas volume in the cask cavity. Both service orifice lids are fastened via cap screws (Item 37). The cask lid is fastened by 72 hexagon head screws [redacted] (Item 62, 63) and sealed via a metal gasket (Item 69) that is fixed within its groove via VMQ clips (Item 30). The three hexagon head screws for sealing (Item 63) enable attaching of a protection seal to be attached by the corresponding authority against unauthorised opening. [redacted]

[redacted] The main components of the cask lid system are shown in Figure 1.2-2.

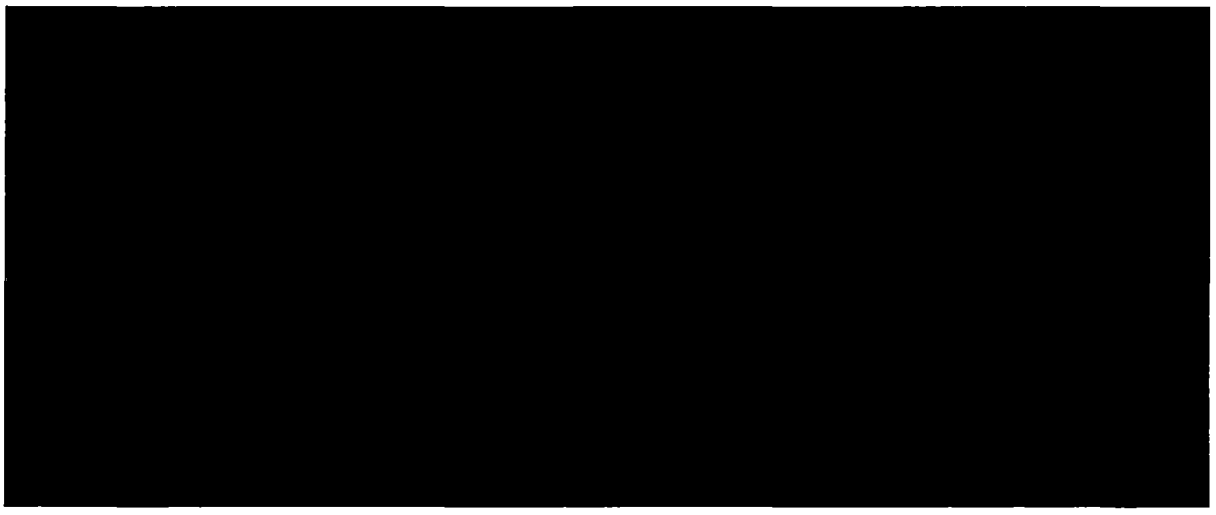

Figure 1.2-2 Lid system of the CASTOR® geo69 cask

On the bottom side of the cask lid, a moderator plate (Item 56) is mounted via six cap screws (Item 52) and bushes (Item 57). Below the cask lid, the retention ring (Item 21) [redacted] to enable adjustment of the gap at the top of the canister e.g. for thermal expansion and to protect the cask lid with the moderator plate from contact with the canister.

1.2.1.3 Canister

The canister consists of the canister body and the canister lid system according to the design parts list 1014-DPL-36855. The welded canister body (Item 2) consist of bottom (Item 2-2), liner (Item 2-3, 2-4) and head ring (Item 2-5). Canister body and canister lid (Item 3) made of stainless steel form the inner containment.

[redacted]

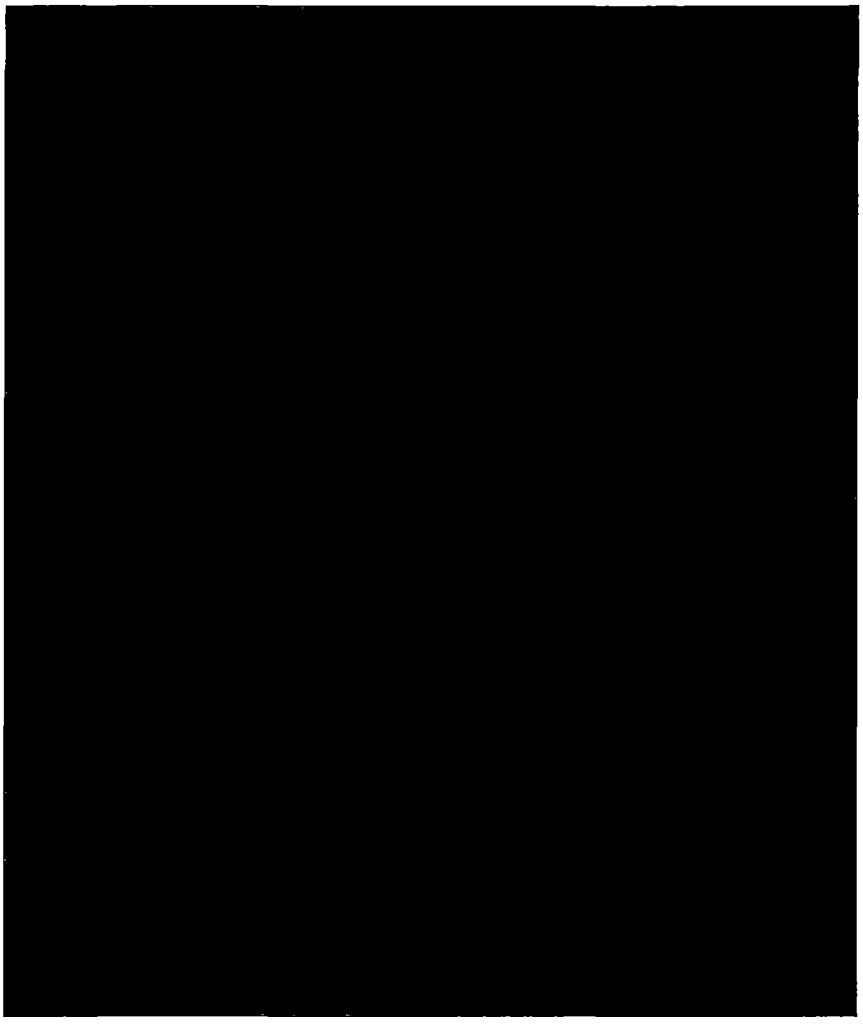

Figure 1.2-3 Closure system of the CASTOR® geo69 canister

The canister lid has two service orifices. One is connected to the interspace between the metal gasket (Item 16) and the sealing ring (Item 17) to test the leak-tightness of the metal gasket and is closed with a sealing screw (Item 26) and an O-ring (Item 74). The second service orifice (see Figure 1.2-4) is used for dewatering, vacuum drying and helium filling of the canister cavity.

Figure 1.2-4 Service orifice and corresponding parts for dewatering, drying and helium filling of the canister

A blind plug (Item 9) with an O-ring (Item 15) is mounted in the service orifice. The quick connect (Item 12) is screwed into the thread in the blind plug with a bonded seal (Item 77). After the canister cavity is dried and filled with Helium, the space above the quick-connect is closed with the tightening plug (Item 10) and sealed with the metal gasket (Item 13). The supporting O-ring (Item 14) limits the test space for leak-tightness testing of the sealing via an orifice in the tightening plug, which is closed by the sealing screw (Item 26) with O-ring (Item 74). The pressure nut (Item 11) is mounted in the canister lid to fasten the tightening plug.

1.2.1.4 Fuel Basket

The fuel basket is designed to ensure criticality safety by accommodation of up to 69 BWR-FA in a secure arrangement inside the canister cavity, as well as the removal of the decay heat released by the fuel. The parts of the fuel basket along with their respective item numbers in parts list 1014-DPL-30984 are described down below.

The fuel basket mainly consists of a grid of stacked sheets, building the separation of the FA receptacles as shown in Figure 1.2-5. Single structural sheets of boronated aluminium (Item 10 – 27) are stacked, serving both for criticality safety and heat dissipation. The stacks are kept together over the total height by the outer sheets (Item 30, 31) made of stainless steel. Round segments (Item 50) for heat transmission, mechanical support and shielding fill the gap between the outer sheets and the canister wall. FA shoes (Item 2) at the bottom of each FA receptacle serve for positioning of the FAs.

Figure 1.2-5 Fuel basket of the CASTOR® geo69 with structural sheets (topmost layer dyed green), outer sheets (pink) and round segments

1.2.1.5 Shielding elements

The circumferential gaps between the four round segments in the corners of the structural skeleton of the basket are filled with four shielding elements (Item 3, 4) according to the design parts list 1014-DPL-33604. The shielding elements are made of solid aluminium profiles, which may consist of several parts. They provide additional shielding, mechanical support and improve the heat conduction. In order to facilitate the draining of the canister cavity after underwater loading, the geometry of one corresponding element (Item 4) provides space for the permanent or temporary dewatering lance. The shielding elements are shown in Figure 1.2-6.

Figure 1.2-6 Shielding elements for the gaps in the corners of the fuel basket

1.2.1.6 Impact limiters

To protect the cask and the content both under NCT and HAC, the package comprises a pair of impact limiters (see Figure 1.2-7) according to the respective parts list 1014-DPL-38772.The lid impact limiter (Item 90) and the bottom impact limiter (Item 95) consist of an aluminium housing with a PU-foam filling to dissipate the impact energy. A penetration protection (Item 91) is arranged between the lid impact limiter and the cask lid system. The penetration protection consists of a load distribution plate (item 91-3), a penetration protection plate (item 91-2) and a spacer (item 91-4).

Figure 1.2-7 Lid-end (left) and bottom-end impact limiter (right)

The lid impact limiter is connected through load distribution plate and spacer to the cask body by ■ cap screws ■ (Item 100). The bottom impact limiter is connected through spacer to the cask body by ■ cap screws ■ (Item 101). The screws are mounted through the closure plate of the cask body.

1.2.1.7 Dimensions, Masses and Volumes

The most important properties of the CASTOR® geo69 components, including dimensions, masses and volumes are summarized in Table 1.2-2 through Table 1.2-4.

Table 1.2-2 Dimensions of the CASTOR® geo69 components

Subject	Dimensions	Reference, Remark
[redacted]	[redacted]	[redacted]
[redacted]	[redacted]	[redacted]
[redacted]	[redacted]	[redacted]
[redacted]	[redacted]	[redacted]
[redacted]	[redacted]	[redacted]
[redacted]	[redacted]	[redacted]
[redacted]	[redacted]	[redacted]
[redacted]	[redacted]	[redacted]

Table 1.2-2 Dimensions of the CASTOR® geo69 components (continued)

Subject	Dimensions	Reference, Remark
[redacted]	[redacted]	
[redacted]	[redacted]	[redacted]
[redacted]	[redacted]	[redacted]
[redacted]	[redacted]	
[redacted]	[redacted]	
[redacted]	[redacted]	

Table 1.2-3 Masses of the CASTOR® geo69 components

Subject	Mass	Reference, Remark
[redacted]		

Table 1.2-4 Volumes in the CASTOR® geo69

Subject	Volume *	Reference, Remark
[redacted]		

1.2.1.8 Components of the Containment System

The containment system consists of all the packaging components that prevent the release of radioactive material. The CASTOR® geo69 features a double-containment system with the outer containment formed by the DCI cask and the inner containment formed by the canister containing the SNF. The item no. refer to the respective parts list acc. to Table 1.2-1.

1.2.1.8.1 Inner Containment

The function of the inner containment is maintained under all conditions of transport.

Table 1.2-5 Components of the inner containment system of the CASTOR® geo69

Component	Quantity	Item	Material
Canister body	1	2	Stainless steel
Canister lid	1	3	Stainless steel
Tightening plug	1	10	Stainless steel
- Pressure nut	1	11	Alloy steel
- Metal gasket	1	16	Ni-alloy, stainless steel, Ag

1.2.1.8.2 Outer Containment

The function of the outer containment is maintained under all conditions of transport.

Table 1.2-6 Components of the outer containment system of the CASTOR® geo69

Component	Quantity	Item	Material
Cask body	1	2	DCI
Cask lid	1	55	Stainless steel
- Hexagonal screws	69	62	Alloy steel
- Hexagon head screws for sealing	3	63	Alloy steel
- Metal gasket	1	69	Ni-alloy, stainless steel, Ag
Protection cap	1	113	Stainless steel
- Pressure nut	6	37	Stainless steel
- Metal gasket	1	44	Ni-alloy, stainless steel, Ag
Blind flange	1	89	Stainless steel
- Pressure nut	12	37	Stainless steel
- Metal gasket	1	71	Ni-alloy, stainless steel, Ag

1.2.1.8.3 Metal Gaskets and Seals

The metal gaskets used in the CASTOR® geo69 consist of a helical spring surrounded by an inner jacket of stainless steel and an outer jacket of silver. [redacted] The selected materials ensure long-term stability and its high leak-tightness over a broad operating temperature range. This metal gasket design has proven itself for more than 30 years of cask operation in more than 1200 loaded and stored CASTOR® casks worldwide.

The various O-rings and sealing rings used in the CASTOR® geo69 are not part of the containment system. They are made of elastomers due to their excellent elastic properties. The elastomer seals serve as test seals and are non-safety related.

The relevant O-Rings in the cask lid system are made of FKM (fluorocarbon rubber). The quick-connect in the cask lid is equipped with a bonded seal plug made of stainless steel and FKM. The hexagon head screw of the closure plate is also equipped with a bonded seal made of stainless steel and FKM and the closure plate exhibits O-Rings made of FKM as well. This FKM material is composed of vinylindene fluoride and fluor alkene and exhibits a high thermal and chemical stability.

The relevant O-Rings in the canister lid system are made of VMQ (vinyl-methyl-silicon rubber). The VMQ elastomeric seals in the canister are auxiliary seals to create a cavity which is necessary for the measurement of the metal seals leakage rate after installation. The cask lid is equipped with a clip made of VMQ. The O-ring of the sealing screw of the closure plate is also made of VMQ. This elastomer material is known to exhibit high resistance against water and weak acids, thermal influences (up to 210 °C) and oxidation.

1.2.1.9 Components Required for Shielding

The major components contributing to shielding are presented as follows, the item no. refer to the respective parts list acc. to Table 1.2-1. Not explicitly mentioned components does only have a minor contribution to shielding and are discussed in the shielding analysis. Dimensions refer to the most relevant shielding contribution and are conservative, if a larger range is permitted.

Table 1.2-7 Cask components required for shielding

Component	Material	Gamma	Neutron
Cask body (Item 2) [redacted]	DCI	Major contribution (radial/wall, axial/bottom)	Contribution due to carbon content (minimum 3%)
Cask lid (Item 55) [redacted]	Stainless steel	Major contribution (axial)	Minor contribution
Trunnions (Item 12) [redacted]	Stainless steel	Major contribution (local)	Minor contribution
Closure plate (Item 7) [redacted]	Stainless steel	Major contribution (axial)	Minor contribution
Steel bar (Item 53, 8) [redacted]	Carbon steel	Major contribution (radial), only bottom end (for activated FA foot piece)	Minor contribution
Moderator rod (Item 141, 4, 54) [redacted]	UHMW-PE	Minor contribution	Major contribution (radial)
Moderator plate (Item 56, 5) [redacted]	UHMW-PE	Minor contribution	Major contribution (axial)

Table 1.2-8 Canister components required for shielding

Component	Material	Gamma	Neutron
Canister body (Item 2) [redacted]	Stainless steel	Major contribution (radial/wall, axial/bottom)	Minor contribution
Canister lid (Item 3) [redacted]	Stainless steel	Major contribution (axial)	Minor contribution

Table 1.2-9 Components of fuel basket and shielding elements required for shielding

Component	Material	Gamma	Neutron
Structure sheets (Item 10 ~ 27) [redacted]	B4C-Al-MMC	Major contribution (radial and diagonal)	Major contribution due to boron-carbide content ([redacted])
Outer sheets (Item 30, 31) [redacted]	Stainless steel	Major contribution (radial)	Minor contribution
Round segments (Item 50) [redacted]	Al	Major contribution (radial)	Minor contribution
FA shoe (Item 2) [redacted]	Stainless steel	Major contribution (axial)	Minor contribution
Shielding elements (Item 2, 3) [redacted]	Al	Major contribution (radial)	Minor contribution

Besides the basket components and the shielding elements, the content itself has a major contribution on the gamma shielding.

1.2.1.9.1 Shielding Material GUR® 4120

The moderator rods and plates installed in the CASTOR® geo69 are made of UHMW-PE [redacted] This treatment leads to isotropic properties until this temperature is reached. The design temperatures of the moderator rods and plates are equal or below this temperature. [redacted]

1.2.1.9.2 Shielding Material [redacted]

[redacted]

1.2.1.10 Components of the Confinement System

The components of the confinement system are intended to preserve criticality safety of the fissile material apart from the confinement function of the fuel assembly itself. This does not only include neutron absorbing materials but also any part of the package that is responsible for maintaining the sub-critical arrangement of the fuel assemblies, as well as components that enclose the fissile material and prevent in-leakage of water under conditions of transport.

1.2.1.10.1 Canister

The canister forms the boundary of the inner confinement system that encloses the fuel basket with the fissile material. Consequently, all components of the containment system (as described in section 1.2.1.8.1) are also confinement components. Under all conditions of transport, the canister forms an independent confinement that prevents in-leakage of water.

1.2.1.10.2 Fuel Basket

Sub-criticality is maintained by the arrangement of the fissile material (spent fuel assemblies) within the fuel basket. As a consequence, all components of the fuel basket that preserve its structural integrity and thus keep the FAs and the neutron absorbing materials in the intended configuration are part of the confinement system. The structural skeleton of the fuel basket (see also section 1.2.1.4) comprises 69 FA shoes (Item 2) as a base for the loaded FAs. The centre, bottom and top sheets (Item 10-27) made of Al-B_4C-MMC are all part of the confinement system, as the boron carbide is required as neutron absorbing material for criticality control. The outer steel sheets (Item 30 and Item 31) and the round segments (item 50) preserve its structural integrity of the structural skeleton of the fuel basket.

1.2.1.11 Components for Thermal Protection

The CASTOR® geo69 does not feature any components specifically aimed as active thermal protection. In case of the thermal test however, the lid and bottom impact limiters (Item 90, 95) protect the lid system and the cask bottom from the direct impact of the fire. The cask body (Item 2) acts as a thermal protection for the inner components due to its high thermal capacity.

1.2.1.12 Components for Heat Dissipation

The maximum acceptable heat load of the CASTOR® geo69 package is 18.5 kW, which is completely passively dissipated. In the following the components are summarised, that are specifically designed for the heat transfer from the FA within the fuel basket to the atmosphere.

1.2.1.12.1 Fuel Basket

The components of fuel basket play a central role in the heat transfer. The decay heat generated in the spent FA is first transferred to the centre, bottom and top sheets (Item 10 to 27) made of Al-B_4C-MMC and the outer steel sheets (Item 30, 31). This heat transfer takes place mainly by radiation and partly by conduction through the helium atmosphere in the canister. Inside the structural skeleton of the fuel basket, the heat is distributed radially and axially by conduction. The heat is radially transferred to the round aluminium segments (Item 50) and the shielding elements (see section 1.2.1.5), which transfer the heat further to the canister body.

1.2.1.12.2 Canister

The canister body consists of a welded stainless steel construction, which allows heat conduction without any gap to its surface, where it is transferred to the cask body by radiation and conduction through the helium atmosphere in the cask cavity. The canister lid system only plays a minor role in the heat transfer due to the gap between fuel basket and canister lid and the subsequent gap between canister and cask lid.

1.2.1.12.3 Cask

Without any gap, the heat is conducted around the moderator bore holes through the monolithic DCI cask body to its surface, where it is dissipated to the atmosphere by convection and radiation. Cooling fins machined into the base material significantly increase the effective surface of the outer cask wall and improve the convective heat transfer.

1.2.1.13 Corrosion Protection

All components of the CASTOR® geo69 packaging that may have contact with the environment during transport or that have contact to water during loading are made of corrosion resistant materials or they are corrosion protected by additional measures such as coating.

1.2.1.13.1 Fuel Basket

After underwater loading, the canister cavity with the fuel basket and the SNF is drained, vacuum-dried and helium-backfilled which ensures a dry and inert canister atmosphere. All components of the fuel basket are made of either stainless steel (FA shoes, outer sheets) or self-passivating aluminium alloys, so that no additional measures for corrosion protection are necessary.

1.2.1.13.2 Canister

Most metallic components of the canister are made of stainless steel, which do not require additional measures for corrosion protection. The thread bolts (Item 6) are an exemption, as they are made of alloy steel bolting material SA-540M, grade B22. They are protected against corrosion by a zinc coating. The metal gaskets are made of highly corrosion resistant material (silver, stainless steel, nickel).

1.2.1.13.3 Cask

Apart from the tilting studs and the recesses for the trunnions, a multi-layer organic painting protects the outer surfaces and the top face of the cask. A nickel coating protects the bearing surface of the cask lid. The cask cavity surface is protected by a coating, which at the same time increases the emissivity for optimising the heat transfer.

The bottom of the cask body is covered by a sealed and leak-tested cover plate (Item 7) made of stainless steel. The cover plate is bolted with galvanised cap screws (Item 9). In addition to the sealing ring (Item 47) which seals the gap between cover plate and cask body, a silicone sealing is applied to the circumferential contact cap between both components.

The tilting studs are corrosion-protected by a stainless steel wear protection (Item 183), which is mounted via stainless steel hexagon screws (Item 185). An O-ring (Item 184) seals the gap between tilting studs and wear protection.

Most components of the cask lid system are made of stainless steel. Only the bolting of the cask lid system, which includes the cap screws (Item 37) and the hexagonal screws (Item 62, Item 63) are made of ferritic steel. The corrosion protection of these screws is ensured by zinc coating.

1.2.1.14 Contamination Protection

The structure of the packaging surface and preservation measures avoid the formation of gathering points for contaminated media. The monolithic cask body provides a closed and gap-free lateral surface of the cask body. In order to ease the removal of possibly adhering contaminations, the outer cask body surface of the CASTOR® geo69 is painted with a multi-layer coating of epoxy resin

that is easy to decontaminate. Other components e.g. lids and the closure plate are made of stainless steel and gaps are filled with sealant which allow for an easy decontamination.

1.2.1.15 Transport Concept

During transport on public roads, the package is mounted via a transport frame in horizontal orientation on the transport vehicle.

Two circumferential support areas, one at the top and another one at the bottom of the cask body, serve as interfaces to the transport frame. The package is resting with these support areas on bearing surfaces of the transport frame. To prevent the package from shifting horizontally during transport, a locking mechanism of the transport frame engages into the circumferential groove in the support area at the bottom end. The cask is also fastened by lashing belts that prevent the cask from moving vertically. The trunnions as well as the tilting studs are covered by the impact limiters, which make it impossible to use these points for load attachment during transport.

1.2.2 Contents

The characteristic values of the cask contents per loading of the CASTOR® geo69 are specified in Table 1.2-10. The cask contents consist exclusively of fuel assemblies (FA) which contain spent nuclear fuel in solid form with the density stated in Table 1.2-11. The characteristics of the fuel assemblies (FA) to be transported in the CASTOR® geo69 which are essential for the safety analyses are denoted in Table 1.2-11. If not explicitly specified otherwise, the values are related to the nominal conditions before irradiation. Maximum heavy metal masses correspond to maximum active fuel rod lengths. Thus, heavy metal (HM) masses decrease for shorter fuel rod lengths. FA which have been deformed or damaged during reactor operation or which are otherwise defective in their structural integrity are not to be loaded into the cask. It is only allowed to load undamaged FA with completely filled grids into the cask. Thus, the FA do not contain any moisture after the cask drying procedure. However, it is allowed to load FA with completely filled grids containing replacement fuel rods and/or replacement rods manufactured from solid material (dummy rods). The FA do not contain any moderating constituents. The cask contents do not contain any coolants.

Table 1.2-10 Characteristic values of the radioactive content per loading of the CASTOR® geo69 package

Maximum number of fuel assemblies	69
Maximum decay heat, kW	18.5
Maximum total activity, PBq	500
Maximum Fa averaged burn-up, GWd/Mg_{HM}	58
Maximum Normal Operating Pressure (MNOP), kPa	■
Maximum metallic heavy metal mass, kg	■■■■
Maximum inventory mass, kg	22000

Table 1.2-11 Characteristics of the fuel assemblies

Internal ID	Footnote	FA No		1	2	3	4	5	6
		Fuel Type		GE 8x8-1	GE 8x8-2	SPC 8x8-2	GE9B 8x8	GE12 LUA	ATRIUM-10A
		Fissile Material		UO_2	UO_2	UO_2	UO_2	UO_2	UO_2
1	1	max. FA mass	kg						
2		max. metallic HM mass	kg						
3	2	max. fuel density	g/cm^3						
4		outer size of the assembly (fuel channel, centre)	mm						
5		outer size of the assembly (corner)	mm						
6		thickness of the fuel channel in centre (corner)	mm						
7		total height of FA (bottom to the top of handle)	mm						
8		fuel rod pitch	mm						
9		number of fuel rods	-	63	62	62	60	92	91
10		number of part length fuel rods	-	0	0	0	0	14	8
11	3	number of water rods	-	1	2	2	1 (2x2)	2 (2x2)	1 (3x3)
12		fuel rod length	mm						
13		fuel pellet stack length (active fuel length)	mm						
14		part length pellet stack length	mm						
15		nominal pellet diameter	mm						
16		tolerance of the pellet diameter	mm						
17		max. dishing+chamfering, pellet volume fraction	vol-%						
18	4	max. ^{235}U initial enrichment	wt-%						
19	5	min. ^{235}U initial enrichment	wt-%						
20		max. FA-averaged discharge burn-up	GWd/Mg_{HM}						
21		min. cooling time	d						
22			-						
23		cladding material	-	Zircaloy-2	Zircaloy-2	Zircaloy-2	Zircaloy-2	Zircaloy-2	Zircaloy-2
24		cladding outer diameter	mm						
25		tolerance of cladding diameter	mm						
26		cladding thickness	mm						
27	6	tolerance of cladding thickness	mm						
28		water rod/channel material	-	Zircaloy-4	Zircaloy-4	Zircaloy-2	Zircaloy-2	Zircaloy-2	Zircaloy-4
29		min. water rod/channel outer dimension	mm						
30		min. thickness of the water rod/channel	mm						
31			-						
32			kg						
33			kg						
34			kg						
35			wt-%						
36			cm^3					39	33
37			cm^3						
38			mm						

All values are given for the cold, non-irradiated state, if not stated otherwise. Tolerances are applied positively and negatively.

[1] the weight of the fuel channel is included

[2] for criticality assessment

[3] FA No 4 to 6 show larger water rods with grid dimensions of 2 by 2 water regular rods or a larger water channel with grid dimensions of 3 by 3 water regular rods

[4] averaged over the cross section of the assembly in the region with highest enrichment including production tolerance

[5] averaged over the cross section of the assembly in the region with lowest enrichment excluding production tolerance

[6] deduced from the tolerances of the inner and outer diameter

Figure 1.2-8 shows the general loading schematic of the cask viewed from the top, including basket position numbers 1 to 69 and position groups (PG) A to F. Position groups are defined by positions which are treated equivalently in terms of shielding and decay heat limit.

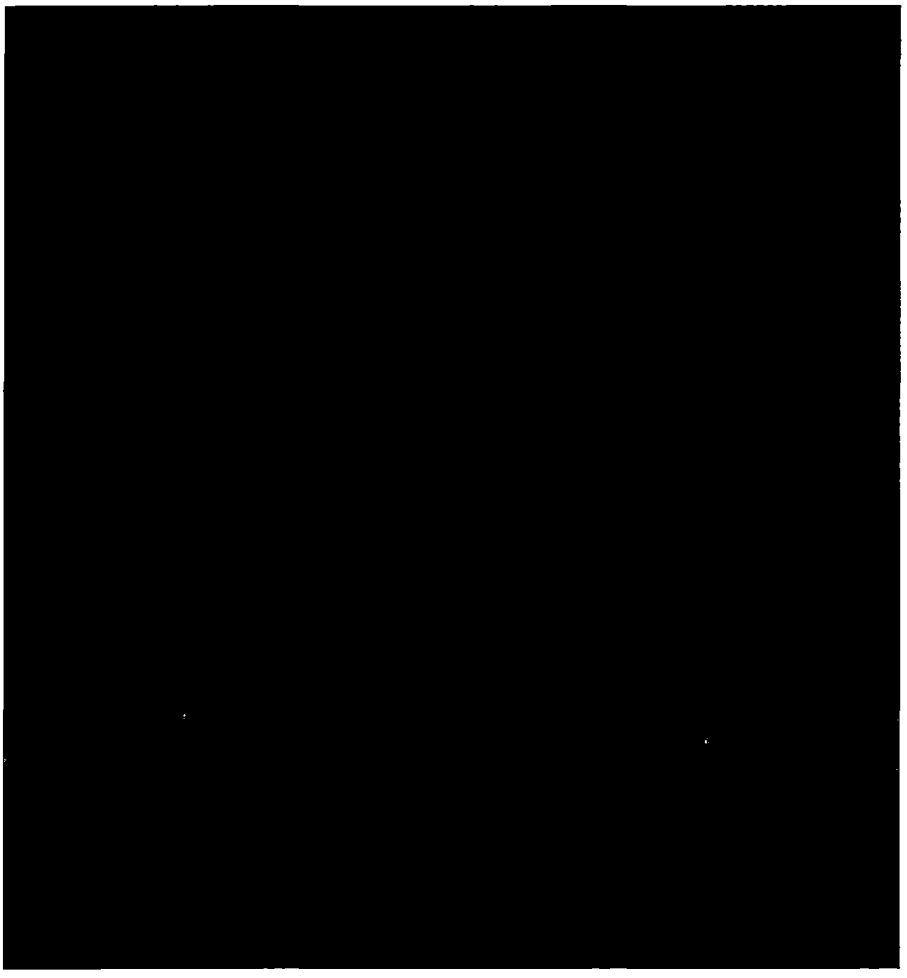

Figure 1.2-8 Loading scheme of the CASTOR® geo69 package with position numbers and position groups (PG), top view

1.2.2.1 Thermal Payload

The BWR FA of the six fuel types listed in Table 1.2-11 are to be loaded into one of three different loading patterns which are defined by overall thermal requirements. At the time of loading into the cask, the decay heat of every FA has to comply with one of the three thermal requirements (TR1-3) presented in Figure 1.2-9. Only one single thermal requirement is admissible for single given loading. The thermal requirements comprise decay heat maxima (in Watts) indicated position wise. Thermal requirements are legit for all FA regardless of their type. In addition to the individual boundaries for decay heat, the overall decay heat of a single loading must not exceed 18.5 kW, as stated in Table 1.2-10. It is possible to combine FA of different types within one single loading respecting the chosen thermal requirement and the overall characteristics of a loading in Table 1.2-10. The bounding thermal parameters are discussed and specified in detail in chapter 3.

Figure 1.2-9 Thermal Requirements (TR1-3) with maximum decay heat per FA position in W, top view

1.2.2.2 Source Specification

The decay heat values, gamma and neutron source terms, nuclide activities, and fissile gas masses are determined with the help of burn-up and depletion calculations. This section briefly describes the approach used for the calculations. Results and details are presented in corresponding chapters of the SAR. The aforementioned physical quantities were calculated using the TRITON [1] and ORIGAMI [2] modules of the SCALE 6.2 system [3].

To enable subsequent ORIGAMI calculations, TRITON is utilized to generate cross-section libraries for all FA types from Table 1.2-11. In Figure 1.2-10 the two-dimensional TRITON models creating the cross-section libraries are shown for the six types FA. Dark blue circles stand for fuel pins,

yellow circles for fuel pins with Gd_2O_3 content. Pin cladding is shown in light blue. Red areas denote the position of the water rods/channels and surrounding moderator. Structural materials of the water rods/channels and the outer fuel assembly are pictured in purple (see Figure 1.2-10).

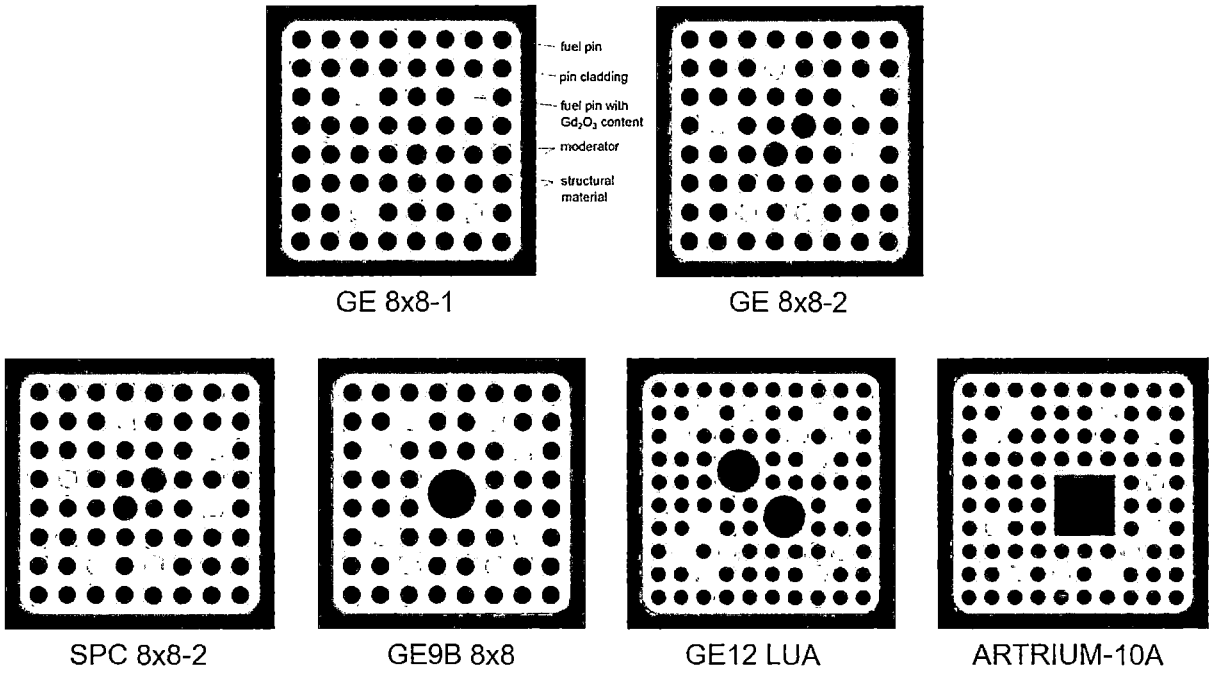

Figure 1.2-10 TRITON models of fuel assemblies

The libraries have been generated using the following parameters:

- ENDF/B-VII 252-group library
- enrichment [redacted] wt-% ^{235}U in steps of [redacted] wt-% ^{235}U for FA types excluding
- [redacted]
- enrichment [redacted] wt-% ^{235}U in steps of [redacted] wt-% ^{235}U for FA type [redacted]
- [redacted]
- [redacted]
- moderator density [redacted] g/cm^3 in steps of [redacted] g/cm^3,
- burn-up up to [redacted] GWd/t_{HM} in steps of [redacted] GWd/t_{HM}.

To take axial variations in source term generation into account, axially varying burn-up profiles and moderator densities are employed in the ORIGAMI calculations. [redacted] Every 2D ORIGAMI model is divided into

[redacted] equidistant axial nodes in the active zone, which leads to a virtual third dimension. In the profiles shown in Figure 1.2-11 and Figure 1.2-12 and summarized in Table 1.2-12, node 1 is at the bottom end of the active region and node [redacted] is at the top end. [redacted] Sample input files for TRITON and ORIGAMI are provided in Appendix 1-1 and Appendix 1-2.

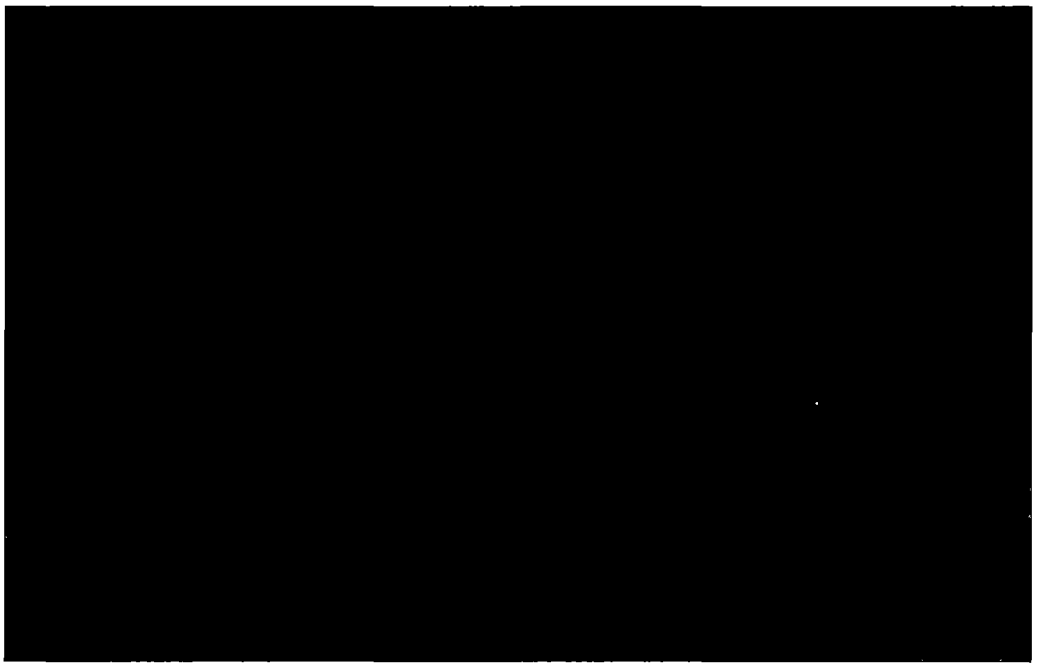

Figure 1.2-11 Moderator density used in the ORIGAMI calculations

Figure 1.2-12 Burn-up profiles used in the ORIGAMI calculations

Table 1.2-12 Moderator density und burn-up profile inputs for ORIGAMI calculations

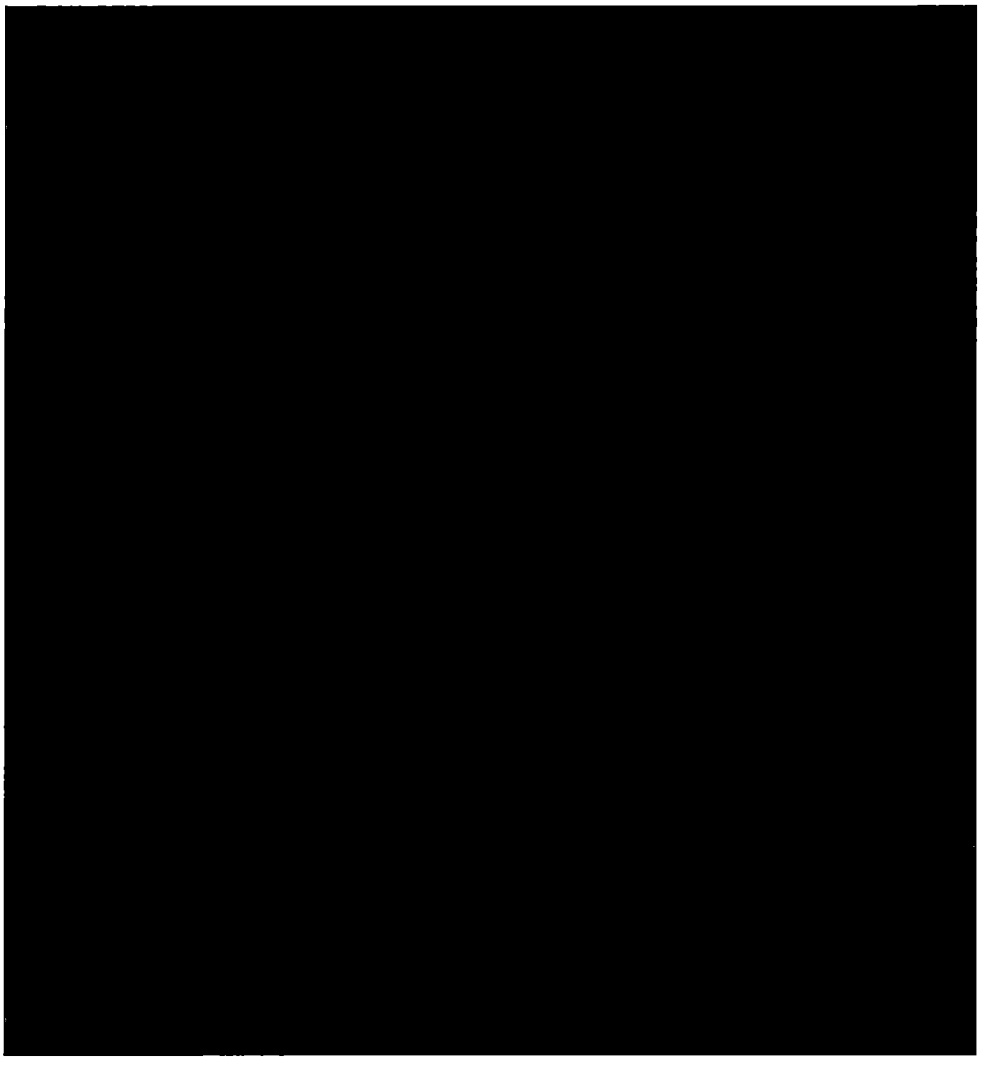

Table 1.2-13 shows the input parameters which are used to generate the ORIGAMI calculation input files resulting in bounding values for decay heat and source terms. Radiation source terms and decay heat increase monotonically with increasing burn-up. Thus, maximum burn-up is a first bounding parameter. Furthermore, it is acknowledged that for decreasing initial fuel enrichments source terms and decay heat are increasing. As a result, minimum initial fuel enrichment is a second bounding parameter.

Table 1.2-13 Input parameters for the ORIGAMI calculations of decay heat and source terms

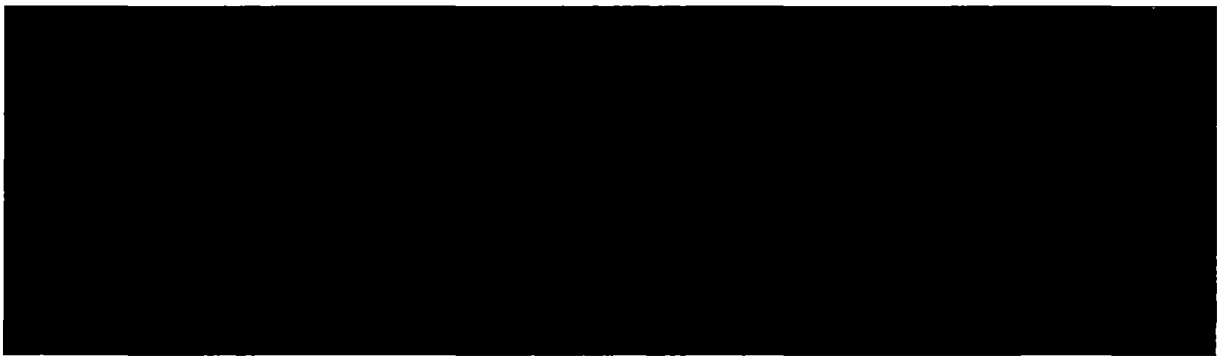

Table 1.2-14 shows the input parameters which are used to generate the ORIGAMI calculation input files resulting in bounding values for nuclide activities and fissile gas masses. As the production of fissile products and actinides differs for varying initial fuel enrichments, a range of this input parameter was taken into account for each fuel assembly type separately. Thus, bounding parameters are determined separately for each nuclide and element, respectively.

Table 1.2-14 Input parameters for the ORIGAMI calculations of nuclide activities and fissile gas masses

Table 1.2-15 contains the calculated values for these quantities. Calculations are performed with respect to 1 Mg_{HM} and for a date at the end of the minimum cooling time stated in Table 1.2-11.

Table 1.2-15 ORIGAMI calculation results for decay heat, nuclide and total activities, and fissile gas masses with regard to 1 Mg_{HM} at the date of minimum cooling time from Table 1.2-11

[redacted]

1.2.3 Special Requirements for Plutonium

The content as described in section 1.2.2 to be transported in the CASTOR® geo69 package contains plutonium in solid form only.

1.2.4 Operational Features

The CASTOR® geo69 is designed to enable the loading and unloading of spent nuclear fuel under consideration of ALARA principles. The closure systems of both containment boundaries (see Fig-

ure 1.2-13 to Figure 1.2-15) are equipped with connection orifices, which are already described in section 1.2.1, to enable the draining, drying and inertizing of the package.

Figure 1.2-13 Containment boundary detail at the cask lid with protection cap

Figure 1.2-14 Containment boundary detail at the cask lid with blind flange

Figure 1.2-15 Containment boundary detail at the canister lid with tightening plug

List of References

1] M. A. Jessee et al.
TRITON: A Multipurpose Transport, Depletion, and Sensitivity and Uncertainty Analysis Module
in: SCALE Code System
ORNL/TM-2005/39, Version 6.2.2, 2017

[2] M. L. Williams et al.
ORIGAMI: A Code for Computing Assembly Isotopics with ORIGEN
in: SCALE Code System
ORNL/TM-2005/39, Version 6.2.2, 2017

[3] SCALE Code System
ORNL/TM-2005/39, Version 6.2.2, 2017

2 Structural Evaluation

2.0 Overview

	Name, Function	Date	Signature
Prepared	[redacted]		
Reviewed			

The following sections of this chapter provides the identification, description, discussion and analyses of the principle structural design of the packaging, components and systems important to safety.

The structural safety evaluation considering the mechanical loads and load combination confirms that the load conditions required according to 10 CFR 71 (Division 3, WA-3351.2 i) are met. For boundary conditions differing from the requirements, it is shown, that assumed loads are covering for those required and represent a conservative scenario.

The structural safety evaluations include e.g. consideration of loads, materials and other specified relevant information. The description how the package complies with the performance requirements of 10 CFR 71 is provided in Section 1.0.

The structural safety evaluation is based on the validation, verification or method reports cited in Section 2.12, Appendix 2-5.

2.1 Description of the Structural Design

	Name, Function	Date	Signature
Prepared	[redacted]		
Reviewed			

In this section the principle structural design of the packaging, components and systems important to safety are identified, described, discussed and analysed separately for the containment, the basket together with the shielding elements, the load attachment points and the impact limiters according to the description in Section 1.2 and the corresponding parts lists and drawing referenced in Section 1.3.

2.1.1 Discussion

The structural evaluation presented in the following sections confirms the integrity of the principal structural members of the packaging important to safe operation under normal conditions of transport (NCT) and hypothetical accident conditions (HAC) by showing that the design criteria specified in 10CFR71 (§§ 71.71 and 71.73) and described in Section 2.1.2 are met. The CASTOR® geo69 transport package consists of the major structural components cask body, canister, basket, shielding elements and lid and bottom impact limiters as described in Section 1.2 and shown in Table 2.1-1 according to the corresponding parts lists cited in Section 1.3.

The evaluation of the integrity of the containment members cask and canister including the corresponding seals and fastenings is performed and verified under NCT, HAC and test conditions for a Type B(U) packaging according to 10 CFR 71 §§71.71 and 71.73. The assessment comprises:

- Proof of sufficient strength for the cask body, canister body, cask lid and canister lid according to Division 3

The evaluation of the basket and the shielding elements comprises the loads for transport conditions based on analytical and numerical calculations with the finite element method (FE-method) as the selected numerical algorithm. Requirements, loads and essential verifications are discussed in detail.

All verifications confirm the adequacy of the basket and the shielding elements regarding the capability of bearing the required loads and thus are sufficiently dimensioned.

The evaluation of the load attachment points confirms that the predefined requirements under handling conditions are met. The assessment comprises the trunnions including bolts and threads, the tilting studs, the threads in the cask lid and the threads in the canister lid.

The analysis of the impact limiters determines the resulting rigid body decelerations of the package under NCT and HAC and proves that the design of the lid impact limiter components [redacted] as well as of the bottom impact limiter compo-

nents [redacted] and their corresponding bolted joints and [redacted] meet the requirements of NCT and HAC.

Furthermore it is shown that the impact limiters remain at the package for NCT and for assembly conditions it is proven that the length of engagement of the impact limiter bolts is sufficient.

The rigid body decelerations of the cask are given for NCT and HAC and it is shown that the deformations of the impact limiter for HAC meet each of the following requirements:

- 9.0-m lid and bottom side flat drop without loads to the lid system and the closure plate
- 9.0-m lid and bottom side edge drop without the cask body touching the ground
- 9.3-m side drop without the trunnions touching the ground

Furthermore the components of the lid and bottom impact limiter are subject to acceptable loads under HAC 9.0 m free drops and 1 m pin drops, respectively.

Table 2.1-1 Principal structural members important to safe operation

No	*Designation*	*Component or Subassembly*	*Safety Aspect*
1	Cask body	Outer containment, cask	Structural resistance against specified load conditions, leak-tightness
2	Cask lid		
3	Bolting		
4	Sealing		
5	[redacted]		
6	Canister body	Inner containment, canister	Structural resistance against specified load conditions, leak-tightness
7	Canister lid		
8	Bolting/fastening		
9	Structural sheets	Fuel basket	Structural resistance against specified load conditions, positioning of FAs
10	PU foam	Impact limiters	Limiting of deceleration loads, protection of lid and cask body from puncture loads
11	[redacted]		
12	Trunnions with fastening	LAP	Safe handling
13	Tilting studs		
14	Cask lid threads		
15	Canister lid threads		

2.1.2 Design Criteria

2.1.2.1 Containment

In general, the assessment criteria are separated into the following categories:

- Normal conditions
- Hypothetical accident conditions
- Testing Limits
- Fatigue Assessment

The design criteria for the stress assessments of the bolts and the cask and canister parts are described in the following.

2.1.2.1.1 Normal Conditions (NC)

Under normal conditions according to 10 CFR 71, the admissible elastic analysis stress intensity limits for the cask and canister parts are as defined in Division 3 (WB-3222) except bolts and gaskets:

General primary membrane stress intensity:	$P_m \leq 1.0 \cdot S_m$
Local primary membrane stress intensity:	$P_l \leq 1.5 \cdot S_m$
Primary membrane (general or local) plus primary bending stress intensity:	$(P_m \text{ or } P_l) + P_b \leq 1.5 \cdot S_m$
Primary plus secondary stress) plus peak stress	$(P_m \text{ or } P_l) + P_b + Q + F \leq S_a$

The welds at the canister are treated as base material considering the allowable stress values and material properties, which is stated in the ASME BPVC Section III Division 1, Subsection NF [1].

The following stress criteria for bolts are considered according to NUREG / CR–6007 [2].

Average stress (Tension):	$\sigma = \frac{F}{A} \leq \frac{2}{3} \cdot S_y$
Average stress (Shear):	$\tau = \frac{Q}{A} \leq 0.4 \cdot S_y$
Stress Ratio (Tension plus shear):	$R_t^2 + R_s^2 < 1$
Maximum stress (Stress intensity S):	$S = \sqrt{(\sigma_m + \sigma_b)^2 + 4 \cdot (\tau + \tau_{res.})^2} \leq 0.9 \cdot S_y$

The evaluation of shear loaded cross sections that are critical to leak tightness conditions are performed by assessments considering the shear forces taken from the simulation results. The evaluated shear stress is compared to the pure shear stress criterion (according to Division 3, WB-3227.2 (a)):

Pure Shear:	$\tau = \frac{F}{A} \leq 0.60 \cdot S_m$

The admissible stress values are summarized in Table 2.1-2.

Table 2.1-2 Admissible stress criteria under normal and hypothetical accident conditions

	Item No.	T [°C]	S_m [MPa]	S_u [MPa]	Admissible stress [MPa]							
					Level A (NC)				Level D (AC)			
					P_m	P_l	P_m+P_b	P_m+P_b+Q+F	P_m	P_l	P_m+P_b	P_m+P_b+Q+F
Cask SA-874M	2	-29	75.0	300.0	75.0	112.5	112.5	772	210.0	300.0	300.0	1544
Cask lid SA-182M Grade F316	55	-29	138.0	517.0	138.0	207.0	207.0	-	331.2	496.8	496.8	-
Canister Headring SA-182M Grade FXM-19	2-5											
Canister Body SA-240M Grade 316L	2-2 2-3 2-4											
Canister Lid SA-965M Grade FXM-19	3											
Clamping element SA-479M Grade XM-19	4											
Form piece SA-479M Grade 316L	5											

The yield strength S_y of the bolts is summarized in Table 2.1-3.

Table 2.1-3 Admissible yield strength [MPa] of the bolts for the cask lid and the canister thread bolts

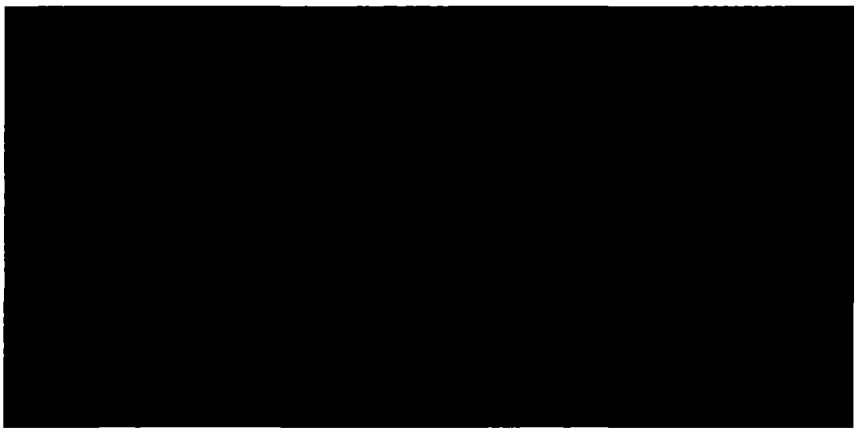

The values for the torsional stress $\tau_{res.}$ are taken from Table 2.1-4. At assembly state the maximum torsional stress is considered. At other load cases half of the above mentioned values are considered according to [2]. A summary of the values is presented in Table 2.1-5.

Table 2.1-4 Calculation of assembly preload; Cask Lid; Items 62 and 63 to 55

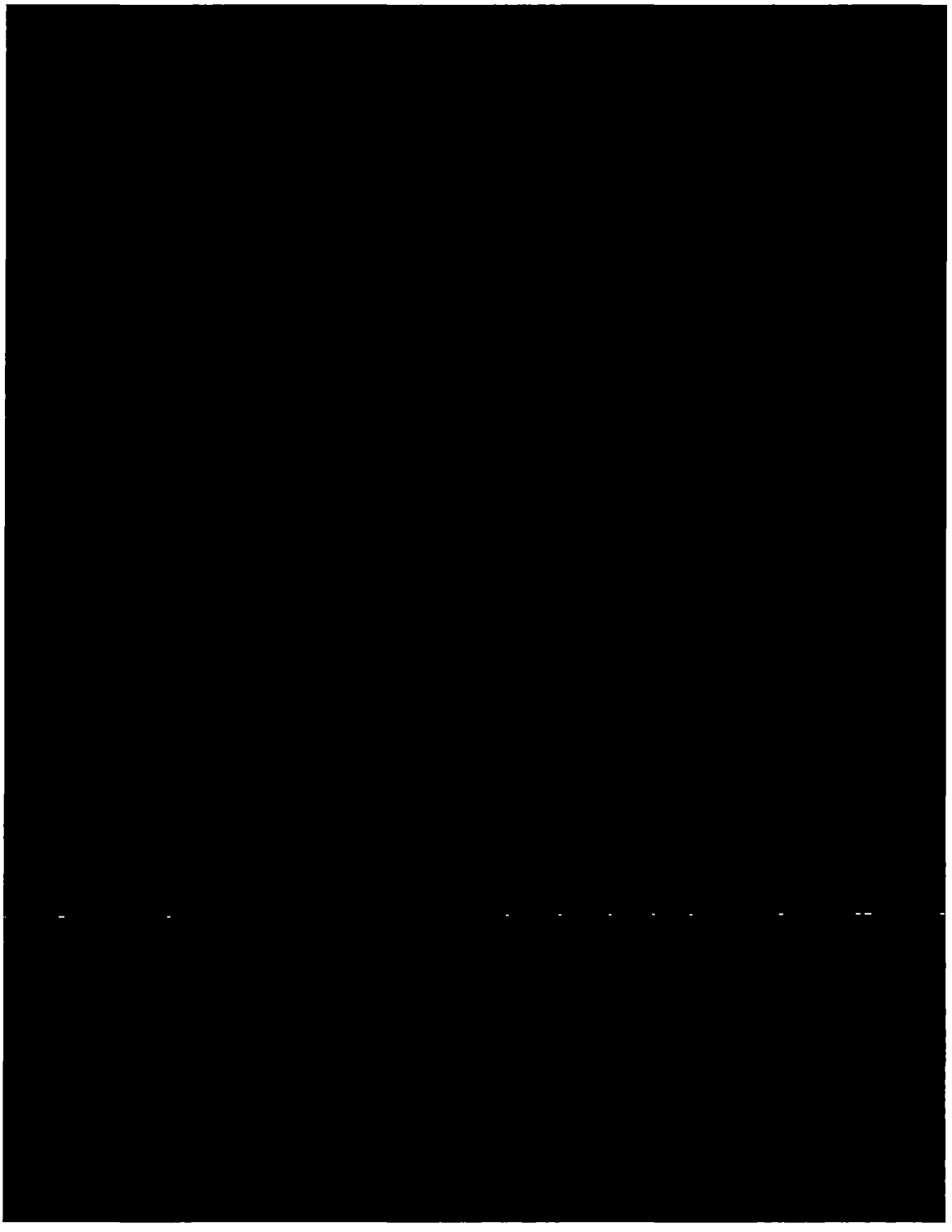

Table 2.1-4 Calculation of assembly preload; Cask Lid; Items 62 and 63 to 55 (continued)

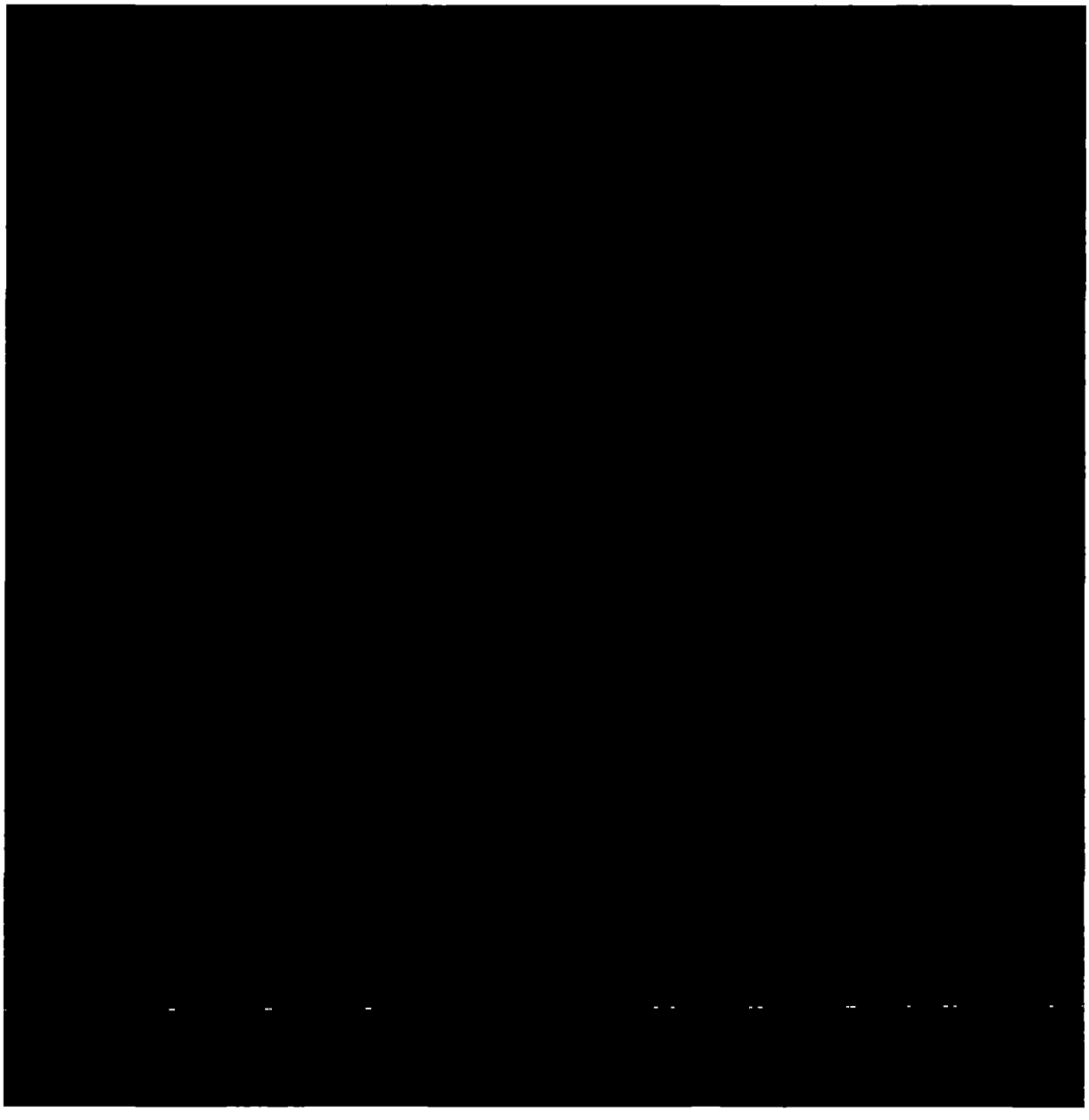

Table 2.1-5 Torsional stress [MPa] from assembly state

Torsional stress τ [MPa] acc. to temperature and pretension.			
	T_{min} -29°C	RT 20°C	T_{max} 110°C
$\tau_{res\ min}$ ($F_{V\ min.}$)	24	28	28
$\tau_{res\ max}$ ($F_{V\ max.}$)	39	39	43

2.1.2.1.2 Hypothetical Accident Conditions (HAC)

Under hypothetical accident conditions, the admissible elastic analysis stress intensity limits for the cask and canister parts are as defined in Division 3 (WB-3234) except bolts and gaskets:

General primary membrane stress intensity (for austenitic steel, high-nickel alloy, and copper-nickel alloy materials):	$P_m \leq Minimum(2.4 \cdot S_m; 0.7 \cdot S_u)$
General primary membrane stress intensity (for ferritic steel materials):	$P_m \leq (0.7 \cdot S_u)$
Local primary membrane stress intensity (for austenitic steel, high-nickel alloy, and copper-nickel alloy materials)	$P_l \leq Minimum(3.6 \cdot S_m; 1.0 \cdot S_u)$
Local primary membrane stress intensity (for ferritic steel materials):	$P_l \leq (1.0 \cdot S_u)$
Primary membrane (general or local) plus primary bending stress intensity (for austenitic steel, high-nickel alloy, and copper-nickel alloy materials):	$(P_m \text{ or } P_l) + P_b \leq Minimum(3.6 \cdot S_m; 1.0 \cdot S_u)$
Primary membrane (general or local) plus primary bending stress intensity (for ferritic steel materials):	$(P_m \text{ or } P_l) + P_b \leq (1.0 \cdot S_u)$
Primary plus secondary plus peak stress intensity	$(P_m \text{ or } P_l) + P_b + Q + F \leq 2 \cdot S_a$, *with* $(2 \cdot S_a)$ *at 10 cycles*

The Sa criterion for canister head ring, liner and bottom of the material is chosen conservatively for a lower material group (BPVC Section III Appendices, Table I-9.5; Nickel-Chromium-Molybdenum-Iron Alloys).

The welds at the canister are treated as base material considering the allowable stress values and material properties according to BPVC Section III Division 1, Subsection NF [1].

The evaluation of shear loaded cross sections that are critical to leak tightness conditions are performed by assessments considering the shear forces taken from the simulation results. The evaluated shear stress is compared to the pure shear stress criterion (according to Division 3, WB-3224.1(d)):

Pure Shear:	$\tau = \frac{F}{A} \leq 0.42 \cdot S_u$

The admissible stress values are summarized in Table 2.1-2.

For the bolts, the stress criteria of the normal conditions (Level A) according to Section 2.1.2.1.1 are applied under HAC. According to Division 3, WB-3234 (Level D service limits) the requirement of leak tightness of the closure may be satisfied by using the rules of Division 3, WB-3232 (Level A

service limits). By ensuring that the Level A service limits are satisfied during HAC, the lid systems of both the cask and canister remain functional. Thus, by demonstrating that the corresponding acceptance criteria for moderator exclusion (i.e. confirmation of the cited Level A service limits) are met, it is shown that two independent watertight boundaries remain intact also under HAC, so that moderator exclusion can be assumed.

The values for the torsional stress are applied as described for the normal conditions above.

2.1.2.1.3 Testing Limits

Under test conditions, the admissible elastic analysis stress limits for the cask and canister parts according to Division 3 (WB-3235) except bolts and gaskets are defined as follows:

General primary membrane stress intensity:	$P_m \leq (0.9 \cdot S_y)$
Primary membrane plus bending stress intensity:	for: $P_m \leq (0.67 \cdot S_y)$ $(P_m + P_b) \leq (1.35 \cdot S_y)$
	for: $(0.67 \cdot S_y) < P_m \leq (0.9 \cdot S_y)$ $(P_m + P_b) \leq (2.15 \cdot S_y - 1.2 \cdot P_m)$

The admissible stress values are summarized in Table 2.1-6.

Table 2.1-6 Admissible stress criteria under testing limits

	T [°C]	S_y [MPa]	Admissible stress [MPa]		
			Testing Limits		
			P_m	P_m+P_b ($0.67S_y$)	P_m+P_b ($0.9S_y$)
Cask SA-874M	RT	200	180	270	214
Cask lid SA-182M Grade F316	RT	207	186	279	221
Canister Headring [redacted]	RT	[redacted]			
Canister Body [redacted]	RT	[redacted]			
Canister Lid [redacted]	RT	[redacted]			
Clamping element [redacted]	RT	[redacted]			
Form piece [redacted]	RT	[redacted]			

The following stress criterion according to Division 3 (WB-3235) has to be met for the bolts in the cask lid and the canister thread bolts:

Maximum stress (Stress intensity S):	$S = \sqrt{(\sigma_m + \sigma_b)^2 + 4 \cdot (\tau + \tau_{res.})^2} \leq S_y$

The values for the torsional stress are applied as described above for the normal conditions.

2.1.2.1.4 Fatigue Assessment

The fatigue assessment of the lid bolting is performed according to the procedure described in Division 3 (WB-3232.4).

The assessment is based on determining the admissible design life for a given stress intensity amplitude. With the calculation of the usage factor as the quotient of design life target cycles and admissible design life cycles for different load cases, the total usage factor is determined. The total usage factor is the sum of the usage factors of each load case:

$$U = \sum_{k=1}^{n} U_k + \cdots + U_n = \sum_{k=1}^{n} \frac{n_k}{N_k} + \cdots + \frac{n_n}{N_n}$$

where n is the given design life target and N is the admissible number of cycles from the equation established in the BPVC Section III Appendices.

The admissible number of load cycles is determined with the stress intensity increased by the following factors:

$$S_a = \frac{1}{2} \cdot S \cdot K_F \cdot K_E \; (for\ pulsating\ load)\ and\ S_a = S \cdot K_F \cdot K_E \; (for\ alternating\ load);$$

Where S = stress intensity, Fatigue strength reduction factor K_F = 4 and correction factor for modulus of elasticity $K_E = \frac{E_{Al}}{E}$.

2.1.2.2 Load Attachment Points

The dimensions of the components are taken from the design parts list according to Section 1.3 and the corresponding drawings and standards.

The material property values are presented in Table 2.1-7 and Table 2.1-8 and are taken from BPVC Section II (Part D) [3]. Not explicitly given values are highlighted in *italics* and are interpolated or taken from the next higher temperature if interpolation is not possible. The coefficients of friction of the components are presented in Table 2.1-9.

Table 2.1-7 Material properties

Component (Dimension)	Item	Classification level	Material [Alternative material]	1: Nominal Composition 2: Product Form 3: Spec. No. 4: Type / Grade 5: Alloy Desig. / UNS No. 6: Class / Cond. / Temper 7: Size / Thickness, mm 8: P-No. 9: Group No.	Temperature T °C	Tensile Strength S_u MPa	Yield Strength S_y MPa	Thermal Expansion α 10^{-6} mm/mm/°C	Modul of Elasticity E 10^3 MPa
Cask body [redacted]	2	■	SA-874M	1: Ductile cast iron 2: Castings 3: SA-874 4: - 5: - 6: - 7: 300<t<530 8: - 9: -	-75	-	-	-	169.00
					-29	***300***	***200***	***10.3***	***165.32***
					20	***300***	***200***	**10.3**	***161.40***
					25	-	-	-	161.00
					40	300	200	-	-
					[redacted]				
			[JIS G 5504]	1: Ductile cast iron 2: Castings 3: SA/JIS G5504 4: FCD 300 LT 5: - 6: - 7: 300<t<530 8: - 9: -	-75	-	-	-	169.00
					-29	***300***	***200***	***10.3***	***165.32***
					20	***300***	***200***	**10.3**	***161.40***
					25	-	-	-	161.00
					40	300	200	-	-
					[redacted]				
Trunnion [redacted]	12	■	SA-479M 13Cr-4Ni (UNS S41500)	1: 13Cr-4Ni 2: Bar 3: SA-479 4: - 5: S41500 6: - 7: - 8: 6 9: 4	-75	-	-	-	208.00
					-29	***793***	***621***	***10.6***	***204.78***
					20	***793***	***621***	**10.6**	***201.35***
					25	-	-	-	201.00
					40	793	621	-	-
					[redacted]				
			[SA-182M Grade F6NM]	1: 13Cr-4Ni 2: Forgings 3: SA-182 4: F6NM 5: S41500 6: - 7: - 8: 6 9: 4	-75	-	-	-	208.00
					-29	***793***	***621***	***10.6***	***204.78***
					20	***793***	***621***	**10.6**	***201.35***
					25	-	-	-	201.00
					40	793	621	-	-
					[redacted]				

Table 2.1-7 Material properties **(continued)**

Component (Dimension)	Item	Classi-fication level	Material [Alternative material]	1: Nominal Composition 2: Product Form 3: Spec. No. 4: Type / Grade 5: Alloy Desig. / UNS No. 6: Class / Cond. / Temper 7: Size / Thickness, mm 8: P-No. 9: Group No.	Tempe-rature	Tensile Strength	Yield Strength	Thermal Expansion	Modul of Elasticity
					T	S_u	S_y	α	E
					°C	MPa	MPa	10^{-6} mm/mm/°C	10^3 MPa
Cap screw [redacted]	13	[redacted]	SA-193M Grade B6	1: 13Cr 2: Bolting 3: SA-193 4: B6 5: S41000 6: - 7: ≤100 8: - 9: -	-75	-	-	-	208.00
					-29	***758***	***586***	***10.6***	***204.78***
					20	***758***	***586***	**10.6**	***201.35***
					25	-	-	-	201.00
					40	758	586	-	-
					[redacted]				
					[redacted]				
					[redacted]				
					[redacted]				

Table 2.1-8 Tensile strengths

Component (Dimension)	Item	Classi-fication level	Material [Alternative material]	Tensile Strength
				S_u
				MPa
Cask body [redacted]	2	[redacted]	SA-874M [JIS G 5504]	300
Cap screw [redacted]	13	[redacted]	SA-193M B6	758
Cask lid [redacted]	55	[redacted]	SA-182M F316 [SA-182 F304, SA-240M 316, SA-240M 304]	517
			[SA-965M F316, SA-965M F304]	483
Canister lid [redacted]	3	[redacted]	[redacted]	689
Load attach-ment point for cask lid handling	-	-	-	1000

Table 2.1-9 Coefficients of friction

Component 1	Component 2	Area of contact	Coefficient of friction
			μ_{max}
Trunnion bolt	Cask body	Bolt thread	0.095
Trunnion bolt	Trunnion	Bolt head bearing area	0.11

2.1.2.3 Basket

2.1.2.3.1 Verifications for the different conditions of transport

The verification is done under the assumption that the decelerations acting on the package are transferred completely to the fuel basket and the content. Since the mechanical loads are modelled as static loads, it is ensured that dynamic effects are covered in the load mapping. The thermal loads are taken into account as steady-state temperature fields.

When determining the mechanical properties of the materials, maximum design temperature is taken as a basis in order to take into account their temperature dependence conservatively.

The verification of the load-bearing capacity of the load-bearing components is accomplished in form of a linear-elastic stress analysis as described in the corresponding paragraph in Section 2.1.2.3.3 below. If this should not be successful, a nonlinear stress-strain analysis is done according to the corresponding paragraph on the verification of the load-bearing capacity in Section 2.1.2.3.3 below. The designation of residual deformations is accomplished according to the corresponding paragraph in Section 2.1.2.3.3 below. The procedure for the verification of stability is described in the corresponding paragraph on the stability analyses in Section 2.1.2.3.3 below.

The stresses and strains are calculated using standard analytical and numerical methods. The numerical algorithm selected is the finite element method (FE-method). The calculations are carried out using the explicit finite element code LS-DYNA® [4].

2.1.2.3.2 Classification of the Conditions of Transport as Load Cases

Load cases to be considered based on the conditions of transport are classified into load categories according to KTA 3201.2 [5]. For this purpose, the load cases corresponding to NCT are classified as "normal operating conditions" (specified operation). The loadings derived for this category are classified as operating level "Level A".

The load cases which correspond to HAC are classified in load category "accidents" (load case class "incidents") based on KTA 3201.2 [5]. The loadings derived for this category are classified as operational level "Level D". The integrity of the fuel basked is verified under HAC loads, which means that structural failure of the load-bearing components is excluded. Furthermore, it is shown that these loads do not cause any deformations which transmit inadmissible loads to the content. If any residual deformations occur, they are quantified and reported. Additionally, it is also proven in the respective verifications for the package, that leak-tight containment and shielding are properly ensured.

The material-dependent allowable stresses used for verifications with elastic and elastic-plastic material behaviour correspond to the classification of operating levels for different conditions of transport based on KTA 3201.2 [5].

2.1.2.3.3 Load-Bearing Components

The verification concept for the load-bearing components with the following analyses is depicted in Figure 2.1-1 in the form of a flow chart:

- linear elastic stress analysis,
- load-bearing capacity analysis (if necessary) with ideally elastic-plastic material behaviour,
- evaluation of the deformations of the fuel basket and
- verification of stability

The allowable stresses and fictitious yield stresses introduced below are valid only for metallic materials, which possess enough deformation capacity (ductility) for the whole range of operating temperatures. This is the case for all components of the fuel basket.

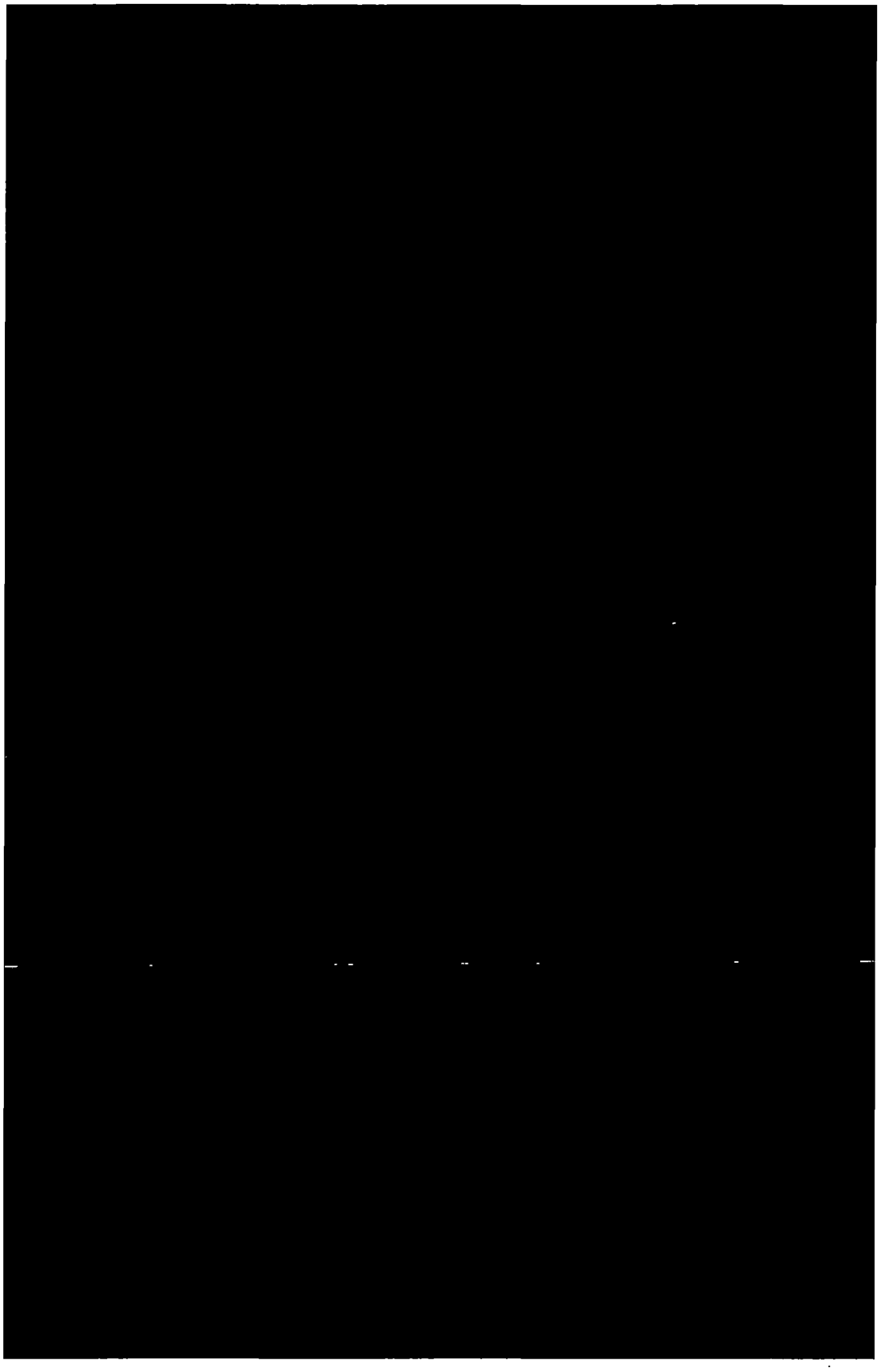

Figure 2.1-1 Verification concept for load-bearing components of the fuel basket

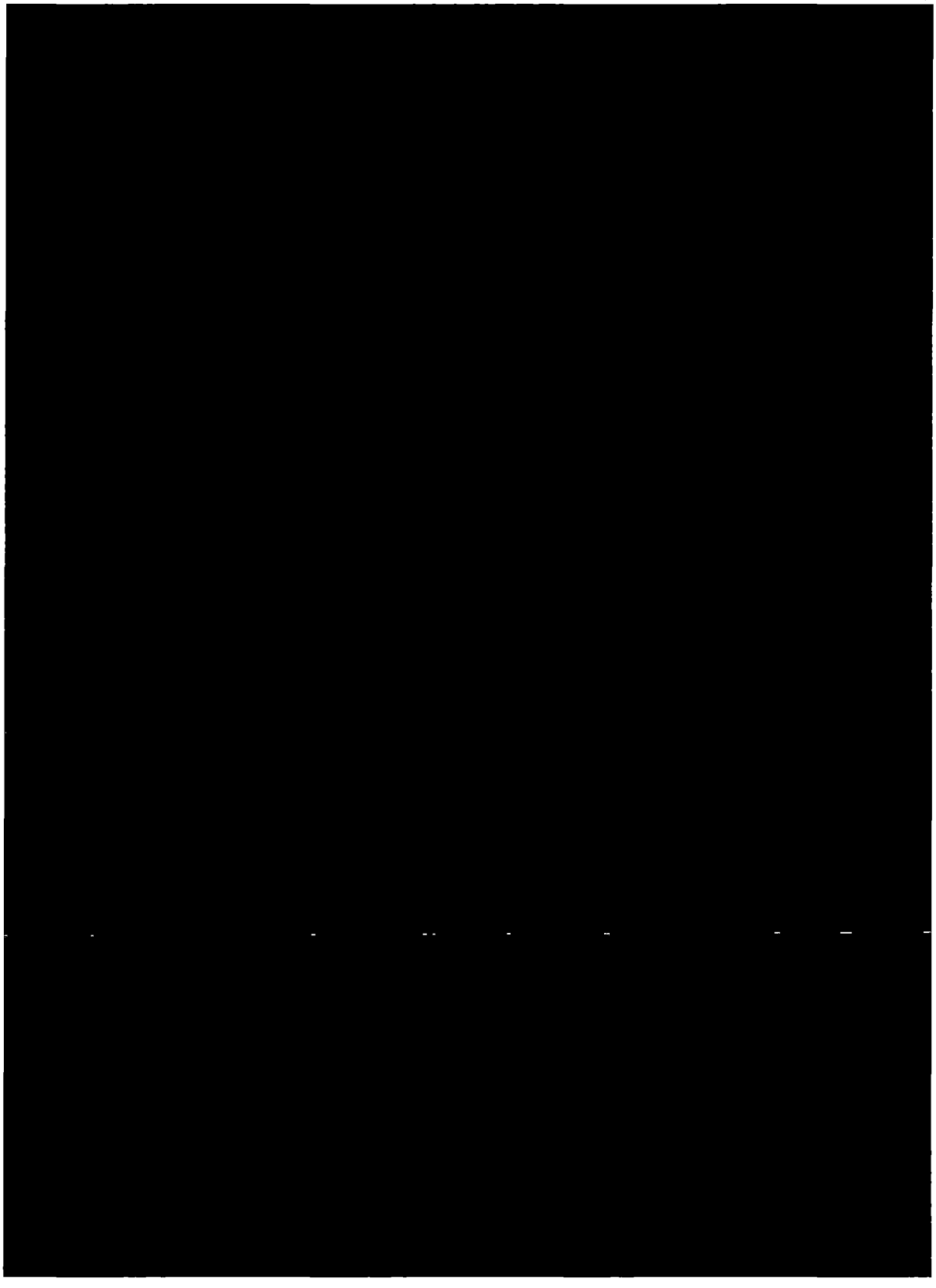

Figure 2.1-1 Verification concept for load-bearing components of the fuel basket (cont.)

Linear-Elastic Stress Analyses

Linear-elastic stress analyses are carried out assuming a linear dependency between stresses and strains using the nominal loads according to Appendix 2-2.

The verification is successful, if the linearized equivalent von-Mises stress σ_V is smaller than the allowable stress σ_{all}.

The allowable stresses σ_{all} according to KTA 3201.2 [5] for metallic materials are shown in Table 2.1-10.

Table 2.1-10 Allowable stresses used for linear-elastic stress analyses

Stress category		*Allowable stresses σ_{all} for*	
		NCT	*HAC*
Primary stresses	P_m	S_m	$0.7\ R_{mT}$
	P_l	$1.5\ S_m$	R_{mT}
	$P_m + P_b$ or $P_l + P_b$	$1.5\ S_m$	R_{mT}
Primary plus secondary stresses	P_e	$3\ S_m$	-
	$P_m + P_b + P_e + Q$ or $P_l + P_b + P_e + Q$		

P_m	general primary membrane stress due to mechanical loads
P_l	local primary membrane stress due to mechanical loads
P_b	bending stress due to mechanical loads
P_e	membrane stress due to constrained thermal expansion
Q	bending stress due to constrained thermal expansion
R_{mT}	tensile strength at design temperature
$R_{p0.2T}$	yield strength at design temperature
S_m	stress reference value according to Table 2.1-13

The higher limit defined for the allowable stresses when considering the additional effect of secondary stresses is explained by the essential characteristic of these stresses, that after exceeding the yield stress, local deformation differences equilibrate and cause plastic strains which are self-limiting.

If the allowable stresses are exceeded in a linear-elastic stress analysis, nonlinear structural analyses must be performed according to the corresponding paragraph on the verification of the load-bearing capacity below.

In case that after at least one of the further analyses the yield strength at design temperature $R_{p0.2T}$ is exceeded, a separate deformation analysis must be performed according to the corresponding paragraph on residual deformations below.

Verification of the Load-Bearing Capacity

Nonlinear structural analyses are performed based on the von Mises plastic distortion hypothesis. The verification of the load-bearing capacity and the calculation of the residual deformations and plastic strains are accomplished by separate analyses according to the corresponding paragraph on residual deformations below.

For the verification of the load-bearing capacity a safety factor on load side γ_F is considered according to KTA 3201.2 [5] as shown in Table 2.1-11.

Table 2.1-11 Safety factor on load side used in a nonlinear load-bearing capacity analysis

Condition of transport	*Safety factor γ_F*
NCT	1.50
HAC	1.10

For the load-bearing capacity analysis an ideally elastic-plastic material behaviour is assumed using the fictitious yield stress σ_F. For the load-bearing components of the fuel basket, the fictitious yield stress values for metallic materials which possess enough ductility over the whole range of operating temperatures according to KTA 3201.2 [5] are shown in Table 2.1-12.

Table 2.1-12 Fictitious yield stress of load-bearing components used in a nonlinear load-bearing capacity analysis

Condition of transport	*Fictitious yield stress σ_F*
NCT	1.5 S_m
HAC	min {2.30 S_m; 0.7 R_{mT}}
R_{mT} tensile strength at design temperature S_m stress reference value according to Table 2.1-13	

The stress reference value is calculated according to KTA 3201.2 [5] as shown in Table 2.1-13.

Table 2.1-13 Stress reference value S_m

Ferritic material	$S_m = \min\left\{\frac{R_{p0.2T}}{1.5}, \frac{R_{mT}}{2.7}, \frac{R_{mRT}}{3.0}\right\}$
Austenitic material	$S_m = \min\left\{\frac{R_{p0.2RT}}{1.5}, \frac{R_{p0.2T}}{1.1}, \frac{R_{mT}}{2.7}, \frac{R_{mRT}}{3.0}\right\}$
$R_{p0.2RT}$ yield strength at room temperature $R_{p0.2T}$ yield strength at design temperature R_{mT} tensile strength at design temperature R_{mRT} tensile strength at room temperature	

[redacted]

The verification is successful if a static equilibrium between external loads and internal forces is achieved, without a structural failure that can lead to the collapse of the frame structure of the fuel basket.

Additionally the limit load can be determined by increasing the mechanical load until a structural collapse occurs. In this way safety margins against structural failure can be identified.

Residual Deformations

The calculation of residual deformations is carried out in a deformation analysis using the nominal loads according to Appendix 2-2.

The analyses must be carried out using either an ideally elastic-plastic material behaviour with yield strength at design temperature $\sigma_y = R_{p0,2T}$ as yield stress or a multi-linear flow curve with the stress-strain relation shown in Table 2.1-14:

Table 2.1-14 Stress-strain relation of multi-linear flow curve for deformation analyses

[redacted]

The effects of residual deformations resulting from NCT on the behaviour under HAC must be taken into account.

The residual deformations from the cumulative loads must be determined for the decisive HAC drop orientations and documented for further safety verifications. Residual deformations which cause loads on the FA are not allowed.

Stability Analyses

Under HAC, stability analyses must be performed for all load-bearing components of the fuel basket. This can be done by applying analytical or numerical methods. The code applied as basis for analytical verification is Eurocode 3 [6] for steel and Eurocode 9 [7] for aluminium structures. For numerical analyses stress-free geometrical imperfections in the structure have to be taken into account for the subsequent nonlinear stability analysis (geometrical and material nonlinearity). The material behaviour is modelled as described in the corresponding paragraph in Section 2.1.2.3.3. The safety factor on load side γ_F is 1.1 (see Table 2.1-11).

2.1.2.3.4 Non-Load-Bearing Components

For the non-load-bearing components, those properties relevant for their usability, such as heat conduction, leak-tight containment, etc., must be maintained under the loads at the conditions of transport.

For components which are relevant for shielding the effects of residual deformations resulting from NCT on the behaviour under HAC must be taken into account in the calculations. The loads are applied according to Appendix 2-2 (Chapter 2). The material behaviour is adopted from the deformation analysis according to the corresponding paragraph on residual deformations in Section 2.1.2.3.3 above.

As all components of the fuel basket are classified as load-bearing components, these requirements do not apply in the framework of this report and are only mentioned in order to complete the description of the verification concept.

2.1.2.3.5 Consideration of the Temperature Influence

Within the superposition of mechanical and thermal loads in nonlinear stress-strain analyses according to 2.1.2.3.3, the temperature loads are applied in the first load step, whereas the mechanical loads are introduced in the next load steps.

2.1.3 Weights and Centres of Gravity

Weights are given in the corresponding table in Section 1.2, the centres of gravity can be taken from the respective drawings, cited in Section 1.3.

2.1.4 Identification of Codes and Standards for Package Design

The design, fabrication, assembly, inspection and examination of the CASTOR® geo69 package will be performed by the use of generally accepted standards which includes:

ASME BPVC Section II 2017 Edition,

ASME BPVC Section III, Division 1, Subsection NF 2017 Edition,

ASME BPVC Section III, Division 3 2017 Edition,

ASME BPVC Section V 2017 Edition,

ASME BPVC Section IX 2017 Edition,

DIN EN 1993-1-5, 2019/10 Eurocode 3: Design of steel structures Part 1-5: Plated structural elements,

DIN EN 1999-1-1, 2014/03 Eurocode 9: Design of aluminium structures Part 1-1: General structural rules,

Safety Standards of the Nuclear Safety Standards Commission (KTA) 3201.2 Components of the Reactor Coolant Pressure Boundary of Light Water Reactors Part 2: Design and Analysis 2017-11

and

American National Standards Institute – ANSI N14.6-1993
American National Standard for Radioactive Materials – Special Lifting Devices for Shipping Containers Weighing 10000 Pounds (4500 kg) or More

Special processes will be applied and documented by evaluated and approved procedures.

List of References

[1] ASME Boiler & Pressure Vessel Code, Sec. III, Div. 1
Subsection NF
2017 Edition

[2] NUREG / CR–6007
UCRL–ID–110637
Stress Analysis of Closure Bolts for Shipping Casks
April 1992

[3] 2017 ASME Boiler & Pressure Vessel Code
Section II – Materials
Part D – Properties (Metric)

[4] LS-DYNA®
Version: smp d R7.1.1, Revision 88541
Livermore Software Technology Corporation

[5] Safety Standards of the Nuclear Safety Standards Commission (KTA) 3201.2
Components of the Reactor Coolant Pressure Boundary of Light Water Reactors
Part 2: Design and Analysis
2017-11

[6] DIN EN 1993-1-5, 2019/10
Eurocode 3: Design of steel structures
Part 1-5: Plated structural elements

[7] DIN EN 1999-1-1, 2014/03
Eurocode 9: Design of aluminium structures
Part 1-1: General structural rules

2.2 Materials

	Name, Function	Date	Signature
Prepared	[redacted]		
Reviewed			

2.2.1 Material Properties and Specifications

This chapter documents the material data to be used for the evaluations of the CASTOR® geo69 transport cask. The report considers the specific materials of parts for the design parts lists of the cask, canister, basket, shielding elements and impact limiters of the CASTOR® geo69 transport cask.

If not stated otherwise, the applicable material properties according to the respective requirements of ASME PBVC, Section II and Division 3 are taken into account. For applied materials other than specified as described above, the properties are considered as given below. Subsection 2.2.1.15 tabulates the emission coefficients of all used materials

In the range of validity of the properties (e.g. temperature), the data can be interpolated linearly.

2.2.1.1 Aluminum EN AW-5051

Table 2-1 Physical Properties acc. to [1]

Tempe-rature	*Yield Strength*	*Tensile Strength*	*Elongation*	*Thermal Expansion*	*Heat Conductivity*	*Specific Heat Capacity*
T [°C]	$R_{p0.2}$ [MPa]	R_m [MPa]	[%]	α [10^{-6}/°C]	λ [W/(m K)]	C_p [J/(kg K)]
20	60	150	16	-	138	900
100	-	-	-	23.8	147	960
150	-	-	-	-	151	-
200	-	-	-	24.8	155	990

Temperature Limit: T_{Limit} [°C] = 121

Poisson's Ratio ν [-] = 0.33

Density ρ [kg/ dm³] = 2.68

Chemical composition according to [1] as given in Table 2-6

2.2.1.2 Aluminum EN AW-5083, condition H111

Table 2-2 Physical Properties acc. to [2]

Tempe-rature	*Yield Strength*	*Tensile Strength*	*Elongation*	*Thermal Expansion*	*Heat Conductivity*	*Specific Heat Capacity*
T [°C]	$R_{p0.2}$ [MPa]	R_m [MPa]	[%]	α [10^{-6}/°C]	λ [W/(m K)]	C_p [J/(kg K)]
20	115	270	15	-	116.1	900
50	-	-	-	-	120.6	913
75	-	-	-	-	123.8	924
100	-	-	-	24.2	126.7	935
125	-	-	-	-	129.5	946
150	-	-	-	-	132.1	957
175	-	-	-	-	134.5	966
200	-	-	-	25.0	136.7	973

Temperature Limit: T_{Limit} [°C] = 66

Poisson's Ratio ν [-] = 0.33

Density ρ [kg/ dm³] = 2.66

Chemical composition according to [2] as given in Table 2-6

2.2.1.3 Aluminum EN AW-5383, condition O/H111

Table 2-3 Physical Properties acc. to [3]

Tempe-rature	*Yield Strength*	*Tensile Strength*	*Elongation*	*Modul of Elasticity*	*Thermal Expansion*	*Heat Conductivity*	*Specific Heat Capacity*
T [°C]	$R_{p0.2}$ [MPa]	R_m [MPa]	[%]	E [10^3 MPa]	α [10^{-6}/°C]	λ [W/(m K)]	C_p [J/(kg K)]
20	125	270	12	66.0	-	116.1	900
50	-	-	-	-	-	120.6	913
75	-	-	-	-	-	123.8	924
100	-	-	-	-	24.2	126.7	935
125	-	-	-	-	-	129.5	946
150	-	-	-	-	-	132.1	957
175	-	-	-	-	-	134.5	966
200	-	-	-	-	25.0	136.7	973

Temperature Limit: T_{Limit} [°C] = 66

Poisson's Ratio ν [-] = 0.33

Density ρ [kg/ dm³] = 2.66

Chemical composition according to [2] as given in Table 2-6

2.2.1.4 Aluminum EN AW-5454, condition O

Table 2-4 Physical Properties acc. to [3]

Temperature	*Yield Strength*	*Tensile Strength*	*Elongation*	*Thermal Expansion*	*Heat Conductivity*	*Specific Heat Capacity*
T [°C]	$R_{p0.2}$ [MPa]	R_m [MPa]	[%]	α [10^{-6}/°C]	λ [W/(m K)]	C_p [J/(kg K)]
20	85	215 - 275	16	23.6	134.0	898
50					137.6	909
75					140.8	923
100					143.6	934
125					145.9	942
150					148.0	951
175					150.0	961
200					151.9	972

Temperature Limit: T_{Limit} [°C] = 121

Poisson's Ratio ν [-] = 0.33

Density ρ [kg/ dm³] = 2.69

Chemical composition according to [3] as given in Table 2-6

2.2.1.5 Aluminum EN AW-7075, condition T651

Table 2-5 Physical Properties acc. to [3]

Temperature	*Yield Strength*	*Tensile Strength*	*Elongation*	*Thermal Expansion*	*Heat Conductivity*	*Specific Heat Capacity*
T [°C]	$R_{p0.2}$ [MPa]	R_m [MPa]	[%]	α [10^{-6}/°C]	λ [W/(m K)]	C_p [J/(kg K)]
20	360	460	3	23.1	130	796
50	-	-	-	-	134	879
100	-	-	-	-	142	921
200	-	-	-	-	176	1005
400	-	-	-	-	176	1005

Temperature Limit: T_{Limit} [°C] = 66

Poisson's Ratio ν [-] = 0.33

Density ρ [kg/ dm³] = 2.80

Chemical composition according to [3] as given in Table 2-6

Table 2-6 Chemical composition for Aluminium alloys in wt-%

Alloy	*Si*	*Fe*	*Cu*	*Mn*	*Mg*	*Cr*	*Zn*	*Ti*	*Add.*	*Bal.*
EN AW-5051	0.30 max	0.45 max	0.05 max	0.10 ~ 0.25	1.60 ~ 2.10	0.30 max	0.20 max	0.10 max	≤ 0.15	Al
EN AW-5083	0.40 max	0.40 max	0.10 max	0.40 ~ 1.00	4.00 ~ 4.90	0.05 ~ 0.25	0.25 max	0.15 max	≤ 0.15	Al
EN AW-5383	0.25 max	0.25 max	0.20 max	0.70 ~ 1.00	4.00 ~ 5.20	0.25 max	0.40 max	0.03 max	≤ 0.15	Al
EN AW-5454	0.25 max	0.40 max	0.10 max	0.50 ~ 1.00	2.40 ~ 3.00	0.05 ~ 0.20	0.25 max	0.20 max	-	Al
EN AW-7075	0.35 max	0.40 max	0.20 max	0.05 ~ 0.50	1.00 ~ 1.40	0.10 ~ 0.35	4.00 ~ 5.00	0.08 ~ 0.25 *	≤ 0.15	Al

* Combined content of Zr + Ti

2.2.1.6 Ultra High Molecular Weight Low Pressure Polyethylene GUR 4120, tempered

Table 2-7 Physical Properties acc. to Section 2.12, Appendix 2-7

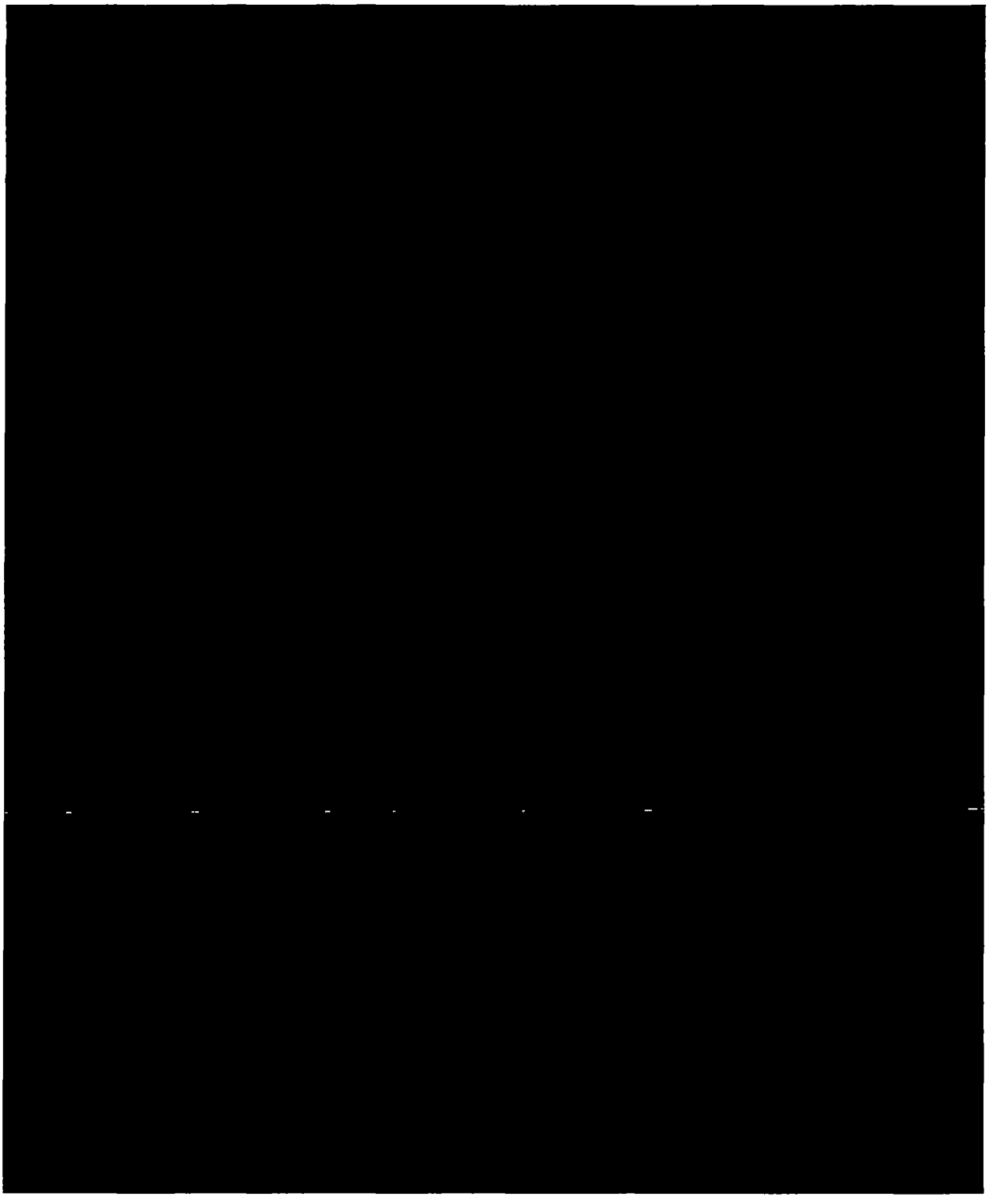

2.2.1.7 Stainless Spring Steel 1.4310

Table 2-8 Physical Properties acc. to [4]

Tempera-ture	*Tensile Strength*	*Thermal Conductivity*	*Thermal Expansion*	*Modulus of Elasticity*	*Specific Heat*	*Density*
T [°C]	**R_m [MPa]**	**λ [W/(m*K)]**	**α [10^{-6}/°C]**	**E [10^3 MPa]**	**[J/(kg*K)]**	**ρ [kg/m^3]**
20	1300 - 1500	14.5	16.1	196	472	7920
100	-	16.0	16.7	-	501	-
200	-	17.6	17.2	-	525	-
300	-	19.1	17.7	-	532	-
400	-	20.4	18.1	-	555	-

Table 2-9 Chemical Composition acc. to [4]

Chemical composition [wt-%]		
	min	max
C	0.05	0.15
Si	-	2.00
Mn	-	2.00
P	-	0.045
S	-	0.015
Cr	16.0	19.0
Ni	6.00	9.50
N	-	0.11
Mo	-	0.80

2.2.1.8 Construction Steel 1.8983

Table 2-10 Physical Properties acc. to [5]

Tempe-rature	*Yield Strength*	*Tensile Strength*	*Elongation*	*Modul of Elasticity*	*Thermal Conductivity*	*Thermal Expansion*	*Specific Heat*
T [°C]	$R_{p0.2}$ [MPa]	R_m [MPa]	A [%]	E [10^3 MPa]	λ [W/(m*K)]	α [10^{-6}/°C]	[J/(kg*K)]
20	890	940	11	212	41.5	-	461
100	828	874	-	207	42.5	12.1	496
200	748	790	-	199	42.5	12.7	533
300	-	-	-	-	41.2	13.2	568
400	-	-	-	-	39.3	13.6	611

Density ρ [kg/ dm³] = 7.84

Poisson's Ratio ν [-] = 0.30

Table 2-11 Chemical Composition acc. to [5]

Chemical composition [wt-%]		
	min	max
C	-	0.20
Si	-	0.80
Mn	-	1.70
P	-	0.020
S	-	0.010
Cr	-	1.50
Ni	-	4.00
N	-	0.015
Mo	-	0.70
Cu	-	0.50
Nb	-	0.06
Ti	-	0.05
V	-	0.12

2.2.1.9 Aluminum-Boron Metal Matrix Composite Al-B4C-MMC

Table 2-12 Physical Properties acc. to Section 2.12, Appendix 2-8

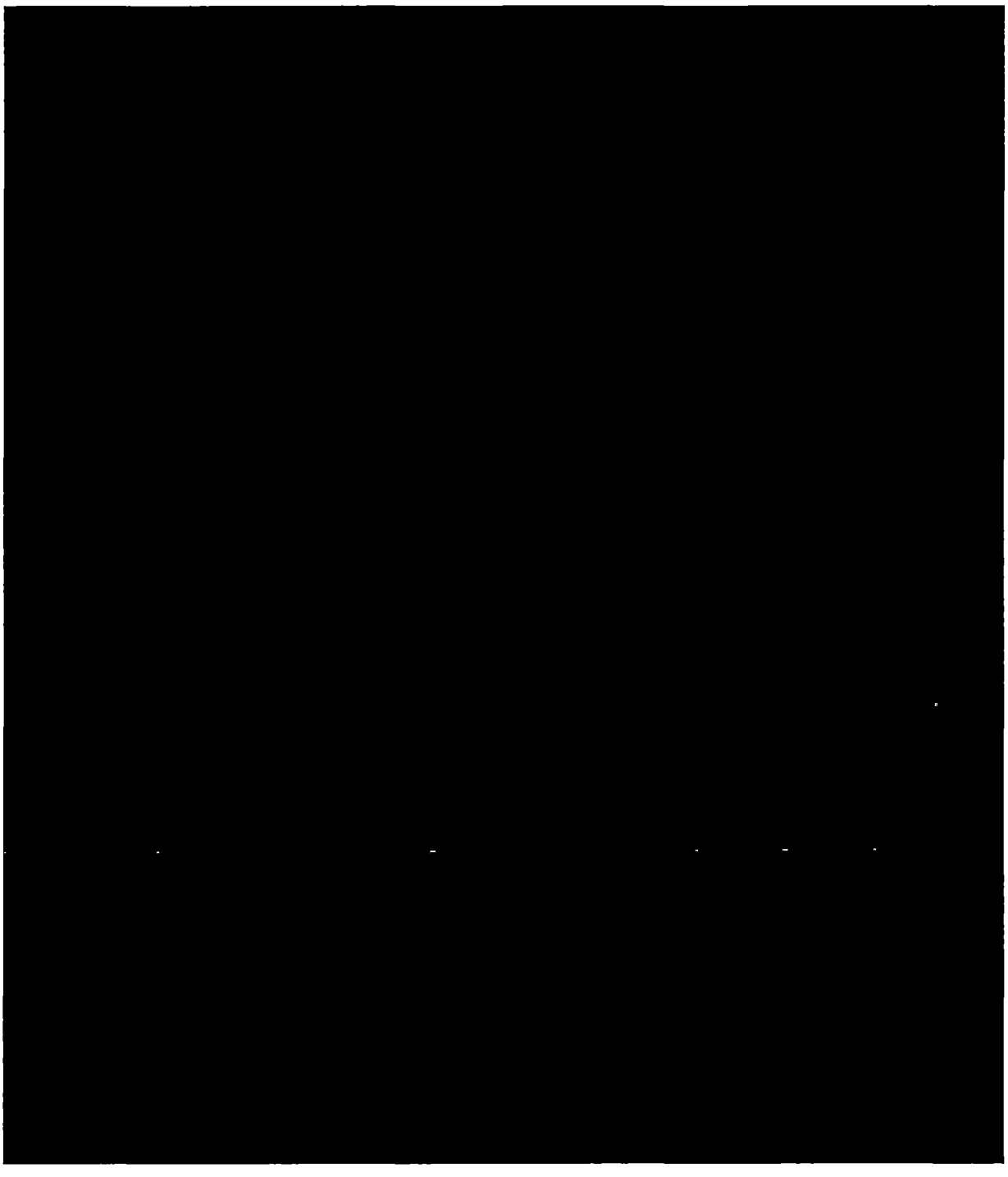

Table 2-13 Chemical Composition acc. to Section 2.12, Appendix 2-8

2.2.1.10 Polyurethane Hard Foam [redacted]

Table 2-14 Physical Properties acc. to Section 2.12, Appendix 2-10

Temperature	*Compressive Strength*		*Density*		
T [°C]	**σ_s [MPa]**		**ρ [kg/m³]**		
	min	**max**	**min**	**max**	**nominal**
20	[redacted]				

Coefficient of Linear Thermal expansion α [10^{-6}/K] = [redacted]

Thermal Conductivity λ [W/(m*K)] = [redacted]

Specific Heat Capacity C_p [J/(kg*K)] = [redacted]

Table 2-15 Chemical Composition acc. to Section 2.12, Appendix 2-10

Chemical composition [wt-%]	
C	[redacted]
H	[redacted]
N	[redacted]
O	[redacted]
P	[redacted]
Si	[redacted]

2.2.1.11 Polyurethane Hard Foam [redacted]

Table 2-16 Physical Properties acc. to Section 2.12, Appendix 2-10

Temperature	*Compressive Strength*		*Density*		
T [°C]	**σ_s [MPa]**		**ρ [kg/m³]**		
	min	**max**	**min**	**max**	**nominal**
20	[redacted]				

Coefficient of Linear Thermal expansion α [10^{-6}/K] = [redacted]

Thermal Conductivity λ [W/(m*K)] = [redacted]

Specific Heat Capacity C_p [J/(kg*K)] = [redacted]

Table 2-17 Chemical Composition acc. to Section 2.12, Appendix 2-10

Chemical composition [wt-%]	
C	[redacted]
H	[redacted]
N	[redacted]
O	[redacted]
P	[redacted]
Si	[redacted]

2.2.1.12 Polyurethane Hard Foam [redacted]

Table 2-18 Physical Properties acc. to Section 2.12, Appendix 2-10

Temperature	*Compressive Strength*		*Density*		
T [°C]	σ_s [MPa]		ρ [kg/m³]		
	min	max	min	max	nominal
20	[redacted]				

Coefficient of Linear Thermal expansion α [10^{-6}/K] = [redacted]

Thermal Conductivity λ [W/(m*K)] = [redacted]

Specific Heat Capacity C_p [J/(kg*K)] = [redacted]

Table 2-19 Chemical Composition acc. to Section 2.12, Appendix 2-10

Chemical composition [wt-%]	
C	[redacted]
H	[redacted]
N	[redacted]
O	[redacted]
P	[redacted]
Si	[redacted]

2.2.1.13 Nickel alloy

Table 2-20 Physical Properties acc. to Section 2.12, Appendix 2-9

Tensile Strength (RT)	*Density [6]*
R_m [MPa]	**ρ [kg/m³]**
[redacted]	8.20

Table 2-21 Chemical Composition acc. to Section 2.12, Appendix 2-9

Chemical composition [wt-%]		
	min	max
Cr	18.0	21.0
Fe	-	2.00
Ti	2.00	3.00
Mn	-	1.00
Si	-	1.00
C	-	0.13
Al	1.00	2.00
Co	15.0	21.0
S	-	0.015
Cu	-	0.2
B	-	0.03
Pb	-	0.0025
Zr	-	0.15
Ni	bal.	

2.2.1.14 Silver

Table 2-22 Physical Properties acc. to Section 2.12, Appendix 2-9 [7]

Hardness
HV
50 ±10

Table 2-23 Chemical Composition acc. to [7]

	Chemical composition [wt-%]	*Density [kg/dm^3]*
		Nominal
Ag	99.99	10.49

2.2.1.15

2.2.1.15 Emission Coefficients

Table 2-24 Table of Emission Coefficients of the Materials Used in Transport Configuration

Material	*Standard*	*Type / Grade / Alloy (Denomination)*	*Emission Coefficient ε [-]*	*Reference*
Carbon Steel	SA-182M	F60	0.36	[8]
Stainless Steel	SA-182M	F304	0.36	[8]
Stainless Steel	SA-182M	F316	0.36	[8]
Stainless Steel	SA-182M	F316L	0.36	[8]
Stainless Steel	SA-182M	FXM-19	0.36	[8]
Stainless Steel	SA-182M	F6NM	0.36	[8]
Chromium Steel	SA-193M	B6	0.36	[8]
Chromium Steel	SA-193M	B7	0.36	[8]
Stainless Steel	SA-240M	(UNS S31803)	0.36	[8]
Stainless Steel	SA-240M	F304	0.36	[8]
Stainless Steel	SA-240M	F304L	0.36	[8]
Stainless Steel	SA-240M	F316	0.36	[8]
Stainless Steel	SA-240M	F316L	0.36	[8]
Stainless Steel	SA-240M	XM-19	0.36	[8]
Stainless Steel	SA-479M	304	0.36	[8]
Stainless Steel	SA-479M	316L	0.36	[8]
Stainless Steel	SA-479M	(UNS S41500)	0.36	[8]
Stainless Steel	SA-479M	XM-19	0.36	[8]
Low Alloy Carbon Steel	SA-540M	B22 Cl. 3	0.36	[8]
Carbon Steel	SA-675M	60	0.36	[8]
Cast Iron	SA-874M	(JIS G 5504)	Untreated 0.50 Coated 0.93	[8], [9]
Stainless Steel	SA-965M	304	0.36	[8]
Stainless Steel	SA-965M	316	0.36	[8]
Stainless Steel	SA-965M	316L	0.36	[8]
Stainless Steel	SA-965M	FXM-19	0.36	[8]
Stainless Steel	EN 10270-3	1.4310	0.40	[10]

Material	*Standard*	*Type / Grade / Alloy (Denomination)*	*Emission Coefficient ε [-]*	*Reference*
Construction Steel	EN 10137-2	1.8983	0.40	[10]
Aluminum	SB-209	5454	Anodized 0.10 Oxidized 0.55	[11]
Aluminum	EN 573-3	AW-5051	Anodized 0.10 Oxidized 0.55	[11]
Aluminum	EN 573-3	AW-5083	Anodized 0.10 Oxidized 0.55	[11]
Aluminum	EN 573-3	AW-5454	Anodized 0.10 Oxidized 0.55	[11]
Aluminum	EN 573-3	AW-7020	Anodized 0.10 Oxidized 0.55	[11]
Aluminum	EN 573-3	AW-7075	Anodized 0.10 Oxidized 0.55	[11]
UHMW LP-PE	-	GUR 4120	0.90	[12]
Alum.-Boron Metal Matrix Composite	-	Al-B4C-MMC	Polished 0.27 Anodized 0.90	Section 2.12, Appendix 2-8
Nickel	-	2.4969	Oxidized 0.40	[13]
Silver	-	-	0.02	[8]

2.2.2 Chemical, Galvanic, or other Reactions

The materials of the CASTOR® geo69 have been reviewed and as a result during loading and transport operations no safety related component is significantly influenced by chemical, galvanic or other reactions.

During the loading operations the parts of the basket and the canister are in contact with the pool water. These materials are stainless steels, aluminium alloys and the aluminium boron carbide metal-matrix-composite (MMC) and all are compatible with the pool water.
The interior of the CASTOR® geo69 is filled with helium after the loading operations. This provides a non-aqueous and inert environment during transportation. Corrosion reactions depend on the presence of water and/or oxygen. The inert helium gas atmosphere in the CASTOR® geo69 precludes corrosion during transport. Exterior surfaces and materials consists of stainless steels, aluminium alloys or coated materials. Therefore no chemical, galvanic or other reaction have to be assumed.

The materials of the CASTOR® geo69 are summarized in the attached table. Under the presence of water dissimilar materials can form a galvanic couple. During the loading the aluminium alloys and the aluminium boron carbide (MMC) form a galvanic couple with stainless steel. Both types of aluminium develop a native passive layer that precludes significant corrosion effects. To minimize other galvanic reactions the aluminium components, which are in contact with stainless steels, are additionally anodized. In consequence no galvanic reactions to the aluminium alloys or the stainless steels occur during the short loading time.

The cask is made of ductile cast iron and the exterior surfaces will be coated to preclude corrosion reactions at the surfaces. The cask cavity is filled with helium and no corrosion has to be assumed.

The lids of the cask are made of stainless steel and are in contact with the zinc-coated alloyed steel bolts. The bolts of the lid are not directly exposed to the ambient weather, because they are covered by the impact limiters. During the time of transport no significant corrosion effects are to be implied for the bolts.

During loading operations of the canister, before drying and refilling with helium, only minor amounts of hydrogen gas will be generated due the minimized galvanic reaction of the aluminium and stainless steel and due to radiolysis of the water. This hydrogen will be evacuated from the canister during the drying process and no concentration of hydrogen can occur.

Lubricants are used to coat the screw thread. Only permitted lubricants are used for the coating of the screw thread. Before assembly or loading all cask components will be inspected and freed from any form of contamination or marking. The lubricants have no significant effect on the cask materials.

In consequence there are no significant chemical, galvanic or other reaction that could reduce the integrity of the cask during the loading and transport operations.

Material / Component	*Loading Operations / Contact to Fuel Pool*	*Transport Environment*
High alloyed stainless Steels: [redacted] Basket Canister	Stainless steels in contact with both borated and unborated water do not exhibit chemical or galvanic reactions or interactions with spent fuel.	The environment for these components will be an inert helium atmosphere. No further chemical, galvanic or other reactions are assumed.
Aluminium boron carbide (MMC) Neutron Absorber Basket	The aluminium boron carbide (MMC) forms a galvanic couple with stainless steels. The aluminium will be anodized to minimise any form of galvanic or other corrosion reactions. Due to the short loading time, in which they are in contact with pool water, the neutron absorber material is not exposed to significant chemical, galvanic or other reactions.	The environment for these components will be an inert helium atmosphere. No further chemical, galvanic or other reactions are assumed.

Material / Component	*Loading Operations / Contact to Fuel Pool*	*Transport Environment*
Aluminium alloys Heatconducting or shielding elements	The aluminium alloy forms a galvanic couple with stainless steels. These aluminium components will be anodized to minimise any form of galvanic or other corrosion reactions. Due to the short loading time in which they are in contact with pool water, the material is not exposed to significant chemical, galvanic or other reactions.	The environment for these components will be an inert helium atmosphere. No further chemical, galvanic or other reactions are assumed.
Steels: SA-193M B7 SA-540M B22 Canister	These components are not in contact with the pool water.	The environment for these components will be an inert helium atmosphere. No further chemical, galvanic or other reactions are assumed.
Ductile cast iron Cask	This component is not in contact with the pool water.	The internal surfaces will be exposed to an inert helium atmosphere. Exposed external surfaces will be coated and will be maintained with a fully coated surface. No further chemical, galvanic or other reactions are assumed.
Polyethylene Neutron absorber Cask	This component is not in contact with the pool water.	The neutron absorber material has no contact to the outer environment. No chemical or galvanic reactions with ductile cast iron or other steels are assumed. Other reactions are insignificant.

Material / Component	*Loading Operations / Contact to Fuel Pool*	*Transport Environment*
High alloyed stainless steels:  Cask	This component is not in contact with the pool water.	Some parts are exposed to ambient weather. Stainless steels exhibit a native corrosion protection layer and no galvanic or other corrosion reactions have to be assumed. No chemical or other reactions are assumed.
Constructional Steel SA-675M 60 Cask	This component is not in contact with the pool water.	This material has no contact to the outer environment. No significant chemical or galvanic reactions with ductile cast iron or other steels are assumed. No other reactions are assumed.

Material / Component	*Loading Operations / Contact to Fuel Pool*	*Transport Environment*
Steels: SA-193M B7 SA-540M B22 Cask	This component is not in contact with the pool water.	Components are exposed to atmosphere. These components are coated with a zinc layer. During the transport time, no loss of function has to be assumed. Components will be inspected prior to transport.
Metallic gasket Silver, stainless steel and nickel based alloy	All materials of the gasket exhibit a native corrosion protection layer and no galvanic or other corrosion reactions have to be assumed. No chemical or other reactions are assumed.	All materials of the gasket exhibit a native corrosion protection layer and no galvanic or other corrosion reactions have to be assumed. No chemical or other reactions are assumed.
Aluminium alloys Impact limiter	This component is not in contact with the pool water.	Components are exposed to ambient weather. Aluminium alloys exhibit a native corrosion protection layer and no significant galvanic or other corrosion reactions have to be assumed. No chemical or other reactions are assumed.
PU-Foam Impact limiter	This component is not in contact with the pool water.	The foam is fully enclosed in the impact limiter. No chemical, galvanic or other reactions are assumed.
Constructional Steel EN 10025-6 1.8983 Impact limiter	This component is not in contact with the pool water.	Components are exposed to atmosphere. Chemical and galvanic reactions are thus only of minor influence. No other reactions are assumed.

Material / Component	*Loading Operations / Contact to Fuel Pool*	*Transport Environment*
High alloyed stainless Steels: [redacted] Impact limiter	This component is not in contact with the pool water.	Some components may be exposed to ambient weather. Stainless steels exhibit a native corrosion protection layer and no galvanic or other corrosion reactions have to be assumed. No chemical or other reactions are assumed.
Organic Coating Cask Impact limiter	The coating is not in contact with the pool water.	The coating on external surfaces is exposed to ambient weather but exhibits a good long-term durability. Discoloration is not a concern. No further chemical, galvanic or other reactions are assumed.

2.2.3 Effects of Radiation on Materials

Metals are not impaired by gamma radiation. Significant radiation damages due to neutron exposure is not expected for metals at neutron fluences below 10^{18} n/cm^2. The expected neutron fluences of the components of CASTOR® geo69 will be significantly lower [redacted]

Elastomeric seals are exposed to gamma radiation and thus may undergo degradation. The elastomeric seals do not have safety related functions and the degradation products have a similar composition as the original molecule but different crosslinking or chain length. Thus no harmful degradation products are expected.

The neutron shielding material polyethylene may be affected by irradiation analogously to elastomeric materials. The irradiation of the neutron shielding amounts [redacted] The impairment through irradiation is insignificant and a loss of the neutron shielding ability does not have to be expected.

There is no significant extend of degradation of any important safety related component caused directly by the effect of the reactions. Same applies for the effects of the reactions combined with the effects of exposure of the materials to neutron or gamma radiation.

List of References

[1] EN 573-3, 2019-08, Aluminium and aluminium alloys - Chemical composition and form of wrought products - Part 3: Chemical composition and form of products
Material data base WIAM-Metallinfo 2002/2.2
EN 755-2, 2016-03, Aluminium and aluminium alloys – Extruded rod/bar, tube and profiles – Part 2: Mechanical properties
ASME Boiler and Pressure Vessel Code Section II Part D, Properties (metric), Edition 2017
Dubbel, Taschenbuch für den Maschinenbau, Seite E 102, 20. Auflage, 2001
Aluminium-Taschenbuch 1995

[2] EN 573-3, 2019-08, Aluminium and aluminium alloys - Chemical composition and form of wrought products - Part 3: Chemical composition and form of products
Material data base WIAM-Metallinfo 2002/2.2
EN 755-2, 2016-03, Aluminium and aluminium alloys – Extruded rod/bar, tube and profiles – Part 2: Mechanical properties
ASME Boiler and Pressure Vessel Code Section II Part D, Properties (metric), Edition 2017
Dubbel, Taschenbuch für den Maschinenbau, Seite E 102, 20. Auflage, 2001
Aluminium-Taschenbuch 1995

[3] EN 573-3, 2019-08, Aluminium and aluminium alloys - Chemical composition and form of wrought products - Part 3: Chemical composition and form of products
EN 485-2, 2018-10, Aluminium and aluminium alloys - Sheet, strip and plate - Part 2: Mechanical properties
ASME Boiler and Pressure Vessel Code Section II Part D, Properties (metric), Edition 2017
Aluminium-Taschenbuch, Band 1, Aluminium-Verlag Düsseldorf, 1995
Aluminium Werkstoffdatenblätter, Aluminium-Verlag Düsseldorf, 1998

[4] Stahl-Eisen-Werkstoffblatt SEW 310, 08.1992
EN 10270-3, 2011-10, Steel wire for mechanical springs - Part 3: Stainless spring steel wire

[5] EN 10137-2, 1995-09, Plates and wide flats made of high yield strength structural steels in the quenched and tempered or precipitation hardened conditions - Part 2: Delivery conditions for quenched and tempered steels
Stahl-Eisen-Werkstoffblatt SEW 310, 08.1992
Dubbel, Taschenbuch für den Maschinenbau, Seite E 102, 20. Auflage, 2001

[6] Datenblatt Nimonic 2.4969 Fa. Metalcor Essen

[7] Physical Properties Silver, G. L. Trigg, E. H. Immergut, Encyclopedia of Applied Physics, Wiley 1992
Kern D.Q. „Process Heat Transfer" McGraw Hill Kogakusha (1950)

[8] Kern, D. Q.: "Process Heat Transfer", McGraw-Hill, Kogakusha/Japan (1965)

[9] VDI Wärmeatlas, Ke4 „Strahlung technischer Oberflächen, VDI-Verlag Düsseldorf/Germany, 2002

[10] Gosse, J.: "Thermodynamik-Kompendium, VDI-Verlag Düsseldorf/Germany, 1986

[11] "Emissionsgradtabelle", VEB Meßgerätewerk "Erich Weinert" Kombinat Elektro-Apparate-Werke "Friedrich Ebert", Berlin/Germany

[12] White, F. M.: "Heat and Mass Transfer", Addison Wesley, 1991

[13] "Emissionsgradtabelle" Company Fa. Kleiber infrared

2.12 Appendix

	Name, Function	Date	Signature
Prepared	[redacted]		
Reviewed			
Reviewed			

Appendix 2-1 GNS Proprietary Report
1014-TR-00024 Rev. 0 Structural Evaluation Containment Transport Package CASTOR® geo69

Appendix 2-2 GNS Proprietary Report
1014-TR-00028 Rev. 1 Structural Evaluation Basket and Shielding Elements Transport Package CASTOR® geo69

Appendix 2-3 GNS Proprietary Report
1014-TR-00026 Rev. 0 Structural Evaluation Load Attachment Points Transport Package CASTOR® geo69

Appendix 2-4 GNS Proprietary Report
1014-TR-00029 Rev. 0 Structural Evaluation Impact Limiters Transport Package CASTOR® geo69

Appendix 2-5 GNS Proprietary Report
1014-TR-00071 Rev. 0 Overview of Documents Related to Methodology, Verification and Validation CASTOR® geo69

Appendix 2-6 GNS Proprietary Report
1014-TR-00009 Rev. 1 Material Data Transport Package CASTOR® geo69

Appendix 2-7 GNS Proprietary Report
1014-TR-00012 Rev. 1 Material Qualification [redacted]

Appendix 2-8 GNS Proprietary Report
1014-TR-00011 Rev. 1 Material Qualification [redacted]

Appendix 2-9 GNS Proprietary Report
1014-TR-00017 Rev. 1 Material Qualification Metal Gaskets

Appendix 2-10 GNS Proprietary Report
1014-TR-00014 Rev. 0 Material Qualification Polyurethane Foam

3.1 Description of Thermal Design

	Name, Function	Date	Signature
Prepared	[redacted]		
Reviewed			

3.1.1 Design Features

A detailed description of the CASTOR® geo69 can be found in section 1.2.1. The packaging consists of a thick-walled cask body made of ductile cask iron (DCI) and an inner canister made of stainless steel. The canister accommodates up to 69 spent fuel assemblies (FA) from boiling water reactors (BWR). Their maximum decay heat amounts to 18.5 kW, while different homogeneous and heterogeneous loading patterns are possible. A description of the different loading patterns can be found in section 3.1.2.

The safe enclosure of the content is ensured by two independent barriers, the canister with reopenable lid and the cask with bolted lid. Both are sealed by metal gaskets. The temperature of the gaskets is examined in the thermal evaluation for NCT and HAC to ensure the long-term tightening function.

The FA are kept in position by the basket sheets and the outer sheets which ensure besides criticality safety a sufficient heat removal from the FA. The basket sheets are made of boronized aluminium, the outer sheets are made of steel. Additional components inside the canister are the round segments and the shielding elements, which are both made of aluminium.

During transportation, the package is positioned horizontally. It is equipped with one lid- and one bottom-side impact limiter. In section 3.3.2.3 it is shown that no personnel barrier is needed to meet the requirements of § 71.43 (g), in which the maximum temperature of the accessible surface under exclusive use is limited to 85 °C.

The heat removal within the package is achieved by conduction, convection and radiation. Conduction takes place mainly inside walls of the cask and the canister and within the basket sheets. Radiation takes place between all surfaces that border a gaseous atmosphere. Heat removal from the package to the environment takes place by convection and radiation without using active cooling mechanisms or other coolants. In order to improve the heat dissipation on the outside, the cask is equipped with radial fins. Due to the high thermal resistance of the impact limiters and the gaps in the lid system, the majority of the thermal energy is dissipated by the fin zone.

To enhance heat removal from the FA, the space between cask and canister and the inner space of the canister are backfilled with the filling gas helium, which has a high thermal conductivity. Additionally, the temperature gradients that occur radially cause a convective flow, which further enhances the heat removal.

The disclosure of the maximum normal operating pressure (MNOP) can be found in chapter 4.

Inside the cask wall, [redacted] moderator rods are placed for radial neutron shielding. Furthermore, moderator plates are placed in the cask bottom and in the lid area for axial neutron shielding. All moderator components are made of [redacted]

The containment relevant components of the package are designed in accordance with the 2017 edition of the ASME Boiler and Pressure Vessel Code (BPVC), Section III, Division 3 [1].

3.1.2 Content's Decay Heat

The cask can be loaded with 69 FA of six different types from BWR according to section 1.2.2. Their summarized maximum decay heat is limited to 18.5 kW. There are three bounding loading patterns, all fitting into a certain scheme of six position groups of FA. These loading patterns are identified by their decay heat per FA and therefore are called thermal requirements. The three thermal requirements are shown in Figure 3.1-1. [redacted] For the thermal evaluation of NCT, all thermal requirements are examined. Based on NCT, the most unfavorable thermal requirement is identified for the evaluation of HAC.

The active length of the FA and the axial heat power distribution depend on the type of the FA, the burnup profile additionally depends on the irradiation time and the decay time. All allowed types of FA are listed in Table 3.1-1. For the modelling of the FA, the most unfavourable conditions are considered, see section 3.3.1 for details.

Figure 3.1-1 Thermal Requirements (TR1-3) with maximum decay heat per FA position in W, top view

Table 3.1-1 Considered types of FA

3.1.3 Summary Tables of Temperatures

The component temperatures of the package are summarized in Table 3.3-5 for NCT and a conservative high ambient temperature (hot case) and discussed in section 3.3.2.1. The influence of the radial displacement of the components inside the cask on the maximum temperatures is summarized in Table 3.3-7. For NCT and a conservative low ambient temperature (cold case), the component temperatures are assumed to be uniformly at -40 °C, as discussed in section 3.3.2.2. The temperature of the accessible surface of the package is given in Table 3.3-6 and discussed in section 3.3.2.3.

The maximum temperatures for HAC and the time of occurrence are given in Table 3.4-2 and discussed in section 3.4.

The applicable temperature limits of the materials and components are given in Table 3.2-9.

3.1.4 Summary Tables of Maximum Pressures

The calculation of the maximum pressures for NCT and HAC and a discussion on flammable gases can be found in chapter 4.

List of References

[1] 2017 ASME Boiler and Pressure Vessel Code, An International Code
Section III Rules for Construction of Nuclear Facility Components
Division 3 Containment Systems for Transportation and Storage of Spent Nuclear Fuel and High-Level Radioactive Material

3.2 Material Properties and Component Specifications

	Name, Function	Date	Signature
Prepared	[redacted]		
Reviewed			

3.2.1 Material Properties

The relevant material data of the components of the package on which the thermal calculations are based, include

- the thermal conductivity k [W / (m · K)],
- the density ρ [kg / m^3],
- the specific heat capacity c, [J / (kg · K)],
- the emissivity ε [-].

Materials used for the package are ductile cast iron for the cask body and stainless steel for the canister, the bottom closure plate, the retention ring and the lids. The moderator material, which is used in the moderator rods and the moderator plates is made of [redacted] The relevant material data of the cask, the canister and the moderator components can be found in Table 3.2-1.

Table 3.2-1 Material data of cask and canister components

Component, material	Reference	Temperature, °C	Heat conductivity, W/(m · K)	Density, kg/m³	Spec. heat capacity, J/(kg · K)
Cask body Ductile cast iron SA-874M	section 2.2.1	20 50 100 150 200 250 300 325	37.5 38.5 39.73 40.45 40.73 40.64 40.23 39.93	7200	455 461 479 495 508 521 535 542
Canister body [redacted]	section 2.2.1	20 100 150 200 250 300 350 400	[redacted]	[redacted]	[redacted]
Canister lid [redacted]	section 2.2.1	[redacted]	[redacted]	[redacted]	[redacted]
Cask lid **Retention ring** [redacted]		See SA-240M 316L			
Closure plate SA-240M 22Cr-5Ni-3Mo-N		See SA-240M 316L			
Moderator rods **Moderator plates (bottom / lid)** (GUR 4120 tempered)	section 2.2.1	[redacted]	[redacted]	[redacted]	[redacted]

The basket sheets are made of boronized aluminium, the round segments and the shielding elements are made of aluminium. The outer sheets are made of steel. The relevant material data of the basket material, the outer sheets and the round segments can be found in Table 3.2-2.

Table 3.2-2 Material data of the basket

Component, material	Reference	Temperature, °C	Heat conductivity, W/(m · K)	Density, kg/m³	Spec. heat capacity, J/(kg · K)
Round segments **Shielding elements** SB-209 Alloy 5454	section 2.2.1	20 50 75 100 125 150 175 200	134.0 137.6 140.8 143.6 145.9 148.0 150.0 151.9	2690	898 909 923 934 942 951 961 972
Basket sheets Al-B4C-MMC	section 2.2.1	[redacted]	[redacted]	[redacted]	[redacted]
Outer sheets SA-240M 316	section 2.2.1	See SA-240M 316L			

The impact limiters use polyurethane foams of various densities as crush material. The sheets of the casing, the spacers and the load distribution plate are made of aluminium. The penetration protection plate is made of steel. The relevant material data of the impact limiters can be found in Table 3.2-3.

Table 3.2-3 Material data of the impact limiters

Component, material	Reference	Temperature, °C	Heat conductivity, W/(m · K)	Density, kg/m³	Spec. heat capacity, J/(kg · K)
Plates **Spacers**[1] EN AW-5083 H111	section 2.2.1				
Load distribution plate EN AW 7075-T651	section 2.2.1				
Penetration protection plate 1.8983	section 2.2.1				
Crush material (PU-Foam FR3720) PUR320	section 2.2.1				
Crush material (PU-Foam FR3740) PUR641	section 2.2.1				

[1] In the calculations, the material data of EN AW-7020 is used for the spacers leading to a by about 10 % higher heat conductivity. An additional calculation with the EN AW-5083 H111 material data shows that the influence on the temperatures is minor (less than 0.2 K difference in the lid and bottom region).

The fuel assemblies contain a various number of fuel rods filled with fuel pellets made of uranium oxide. The structural components such as cladding, water rods, spacers and fuel channels are made of zircaloy. The space between the fuel rods is filled with helium. Within the numerical model of the package, the FA are not modelled in detail, but they are replaced by homogenized zones. The material data of these zones are calculated separately, which is described in section 3.3.1. The material data of FA-components are listed in Table 3.2-4, the calculated material data, which are applied in the homogenized zones, can be found in Table 3.2-5.

Table 3.2-4 Material data of the fuel assemblies

Component, material	Reference	Temperature, °C	Thermal conductivity, W/(m · K)	Density, kg/m³	Spec. heat capacity, J/(kg · K)
Fuel pellets (UO_2)	[1]	20 - 400	5 / 2.5 (radial / axial)	10600	303
Cladding tubes **Water rods** **Fuel channel** (Zircaloy)	[2]	20	13.6	6550	296
		100	14.3		310
		200	15.2		323
		300	16.4		334
		400	18.0		344

Table 3.2-5 Calculated material data of the homogenized FA-zones applied in the 3D-FE model

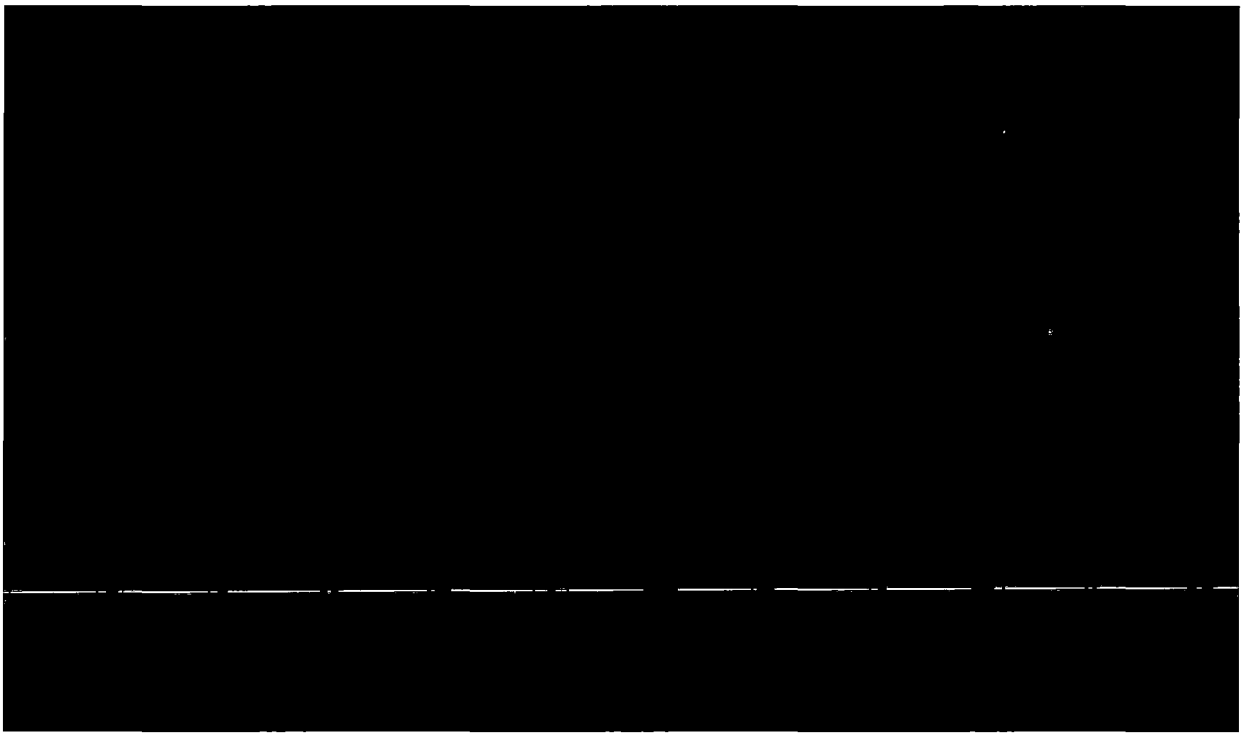

The coefficients of thermal expansion in Table 3.2-6 are used to evaluate the radial and axial gaps between the components. The emissivities of the relevant components can be found in Table 3.2-7.

The internal space of the canister and the space between cask and canister are backfilled with helium. The gaps between cask and impact limiters as well as the gap around the bottom moderator plate are filled with dry air. The material data of the gases can be found in Table 3.2-8.

Conservatively, the solar absorption coefficients of all outer surfaces are assumed to be 1.

Material properties of ASME-material are taken from 2.2.1 in accordance with the ASME Boiler and Pressure Vessel Code, Part II Section D (Metric). Other material properties base on manufacturers specifications and individual material qualification. The material properties of the gases and the emission coefficients are taken from reliable literature sources.

Table 3.2-6 Coefficient of thermal expansion of the relevant components

Table 3.2-7 Applied emissivity of the relevant components

Component	Reference	Emissivity
Cask body, outer surface (painted)	section 2.2.1	0.93
Cask body, inner cavity (Thermaline®)	section 2.2.1	0.6
Cask body (untreated)	section 2.2.1	0.5
Canister (stainless steel)	section 2.2.1	0.36
Cask lid (stainless steel)	section 2.2.1	0.36
Canister lid (stainless steel)	section 2.2.1	0.36
Closure plate (stainless steel)	section 2.2.1	0.36
Retention ring (stainless steel)	section 2.2.1	0.36
Moderator rods and discs (polyethylene)	section 2.2.1	0.9
Impact limiter sheets (aluminium, untreated)	section 2.2.1	0.1
Load distribution plate (aluminium, untreated)	section 2.2.1	0.1
Cladding and water rods (zircaloy, untreated)	[2]	0.8
Basket sheets (aluminium, anodized)	section 2.2.1	0.55
Outer sheets (stainless steel)	section 2.2.1	0.36
Fuel channels (Zircaloy, untreated)	[2]	0.8
Round segments (aluminium, anodized)	section 2.2.1	0.55
Shielding elements (aluminium, anodized)	section 2.2.1	0.55
Ambience	chosen	1
Emissivity of the fire	§ 71.73 c)	0.9
Cask surface (During fire and cooling phase)	§ 71.73 c)	0.8

Table 3.2-8 Material data of the gases

Fluid	Literature	Temperature, °C	Heat conductivity, W/(m · K)	Density kg/m³	Spec. heat capacity, J/(kg · K)
Air (dry)	[3]	20 100 200 300 400 500	0.0257 0.0314 0.0380 0.0441 0.0500 0.0556	1.188	720 (ρ = const.)
Helium	[3]	25 100 200 300 400	0.1536 0.1793 0.2116 0.2420 0.2708	0.166	3115 (ρ = const.)

3.2.2 Component Specifications

The temperatures of the following components of the package are limited to certain admissible values under NCT:

- the fuel rods,
- the lid gaskets,
- the moderator material,
- the surface of the package.

The integrity of the fuel rod cladding must be ensured. For this purpose, the maximum cladding temperature must not exceed the admissible limit of 400 °C for normal conditions of transport according to [4].

The safe enclosure of the content must be ensured. For this purpose, the temperatures of the design-relevant lid gaskets must stay below the admissible limit value of [redacted] according to section 2.2.1 for continuous operation. Furthermore, the temperatures of the lid gaskets and the mean temperature of the filling gas in the cask cavity are used for the verification of the containment.

The effectiveness of the shielding is ensured when the maximum temperatures of the moderator components are below the maximum admissible application temperatures of [redacted] according to section 2.2.1. Furthermore, the mean temperatures of the moderator components are used for the shielding analyses and the moderator design.

The shielding elements and the round segments in the fuel basket are made of aluminium (SB-209 Alloy 5454). For these components it is shown that the calculated temperatures are far below the melting temperature of 603 °C.

The maximum temperature at the accessible surface of the package must remain under 85 °C during transport in an exclusive use shipment according to §71.43 (g).

During hypothetical accident conditions, the safe enclosure of the content must be ensured. Therefore, the maximum temperatures of the cask and canister lid gaskets are limited to [redacted] These are the maximum temporary temperatures for which failure of the metal gaskets can be excluded according to section 2.2.1.

The cladding temperatures are shown to remain below the admissible value of 570 °C for accidents according to [4].

As the thermal degradation of the moderators shielding effectiveness under accident conditions of transport is taken into account in the shielding analyses, assessment of the moderator component temperatures is omitted.

Table 3.2-9 Temperature limits of components

Component, material	Literature	Maximum temperature NCT, °C	Maximum temperature HAC, °C
Cladding	[4]	400	570
Gaskets	section 2.2.1	[redacted]	
Moderator material [redacted]	section 2.2.1	[redacted]	-
Cask surface (accessible surface)	§71.43 (g)	85	-
Cask body Ductile cast iron SA 874	section 2.2.1	343	-
Canister body [redacted]	section 2.2.1	427	-
Head ring [redacted]	section 2.2.1	427	-
Canister lid [redacted]	section 2.2.1	427	-
Cask lid **Retention ring** [redacted]	section 2.2.1	427	-
Closure plate SA-240M 22Cr-5Ni-3Mo-N	section 2.2.1	316	-
Basket sheets Al-B4C-MMC	section 2.2.1	250	-
Outer sheets SA-240M 316	section 2.2.1	427	-
Plates of the impact limiter [redacted]	section 2.2.1	66	-
Crush material [redacted]	section 2.2.1	127	-

List of References

[1] SCALE 4.4a: A Modular Code System for Performing Standardized Computer Analyses for Licensing Evaluation for Workstations and Personal Computers
Oak Ridge National Laboratory NUREG/CR-0200
ORNL/RSIC, CCC-545, 2000

[2] MATPRO-Version 11 (Revision 2): A Handbook of Materials Properties for Use in the Analysis of Light Water Reactor Fuel Rod Behaviour
US Nuclear Regulatory Commission, NUREG/CR-0497-REV-2, 1981

[3] McAdams W. H.
Heat Transmission (3rd edition)
McGraw Hill (1985)

[4] Cladding Considerations for the Transportation and Storage of Spent Fuel
Interim Staff Guidance – 11, Rev. 3
Spent Fuel Project Office
U.S. Nuclear Regulatory Commission (2003)

3.4 Thermal Evaluation under Hypothetical Accident Conditions

	Name, Function	Date	Signature
Prepared	[redacted]		
Reviewed			

According to 10 CFR 71, the effects of a series of sequent hypothetical accident scenarios has to be evaluated. In this chapter the effects of a 30 min fire test on the temperature distribution are described. Therefore, safety-important temperatures are evaluated. The maximum temperature of the fuel rods and the lid gaskets remain below their temperature limits.

For the thermal evaluation under hypothetical accident conditions, the package is exposed to a fully-engulfing pool fire with an average flame temperature of 800 °C for a duration of 30 minutes and a subsequent cooling phase. For HAC, only thermal requirement 2 is considered, as it leads to slightly higher temperatures than the thermal requirements 1 and 3

3.4.1 Initial Conditions

The initial conditions of the hypothetical fire accident comply with the results of the stationary calculation (hot case). The package dissipates heat by natural convection and radiation according to section 3.3.1.6.1, the ambient temperature amounts to 38 °C and the package is exposed to the sun according to section 3.3.1.6.2. Therefore, the initial temperature field of the package is equivalent to the one shown in Figure 3.3-9 (Thermal requirement 2).

3.4.2 Fire Test Conditions

The temperature distribution during the fire test is calculated by a transient FEM analysis, which consists of three parts, an initial phase with a stationary temperature distribution, a 30 min fire phase and a subsequent cooling phase of 35.5 hours. Due to the thermal inertia of the package, the maximum temperatures inside the package are reached several hours after the end of the fire phase. For the analysis, the same 3D-FE model is utilized as for NCT, (described in section 3.3.1.5), while several boundary conditions and modelling assumptions differ.

For the transient calculation under HAC, the heat storage capacity of the fins is taken into account.

[redacted]

The heat flux caused by insolation according to section 3.3.1.6.2 is considered during all three phases, conservatively.

3.4.2.1 Thermal Boundary Conditions during the Fire Phase

As stated in section 3.3.1.6.2, the HTC consists of a convective and a radiative amount. For the fire phase, h_{conv} is derived from the Nusselt law according to [1]

$$\overline{Nu} = C \cdot Re_D^m \cdot Pr^{1/3}$$

where Pr is the Prandtl number, as defined in section 3.3.1.6.1 and Re denotes the Reynolds number based on the diameter D

$$Re_D = \frac{v \cdot D}{\nu},$$

where

- v: velocity of the fluid [m/s],
- D: cask diameter [m],
- ν: kinematic viscosity [m^2/s].

The parameters C and m depend on the Reynolds number Re. The heat transfer coefficient is calculated for a temperature of 800 °C according to the fire test regulations and additionally for a sufficiently low temperature of 400°C.

The gas velocity inside the fire can be estimated by 5 m/s according to [2]. For the kinematic viscosity ν, the Prandtl Number Pr and the thermal conductivity k, the material properties of dry air from Table 3.3-4 according to [3] are used. [redacted] In Table 3.4-1, the input variables and the results for Re, Nu and h are summarized.

Table 3.4-1 Input values and calculated values of the heat transfer coefficient

For the flame temperature of 800 °C, a heat transfer coefficient of around 6.7 W / ($m^2 \cdot K$) is calculated, for a lower temperature of 400 °C, the HTC is around 8.7 W / ($m^2 \cdot K$) due to the higher Reynolds number. Conservatively, a reasonably high convective HTC of 15 W / ($m^2 \cdot K$) is applied during the fire phase.

The higher HTC takes into account that the gas atmosphere under pool fire conditions is a complex composition of mainly air, CO_2, water vapor and additional components such as soot particles. The exact gas mixture is varying locally and over the time. As the real material properties of the gas cannot be evaluated, the HTC is calculated using the material data of air, which represents the major part of the flue gas.

The convective HTC is applied on the outer surface of the package and set constant during the fire phase. Within the finned zone of the cask, the convective HTC is multiplied by the surface enlargement factor of [redacted] (see section 3.3.1.3).

The radiative heat transfer coefficient during the fire phase is calculated as described in section 3.3.1.5. For the ambient temperature, the flame temperature of 800 °C is set. For the emissivity ε an effective emissivity is calculated. Therefore, the fire is treated as a cylinder that surrounds the cask. According to [1], the effective emissivity between two concentric cylinders is given by

$$\varepsilon_{eff} = \frac{1}{\frac{1}{\varepsilon_1} + \frac{1-\varepsilon_2}{\varepsilon_2} \cdot \frac{r_1}{r_2}} \cdot$$

[redacted]

The ambient temperature for convection and radiation is set to 800 °C according to, §71.73 (c). The described boundary conditions lead to a heat flux shown in Figure 3.4-1, which is in the range recommended in [2].

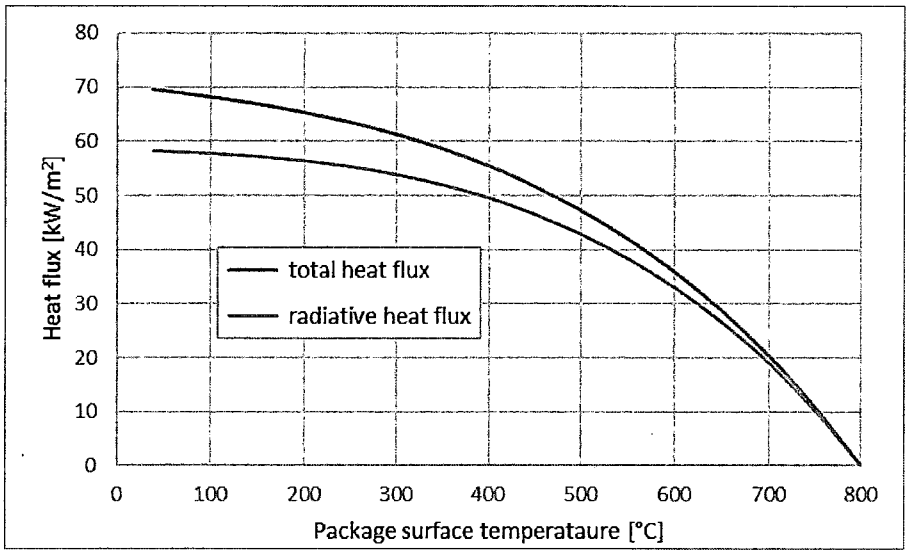

Figure 3.4-1 Resulting heat flux during fire phase (surface enlargement factor is not considered)

3.4.2.2 Thermal Boundary Conditions during the Cooling Phase

During the cooling phase, the same temperature dependent heat transfer coefficients than for NCT are applied (see section 3.3.1.5). The emissivity of the package surface is the same as for the fire phase. The ambient temperature is also set to 38 °C and insolation is considered by heat fluxes according to section 3.3.1.6 (constant over time).

3.4.2.3 Modelling of the Impact Limiters during HAC

According to section 2.7, the impact limiters remain on the package after the hypothetical accident conditions "9 m free drop onto an unyielding surface" and "1 m drop on to a mild steel bar", thus, their isolating effect can be credited. The resulting deformation of the impact limiters affects the thermal resistance and therefore has to be examined. The deformation leads to, first a reduced thermal resistance due to the smaller transport distance of the heat, and second, an increased thermal conductivity of the material due to a higher density. During the fire phase, this leads to a higher heat input, during the cooling phase, this leads to a better heat removal. In section 3.4.3.1,

undeformed impact limiters are assumed, the effect of a deformation is examined by an additional calculation in section 3.4.3.2.

[redacted]

As the heat storage capacity of the impact limiters is not affected by the compression, the density and specific heat capacity is the same for both cases.

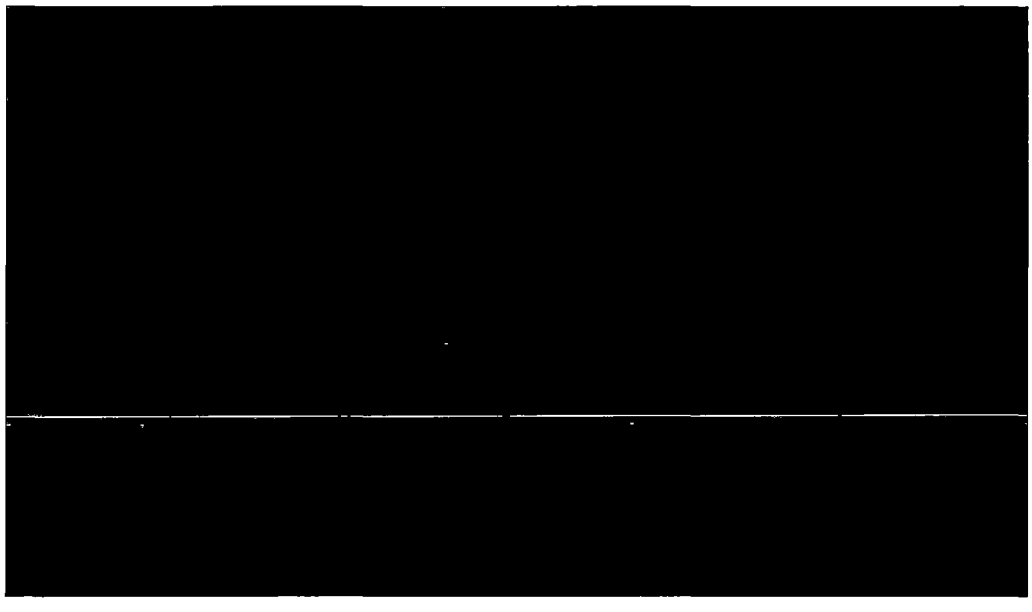

Figure 3.4-2 Correlation between thermal conductivity and density of the polyurethane foam

3.4.3 Maximum Temperatures and Pressures

3.4.3.1 Maximum Temperatures

In Table 3.4-2, the maximum temperatures and their time of appearance (t = 0: ignition of fire) is shown for all relevant components. Below, the design relevant temperatures are compared with their limit values according to section 3.0.

The hottest fuel rod reaches after 17 h its maximum temperature of 237 °C, which is considerably lower than the maximum allowable fuel rod temperature for HAC of 570 °C.

The temperatures of the gaskets are between 121 °C and 127 °C, which is lower than the maximum allowable gasket temperature of at least 370 °C.

Table 3.4-2 Maximum component temperatures for HAC and time of appearance after ignition of the fire

Component, type of temperature	Maximum temperature [°C]	Time of appearance [h]
Fuel rods – maximum	237	17
Cask surface – maximum	380	0.5
Cavity surface – maximum	183	2.3
Moderator rods (inner row) (MR-i) – maximum	199	1.1
MR-i – area-average hottest plane, hottest rod	180	2.2
MR-i – volume-averaged, hottest rod	174	2.5
Moderator rods (outer row) (MR-o) – maximum	310	0.5
MR-o – area-average hottest plane, hottest rod	186	0.6
MR-o – volume-averaged, hottest rod	183	1.7
Moderator plate (bottom) – maximum	145	15
Moderator plate (bottom) – volume averaged	137	10.5
Moderator plate (lid) – maximum	126	29
Moderator plate (lid) – volume averaged	119	21
Canister wall – maximum	180	3.0
Basket sheets – maximum	223	19
Shielding elements – maximum	193	11
Filling gas canister – volume averaged	192	15
Filling gas cask – volume averaged	145	3
Canister lid gasket – maximum	127	12
Cask lid gasket – maximum	127	4.5
Protection cap gasket – maximum	121	8.5
Blind flange gasket – maximum	122	7.5
Tightening plug gasket – maximum	127	19

In Figure 3.4-3, the temperature distribution of the package is shown for two different time steps. First, the end of the fire phase after 0.5 h, where the maximum cask surface temperature is reached. Second, after 17 h, when the hottest fuel rod reaches its maximum temperature.

In Figure 3.4-4, the temperature distribution of the lid system is shown for the maximum temperatures of both gaskets.

In Figure 3.4-5– Figure 3.4-7, the temperature development over time for relevant components is shown.

In Figure 3.4-8 and Figure 3.4-9 the volume averaged temperatures of the moderator rods for different heights over the time are shown, which are used for the moderator evaluation.

The temperatures for the post-fire steady state conditions are similar to the temperatures for the stationary results. Exemplarily, the post-fire steady state temperature for the package surface amounts to approx. 93 °C, which is 9 K above the temperature of the stationary results, as shown in Figure 3.4-7. This is due to the fact that the emissivity after the fire [redacted] is lower than for NCT [redacted]. All other component temperatures shift accordingly.

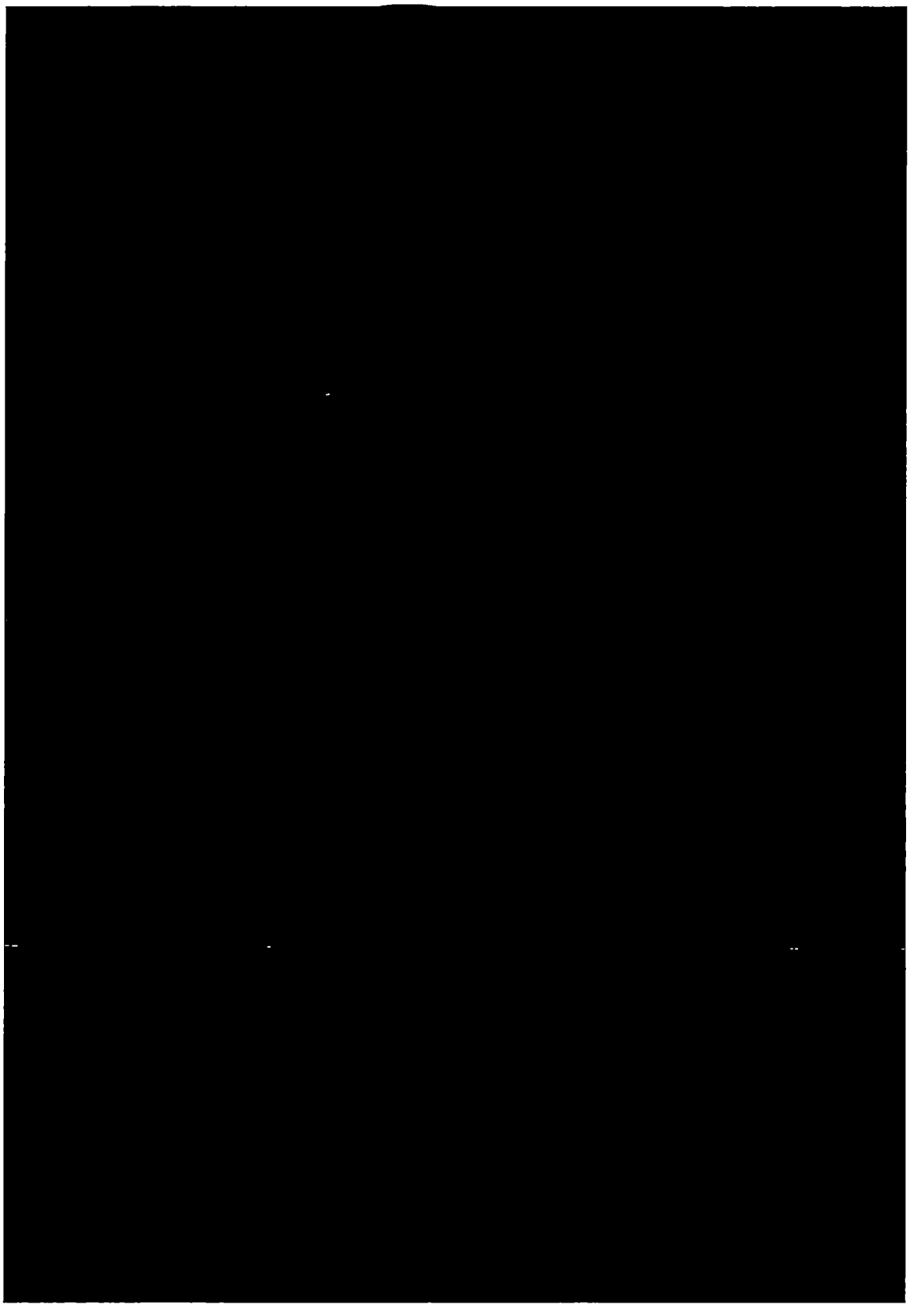

Figure 3.4-3 Temperature distribution of the components after 0.5 h and 17 h (HAC)

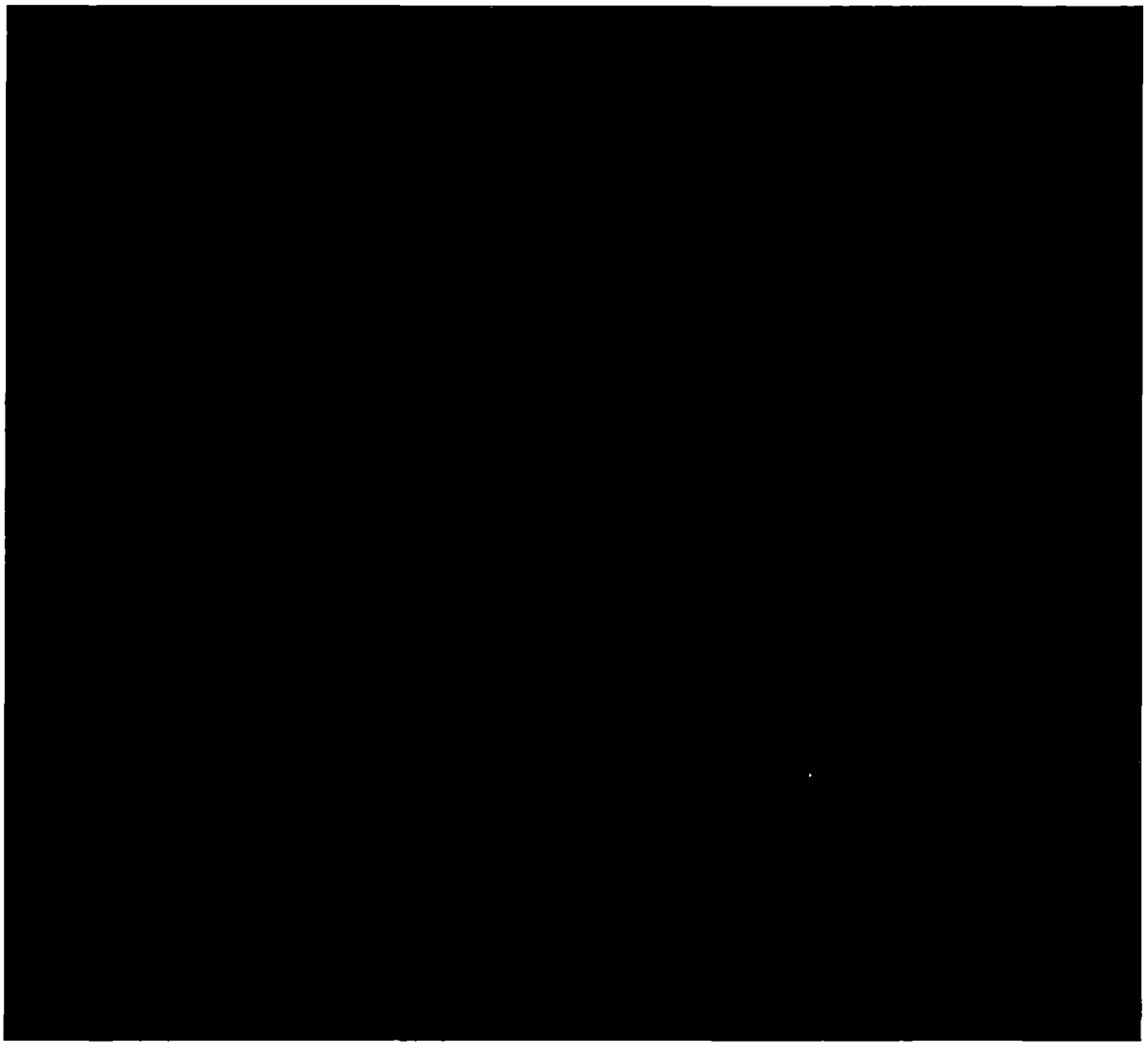

Figure 3.4-4 Temperature distribution in the lid system for maximum gasket temperatures (HAC)

Figure 3.4-5 Temperatures of the filling gases and the hottest fuel rod over time (HAC)

Figure 3.4-6 Temperatures of the gaskets over time (HAC)

Figure 3.4-7 Temperatures of cask and cavity surfaces and canister over time (HAC)

Figure 3.4-8 Volume-averaged temperatures of the inner moderator rods for different heights over time (HAC) (z = 0: upper side of closure plate)

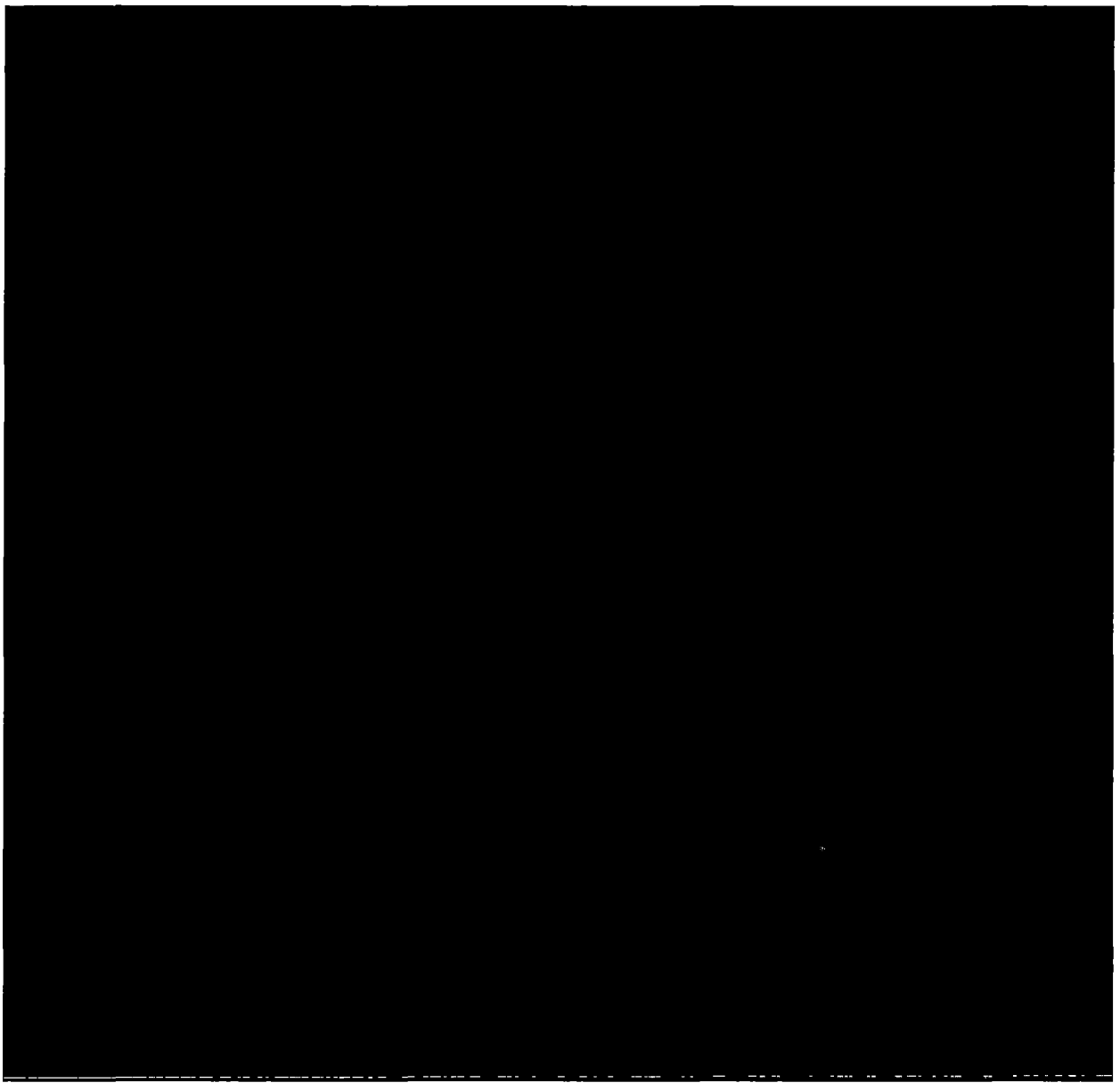

Figure 3.4-9 Volume-averaged temperatures of the outer moderator rods for different heights over time (HAC) (z = 0: upper side of closure plate)

3.4.3.2 Maximum Temperatures for Deformed Impact Limiters

An additional calculation is performed in order to quantify the effects of deformed impact limiters. The initial temperature field is calculated with undeformed impact limiters (equivalent to NCT from section 3.3.2.1). The resulting temperatures over the time are shown in Figure 3.4-10 for the gaskets, the results for the undeformed impact limiters from section 3.4.3.1 are shown by the dashed lines. The comparison shows that the even very conservative assumptions

for the deformation have only a minor effect on the resulting temperatures. The maximum temperatures of the undeformed state are higher than for the deformed state, which means that the positive effect of the better heat removal during cooling phase outweighs the negative effect of a higher heat input during fire phase. The highest temperature differences appear in the direct surrounding of the impact limiters (difference for the cask lid gasket: 1.4 K), further inside the package, the effect can be neglected (difference for the canister lid gasket: 0.2 K, tightening plug gasket: 0 K). The results show that the assumptions made for section 3.4.3.1 are sufficiently conservative.

Figure 3.4-10 Temperatures of the gaskets over time (HAC) for deformed (continuous lines) and undeformed (dashed lines) impact limiters

3.4.3.3 Maximum Pressures

The calculation of the maximum pressures under HAC and a discussion on the generation of flammable gases can be found in chapter 4 "Containment".

3.4.4 Maximum Thermal Stresses

The occurrence of thermal stresses is minimized by sufficiently large gaps in axial and radial direction, which allows for free thermal expansion of the different components without contact and restraint. The discussion of thermal stresses due to temperature gradients within the components can be found in the structural evaluations.

In Figure 3.4-11, the axial gap width of the gaps between canister and basket sheets and cask and canister is shown. [redacted]

The gaps in radial direction behave in a similar manner as the corresponding components (cask, canister, basket) are the same. [redacted]

This shows that, at any time, the gap widths in axial and radial direction are sufficiently large to prevent restraint forces.

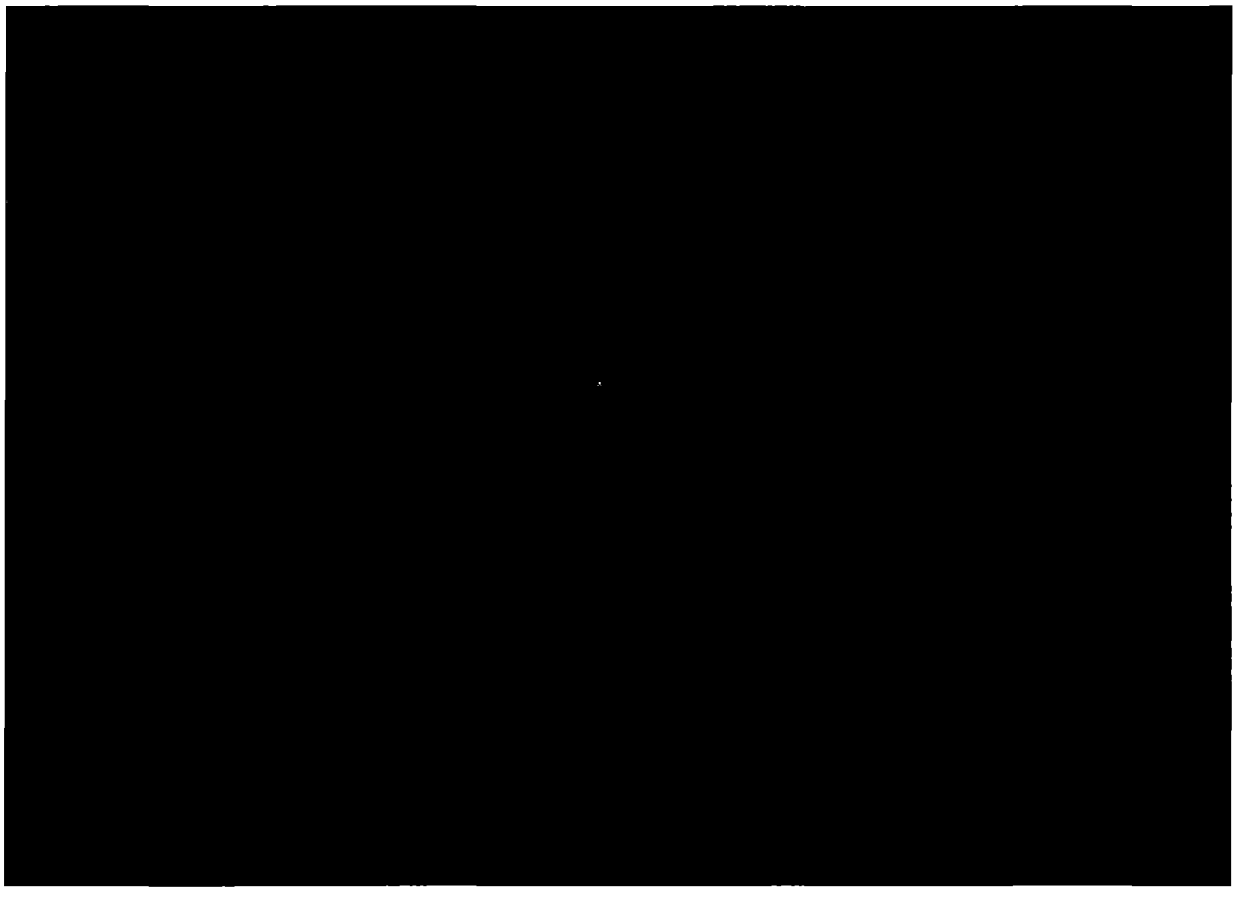

Figure 3.4-11 Development of the axial gaps over time (HAC)

3.4.5 Accident Conditions for Fissile Material Packages for Air Transport

Air transport is excluded for the CASTOR® geo69 package.

List of References

[1] Theodore L. Bergman
Fundamentals of Heat and Mass Transfer (7th edition)
2011

[2] A Guide For Thermal Testing Transport Packages For Radioactive Material
– Hypothetical Accident Conditions –
Division of Transportation and Packaging Safety, Office of Risk Analysis and Technology
1993

[3] VDI Heat Atlas
Springer (2010)

3.5 Thermal Evaluation for Fuel Rod Failure

	Name, Function	Date	Signature
Prepared	[redacted]		
Reviewed			

Since for at least one of the fuel types which are intended to be loaded into the canister of the CASTOR® geo69 package the burn-up exceeds 45 GWd/t_{HM} and for all fuel types the intended dry storage time is beyond 20 years, according to NUREG-2224 [1] age-related uncertainties connected with transport after extended dry storage of high burn-up SNF) are to be considered in the safety analyses.

The chosen approach is to supplement the design basis with safety analyses that demonstrate that the cask still meets the pertinent regulatory requirements by assuming hypothetical reconfiguration of the HBU SNF contents into justified geometric forms. This approach demonstrates that during transport after 20 years of dry storage, even if reconfigured, SNF can still meet the 10 CFR Part 71 requirements for thermal, criticality safety and shielding during NCT and HAC.

Following NUREG-2224 [1], the impact of cladding failures of Category 1 with breached rods (Scenario 1(a) according to [1]) and with damaged rods (Scenario 1(b) according to [1]) is considered by the external dose rate evaluation in chapter 5 assuming rupture of 3 % and 100 % of the fuel rods for NCT and HAC, respectively.

The cask is designed to exclude the water leakage into the canister cavity under NCT and HAC. Due to very low reactivity of dry fuel, the behavior of the spent fuel as a result of accident conditions during transport after more than 20 years of storage does not need to be explicitly evaluated and is bounded by the reactivity of the fully flooded cask with pure unborated water, as assumed in the bounding criticality safety model for NCT (see chapter 6).

The impact of cladding failures of Category 1 with breached rods (Scenario 1(a) according to [1]) and with damaged rods (Scenario 1(b) according to [1]) on the fuel cladding and package component temperatures as well as on the canister pressure assuming rupture of 3 % of the fuel rods for NCT and of 100 % for HAC, respectively, is evaluated in the following passage.

The case of 100 % fuel rod failure for HAC with a fraction of fission gas release of 0.3 leads to a strongly reduced heat conductivity of the gas atmosphere in the canister resulting in a temperature increase of about [redacted] inside the canister. The maximum heat power per FA decreases to [redacted] of dry storage leading to a reduced maximum total heat power of about [redacted] (instead of 18.5 kW) for the cask loading. In that case, about [redacted] lower temperatures inside the canister result. Altogether, both effects lead to about [redacted] higher temperatures for the components and the fuel rods in the canister in sum.

Maximum FA temperatures occur if the fuel remains inside the fuel cladding. A variation calculation with a concentration of the [redacted] heat power in the bottom (or lid) part of the canister (fuel reconfiguration) shows that higher heat power density is compensated by the higher thermal conductivity

within an assumed fuel pouring in the bottom part of the canister ([redacted]), see Figure 3.5-1.

For this variation calculation, the maximum temperature of the fuel is slightly but not significantly lower than for the case if the fuel remains inside the fuel cladding. The mean gas temperature in the canister is much lower, because the main gas volume is now present in the colder zones above the fuel pouring. A slight temperature increase occurs only for some cask components in the bottom (or lid) part, but the admissible temperatures for all cask components are still not reached.

The maximum temperature of the inventory for HAC without fuel rod failure amounts to 237 °C according to section 3.4.3.1. The maximum temperature of the inventory for HAC in case of 100 % fuel rod failure after 20 years dry storage amounts to [redacted]. This temperature is below the admissible value of 400 °C for NCT and 570 °C for HAC according to section 3.0 with very large safety margins. Accordingly, the maximum mean gas temperature inside the canister amounts to [redacted] The admissible temperatures for FA and all cask components are not reached.

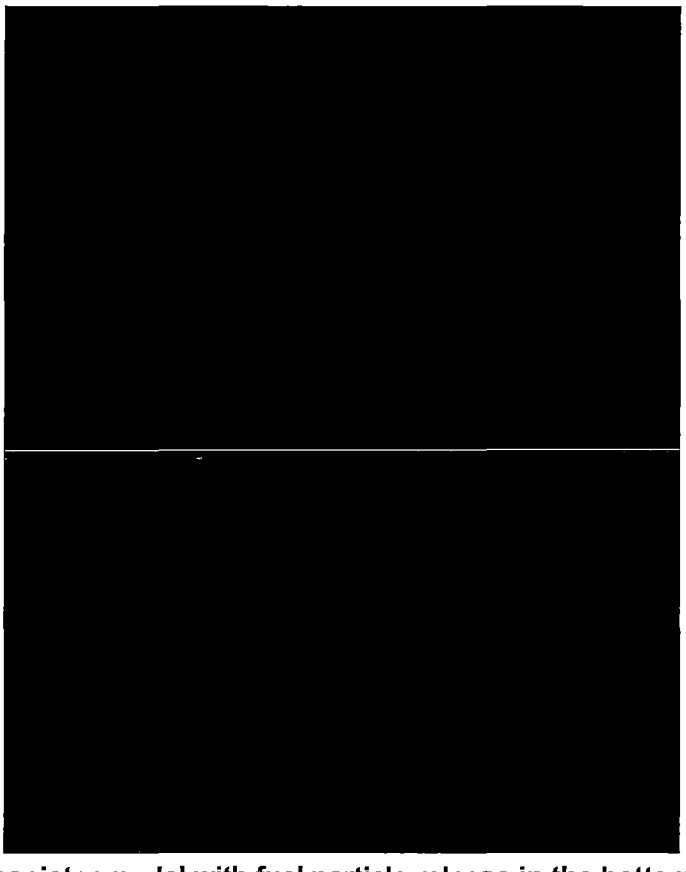

Figure 3.5-1 Thermal canister model with fuel particle release in the bottom part

List of References

[1] NUREG-2224
Dry Storage and Transportation of High Burnup Spent Nuclear Fuel
U.S. Nuclear Regulatory Commission, Final Report (2020)

3.6 Thermal Evaluation for Short-Term Operations

	Name, Function	Date	Signature
Prepared	[redacted]		
Reviewed			

The short-term operations foreseen for the CASTOR® geo69 transport and storage cask are described in Chapter 7. Short-term operations comprise loading and unloading of cask and canister including dewatering, drying and transfer of the loaded canister from the SNF pool to the CASTOR® geo69 cask. The CASTOR® geo69 cask loading unit (CLU) is used for these operations.

The maximum allowable temperatures of components of the cask during short-term operations are equal to those given in Table 3.2-9 for NCT, the maximum fuel cladding temperature during short-term operations is limited to 400 °C in accordance with ISG 11 [1].

A detailed description of the CLU and its components including functionality is given in the SAR for the Dry Storage System CASTOR® geo69 [2]. The thermal evaluations in [2] include detailed analysis regarding short-term operations including evaluations of

- underwater loading of FA into the canister,
- the flooded and closed canister (time-to-boil analysis),
- vacuum drying
- completely dispatched (including helium backfilling) canister.

These evaluations result in some constraints, which are mentioned in Chapter 7 as boundary conditions for FA loadings. As long as these boundary conditions are satisfied during the operations, no impacts on the CASTOR® geo69 transport package are to be assumed.

List of References

[1] Interim Staff Guidance - 11, Revision 3
Cladding Considerations for the Transportation and Storage of Spent Fuel
Spent Fuel Project Office

[2] GNS report 1014-SR-00002 Revision 0
Safety Analyses Report, Dry Storage System CASTOR® geo69
NRC Docket No.: 72-1052

3.7 Appendix

	Name, Function	Date	Signature
Prepared	[redacted]		
Reviewed			

Intentionally no items.

5.1 Description of Shielding Design

	Name, Function	Date	Signature
Prepared	[redacted]		
Reviewed			

5.1.1 Design Features

The principal sources of radiation from SNF are:

- Gamma radiation originating from a decay of actinides and radioactive fission products, of fuel and hardware activation products generated during reactor operation, as well as secondary gamma particles from neutron capture,
- Neutron radiation from spontaneous fission, from (α,n)-reactions in fuel materials, from secondary neutrons produced by fission via subcritical multiplication, and from (γ,n)-reactions. The latter source is however negligible.

The major parts of the package relevant for the shielding of radiation sources are:

- the basket with 69 positions to accommodate SNF,
- the canister with its lid,
- the cask body (with its lid) incorporating moderator rods and plates.

Shielding from gamma radiation is provided by the steel structure of the canister and the lid system and by the ductile cask iron (DCI) of the cask body. In order to make neutron shielding effective, the neutrons have to be thermalised and then absorbed. For this purpose, the moderator rods and plates made of unborated ultra high-molecular polyethylene (UHMW PE) are incorporated into the cask body. Together with relatively high carbon contents in the DCI, they provide an effective way to thermalise neutrons. Sufficient DCI behind the polyethylene rods towards the external surface of the cask not only allows for an efficient absorption of neutrons, but greatly supresses the high energetic secondary gamma radiation.

The borated structures of the basket (NEXUS-3000®) are not primarily aimed to improve the shielding performance of the cask, but nevertheless diminish the thermal part of the neutron spectrum around the SNF to some extent. This helps to reduce the dose rate contributions (mostly) from the inner fuel assemblies.

Additional basket elements (round segments and shielding elements) made of aluminium are added to the basket not only to stabilise it, but to provide some additional gamma shielding.

The cross-sectional top view of the package (quarter cut) is presented in Figure 5.1-1, while the elevation section of the package is displayed in Figure 5.1-2. These views are directly generated from the calculation inputs (here the NCT input). The colour code corresponds to the materials used in the calculations. Different colours selected for the moderator rods are used to distinguish longer and shorter rods. In section 5.3 the shielding model of the package is presented in greater detail.

Figure 5.1-1 Cross section of the package model (2020 mm above cask bottom)

Figure 5.1-2 Elevation section of the package model

The most important dimensions of the package for the shielding calculations in its central plane are presented in Figure 5.1-3 (standard MCNP colours are desaturated). The dimensions according to the technical drawings in section 1.3 are highlighted as blue text, the implementation into the shielding model as green text. The thicknesses of the materials relevant for the shielding analysis are set to their minimum. The occurring gaps are filled with air.

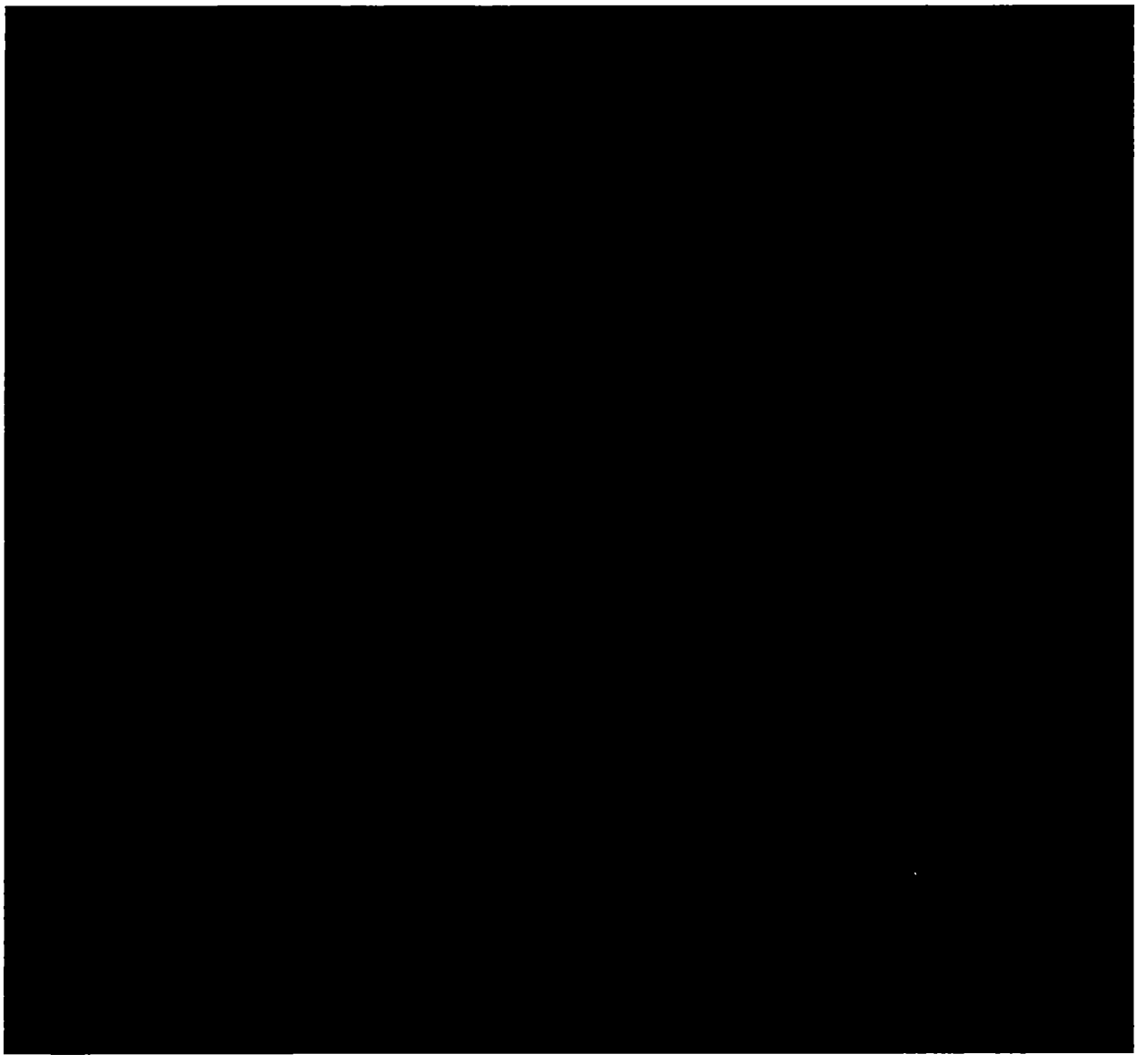

Figure 5.1-3 Cross section of the package model with major dimensions (in mm)

Axially the main shielding is provided by:

- a [redacted] bottom part consisting of thick DCI part ([redacted]), [redacted] bottom moderator plate, and a [redacted] (in its middle part) closure plate;
- the lid system consisting of the canister lid ([redacted]), moderator plate ([redacted]), and cask lid [redacted].

The dose rates on the face sides of the package are much smaller than on the shell side, which is decisive for the design, [redacted]

Besides polyurethane foam (varying thickness) both impact limiters include steel as housing and inner lying structure sheets, it is however conservatively not modelled. The impact limiters do not bear a dedicated shielding function.

Present shielding analysis is not based on the latest version of the design drawings for the impact limiters (from 12/02/2020). Although the radial structure of the impact limiters has not been changed, there are some minor deviations in the axial dimensioning of the pieces which are addressed here.

In general, both impact limiters have gained in the length along the cask axis. This means that there is less material modelled compared to the actual build. Probably the most important aspect for the evaluation of the external dose rate is that [redacted] which is conservative.

The thicknesses of the components relevant for shielding, mainly the penetration protection assembly, remain; the openings for the trunnions are even smaller than before, which in turn has a small positive effect on the dose rates.

Possible negative impact of the bigger lid side central opening ([redacted]) on the dose rates of the lid side of the cask should be more than compensated by other conservative assumptions made. Firstly, the plating of the polyurethane foam is not taken into account in the shielding model at all; its presence would provide a better shielding. And secondly, the length growth would not only provide more material but also shift the normally occupied space further from the package.

Overall, the final design of the impact limiters should not negatively affect the dose rate outside the package. It is expected that the dose rates around the gap between cooling fins and the lid side impact limiter become smaller.

[redacted]

5.1.1.1 Classification of the Fuel Assemblies

The fuel assemblies are generally classified by their type (SNF number, see section 1.2.2) and by their maximum allowed decay heat. These two quantities, geometry and heat, complemented by the minimum initial enrichment and maximum burn-up including burn-up uncertainty unambiguously define the bounding source terms described in detail in section 5.2.

In the shielding model, the design of the SNF No 6, Atrium-10A, is used. The choice is governed by the presence of the part length rods, by the thickness of the fuel pellets and cladding, and by the largest water channel (3x3), which minimises the self-shielding of the peripheral SNF. With this choice, the conservative configuration is realised.

5.1.1.2 Package during Normal Conditions of Transport

The 10CFR71.47 external radiation requirements during NCT for an exclusive shipment addressed in the present shielding analysis are as follows:

- 2 mSv/h on the external surface of the package. No credit has been taken of closed transport vehicle.
- 2 mSv/h at any point on the outer surface of the vehicle, including the top and underside of the vehicle. No credit has been taken of the vehicle or enclosure. Since the dose rate values on the surface of the arbitrary vehicle or enclosure are lower than on the surface of the package, and the same dose rate limit requirements apply, no separate dose rate values are calculated.
- 0.1 mSv/h at any point 2 meter from the outer lateral surfaces of the vehicle. Conservatively, the dose rates are calculated at a distance of 2 meters from the outer surfaces of the package.
- 0.02 mSv/h in any normally occupied space. This is supposed to be the lid side of the package.

In case of shipment under non-exclusive use, the NCT dose rate limit is:

- 0.1 mSv/h at 1 m from the surface of the package.

The CASTOR® geo69 will be transported with impact limiters. The width of the transport vehicle is yet unknown; therefore, no credit is taken of the transportation means. The lateral surfaces of the vehicle are conservatively assumed to be directly located at the tips of cooling fins.

The information about particular dose rates is gained from detectors positioned all around the cask. Besides this geometry-independent mesh of detectors ([redacted]), separate volumetric detectors are modelled in order to control the calculation process. The maximum dose rates are always searched for in different dose rate locations.

A unique feature of the CASTOR® geo69 are the moderator rods placed directly in the cask body. The rods are made of UHMW PE without neutron absorbing additives and serve the neutron moderation purpose only. From the transportation point of view, few standard situations are to be considered:

[redacted]

In case the transportation takes place in winter, the low ambient environment temperature can compensate the increase of the moderator rod temperature. With the normal operational temperature of above 100° C due to the maximum contents, this temperature cannot fall off below 20° C, therefore a shrinkage of the polyethylene is excluded. This effect can only be observed, once SNF loaded into the cask are strongly cooled down, so that the heat produced is not able to warm up the moderator. But in this case the radiation source is also significantly weaker and will not generate comparable external dose rates.

Two shielding models, cold and hot, are analysed. One of the two delivering the highest external dose rates is considered as representative for the package design. Figure 5.1-4 and Figure 5.1-5 illustrate these two shielding models for the inner and outer moderator rods, respectively. In both cases the geometry of the setup is implemented according to section 2.2.1, and the tolerances are chosen such that the air gaps are maximised.

CASTOR® geo69 will transport high burn-up spent fuel, therefore, the impact of the 3-percent fuel failure under NCT is evaluated according to [1]. The source occurring due to fuel failure is relocated to the bottom and to the top regions of the canister, the regions with potentially lower shielding performance due to flattenings in the trunnion regions and due to finite axial size of the moderator rods.

Figure 5.1-4 Inner moderator rods under different operating conditions (dimensions in mm)

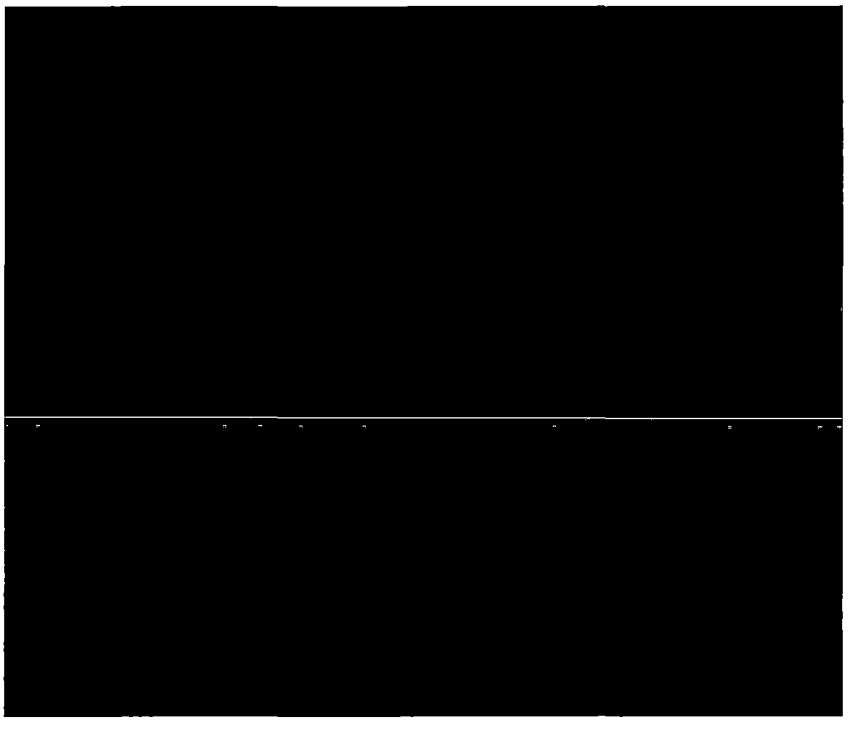

Figure 5.1-5 Outer moderator rods under different operating conditions (dimensions in mm)

5.1.1.3 Package during Hypothetical Accident Conditions

The 10CFR71.51 external radiation dose rate limit for hypothetical accident conditions is:

- The external radiation dose rate shall not exceed 10 mSv/h at 1 m from the external surface of the package.

The hypothetical accident conditions of transport have two bounding consequences which affect the shielding performance of the package. These are the (partial) loss of the neutron moderator as a result of the design basis fire and damage of the impact limiters as a result of the drop.

In a conservative fashion, the shielding analysis of the accident assumes that the moderator material and the impact limiters are completely lost. These assumptions are highly conservative, since neither the moderator material, not the impact limiters are destroyed by the accident according to chapter 2.

The Structural analysis in chapter 2 shows that the basket, canister, and the cask remain largely unaltered throughout the HAC. Localised damage to the cask shell experienced after the pin puncture will have a negligible impact on the dose rate at 1 m from the surface.

The impact of the 100-percent fuel failure under HAC according to [1] is evaluated. The damaged fuel relocation is considered. The dose rates are analysed when the fuel is kept within the basket cell but pushed either to the bottom or to the top of the canister.

5.1.1.4 Computer Codes

The code system MCNP6 in version 2.0 [2] is used to calculate the dose rates. The source terms are calculated with the SCALE 6.2 code system [3] using TRITON [4] and ORIGAMI [5] modules. These codes are described in Appendix 5-1.

5.1.2 Summary Table of Maximum Radiation Levels

Table 5.1-1 provides the maximum dose rates at the package surface, at 1 m from the surface of the cask (package) and at 2 m from the surface of the cask (package) for normal conditions of transport. A location 1 m from the package at its lid side is identified as a normally occupied space (vehicle driver). The values presented are the most unfavourable ones among all considered loading patterns (TR1 through TR3) and fuel arrangements including fuel reconfiguration.

Since the maximum total dose rate exceeds 0.1 mSv/h at 1 m from the surface of the package, the shipments have to be carried out under exclusive use.

Table 5.1-1 Maximum dose rates at different locations for the CASTOR® geo69 package under normal conditions of transport

Dose Rate Location		Gammas, mSv/h	Neutrons, mSv/h	Totals, mSv/h	10CFR71.47 Limit, mSv/h
Shell Side	Cask Surface	[redacted]		1.578	2
	1 m from package	[redacted]		0.158	0.1*
	2 m from package	[redacted]		0.088	0.1
Lid Side	Cask Surface	[redacted]		0.005	2
	1 m from package / normally occupied space	[redacted]		0.004	0.1* / 0.02
	2 m from package	[redacted]		0.002	0.1
Bottom Side	Cask Surface	[redacted]		0.033	2
	1 m from package	[redacted]		0.021	0.1*
	2 m from package	[redacted]		0.009	0.1

** non-exclusive use*

Table 5.1-2 provides the maximum dose rates at 1 m from the cask (package) surface for the hypothetical accident conditions. The values presented are the most unfavourable ones among all considered loading patterns and fuel arrangements.

Table 5.1-2 Maximum dose rates at 1 m for the CASTOR® geo69 package under hypothetical accident conditions

Dose Rate Location	Gammas, mSv/h	Neutrons, mSv/h	Totals, mSv/h	10CFR71.51 Limit, mSv/h
Shell Side	[redacted]		2.461	10
Lid Side	[redacted]		1.531	10
Bottom Side	[redacted]		1.374	10

List of References

[1] NUREG-2224, Dry Storage and Transportation of High Burnup Spent Fuel (Draft for Comment), Washington, DC, July 2018

[2] C.J. Werner (ed.), MCNP User's Manual - Code Version 6.2, LA-UR-17-29981, 2017

[3] SCALE Code System, Version 6.2.2. B. T. Rearden, M. A. Jessee, Eds. ORNL/TM-2005/39, 2017

[4] TRITON: A Multipurpose Transport, Depletion, and Sensitivity and Uncertainty Analysis Module in: SCALE Code System ORNL/TM-2005/39, Version 6.2.2, 2017

[5] ORIGAMI: A Code for Computing Assembly Isotopics with ORIGEN in: SCALE Code System ORNL/TM-2005/39, Version 6.2.2, 2017

5.2 Source Specification

	Name, Function	Date	Signature
Prepared	[redacted]		
Reviewed			

The procedure to identify bounding source terms for each loading pattern TR1 to TR3 is presented in this section. For each fuel assembly described in section 1.2.2 the following quantities are known:

- lattice parameters and geometry,
- minimum initial enrichment (see also Table 5.2-1),
- maximum end burn-up (with burn-up uncertainty, see Table 5.2-1),
- maximum allowed decay heat.

With these parameters burn-up and depletion calculations are performed (see section 1.2.2 for an extended description). The nodal burn-up profile data as well as the nodal value for the moderator density are provided in Table 1.2-12. To accurately account for an axial distribution, 24 individual calculations are executed for a single geometry resulting in nodal values for the physical SNF properties. Cooling times of up to more than 45 years are analysed for each SNF separately, and decay heat, gamma and neutron source terms are compared to find the maximum values. This helps to unambiguously identify the minimum cooling times, at which the decay heat required by the certain loading pattern (in each position group) is just reached. Otherwise, the particular SNF are not authorised for loading.

The decay heat as well as the radiation sources are calculated for every SNF geometry using ORIGAMI with the necessary libraries generated beforehand using TRITON (see Appendix 5-1) as discussed in section 1.2.2. The validity of the ORIGAMI output is checked against multiple TRITON calculations (see Appendix 5-2).

The burn-up profiles used in the analysis compare nicely with the representative profiles utilised in [1]. The moderator density axial profile used in the analyses represents a bounding node-wise minimum of profiles corresponding to the complete irradiation histories of the considered fuel assemblies. [redacted] It also compares nicely to the cycle-average axial void fraction from [1], which in turn is representative for the assemblies with a discharge burn-up of above 30 GWd/Mg_{HM} [2].

The radiation sources relevant for the dose rate outside of the cask consist of gamma and neutron radiation from the active zone of the SNF as well as from gamma radiation due to ^{60}Co from the activated hardware including fuel rod plena and tie plates.

The minimum cooling times required to reach a certain decay heat according to loading patterns TR1 to TR3 are given in Table 5.2-2. The values from SNF GE 8x8-1 and GE 8x8-2 are practically undistinguishable and hence are not separated. Some field are left vacant, because the cooling times are smaller than the minimum cooling times for this particular SNF type (section 1.2.2).

Table 5.2-1 Boundary conditions for the burn-up calculations

[redacted]

Table 5.2-2 Minimum cooling times (in years) needed to reach certain decay heat

[redacted]

5.2.1 Gamma Source

The gamma-radiation of the spent fuel is analysed in seven energy groups (see Table 5.2-3), representing energies relevant for the dose rate outside of the cask. The gamma particles with even lower energy are so well shielded that they do not significantly contribute to the outer dose rate. The high energy gamma particles possess tiny source term strengths and, therefore, do not contribute to the dose rate either. [redacted]

Table 5.2-3 Gamma energy structure

Energy group, i =	1	2	3	4	5	6	7
Average group energy, MeV	0.575	0.85	1.25	1.75	2.25	2.75	3.5
Lower group energy, MeV	0.45	0.7	1	1.5	2	2.5	3
Upper group energy, MeV	0.7	1	1.5	2	2.5	3	4

The gamma source is determined for every SNF type described in section 1.2.2. The total source strength in each gamma energy group is calculated by summation of the 24 axial nodal values stemming from the conservative axial burn-up profile discussed above.

[redacted]

This confirms close to linear behaviour of the total gamma source as a function of the assembly burn-up.

This justifies the use of the high burn-up profile for the generation of the axial source strength distributions. The axial gamma source strength profile used in present shielding calculations are displayed in Figure 5.2-1. Different shapes of the profiles in various groups can be related to the most contributing nuclides.

Figure 5.2-1 Axial gamma source strength distributions

As discussed above, the nodal gamma sources are determined. It is checked that no increase of the source terms over time occurs. For all seven groups the sources monotonously decrease.

The resulting gamma sources calculated based on Table 5.2-2 for every SNF type are summarised in Table 5.2-4 to Table 5.2-10. The sources are normalised to one megagram of heavy metal to account for the differences in the mass of the SNF including the mass in the shielding model. The bold value are the maximum sources for each fixed decay heat.

Besides gamma particles stemming from the fuel pellet stack, there is also a gamma radiation from activated hardware: the end fittings, the plenum springs, and the grid spacers. The primary source of activity in the non-fuel regions of a SNF arise from the activation of ^{59}Co to ^{60}Co. The activity (and the source) of ^{60}Co is determined during burn-up calculations as well.

[redacted]

[redacted] This value is scaled with the maximum burn-up of the particular SNF and corresponding masses of the end fittings and plena. The flux scaling factors of 0.1 for the top end fittings and of 0.2 for the bottom end fittings and plenum springs are applied according to PNL-6906 [3]. [redacted]

[redacted] The activities are finally decayed to the desired cooling time from Table 5.2-2. The gamma sources for each SNF type are given in Table 5.2-11 to Table 5.2-14.

Some older SNF may have higher ^{59}Co impurity level in their structural elements (including spacers), the minimum cooling times specified in section 1.2.2, however, imply that the activity of ^{60}Co is largely cooled down.

Yet another gamma source arises from (n,γ) reactions in the package materials. This source is properly accounted for in MCNP, when neutron calculations are performed in a coupled neutron-gamma mode, which is the case for the present shielding analysis.

The bounding gamma source for each loading pattern TR1 to TR3 is constructed from the maximum individual sources corresponding to the selected decay heat. The final sources used for the shielding analysis are reported in Table 5.2-15 for TR1, in Table 5.2-16 for TR2, and in Table 5.2-17 for TR3 decoded after position groups (see Figure 5.0-1). [redacted]

The bounding gamma energy release rate for the gamma radiation from the spent fuel is summarised in Table 5.2-18.

Table 5.2-4 SNF type dependent gamma sources for energy group i=1

[redacted]

Table 5.2-5 SNF type dependent gamma sources for energy group i=2

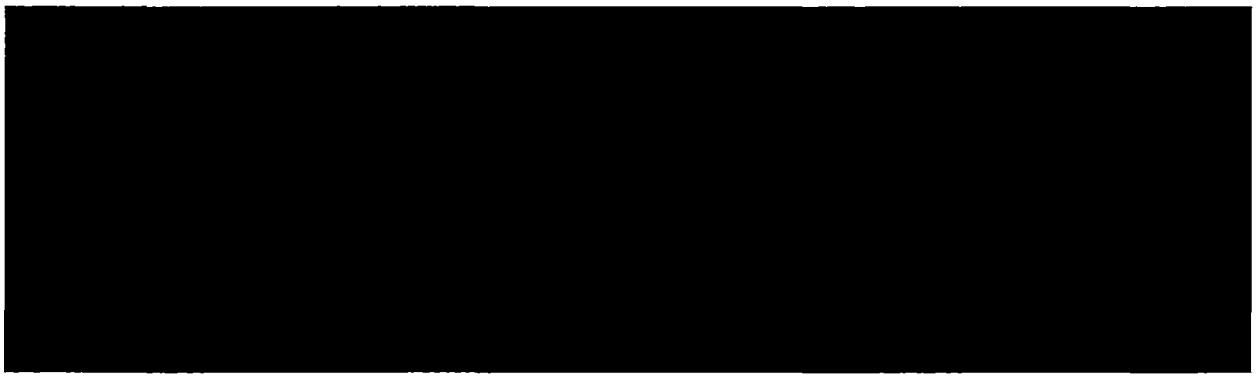

Table 5.2-6 SNF type dependent gamma sources for energy group i=3

Table 5.2-7 SNF type dependent gamma sources for energy group i=4

Table 5.2-8 SNF type dependent gamma sources for energy group i=5

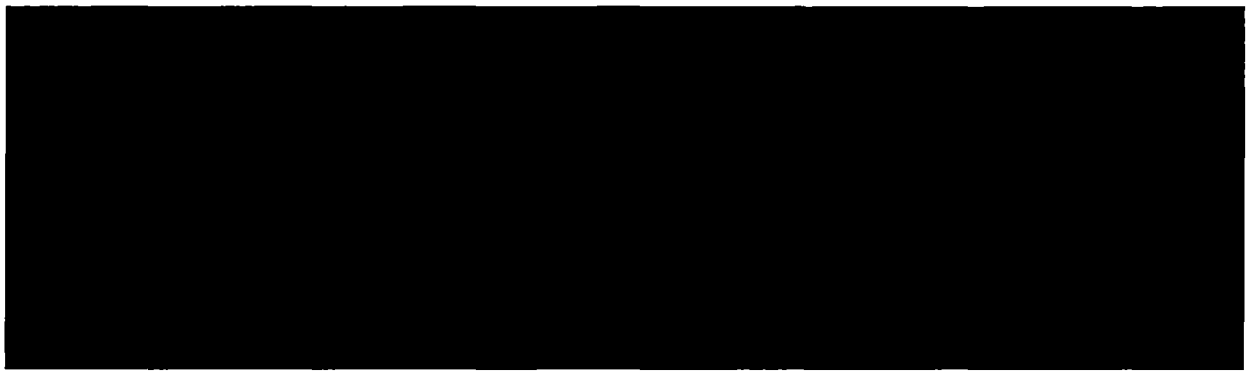

Table 5.2-9 SNF type dependent gamma sources for energy group i=6

Table 5.2-10 SNF type dependent gamma sources for energy group i=7

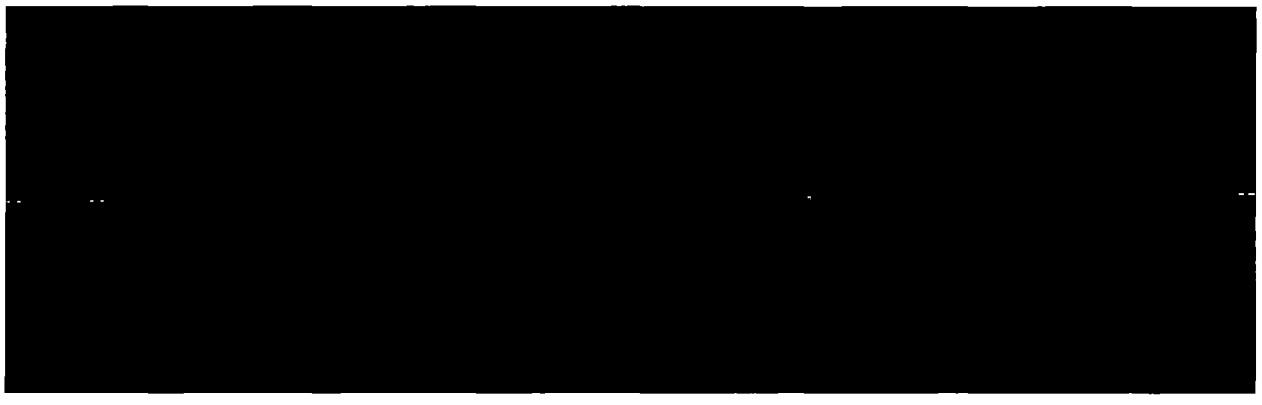

Table 5.2-11 SNF type dependent gamma sources for the bottom end fittings

Table 5.2-12 SNF type dependent gamma sources for the top end fittings

Table 5.2-13 SNF type dependent gamma sources for the plenum springs

Table 5.2-14 SNF type dependent gamma sources for the grid spacers

[redacted]

Table 5.2-15 Bounding gamma source for TR1

Gamma Source for Thermal Requirement 1		
Position Group		A to F
Decay Heat, W		260
γ1	$1/s/Mg_{HM}$	3.90E+15
γ2	$1/s/Mg_{HM}$	3.50E+14
γ3	$1/s/Mg_{HM}$	1.02E+14
γ4	$1/s/Mg_{HM}$	3.83E+12
γ5	$1/s/Mg_{HM}$	1.05E+11
γ6	$1/s/Mg_{HM}$	1.39E+10
γ7	$1/s/Mg_{HM}$	1.80E+09
Bottom End Fitting	1/s	1.38E+12
Top End Fitting	1/s	3.18E+11
Plenum Spring	1/s	2.97E+11

Table 5.2-16 Bounding gamma source for TR2

Gamma Source for Thermal Requirement 2							
Position Group		A	B	C	D	E	F
Decay Heat, W		150	200	450	200	330	200
γ1	$1/s/Mg_{HM}$	1.95E+15	2.87E+15	6.00E+15	2.87E+15	4.06E+15	2.87E+15
γ2	$1/s/Mg_{HM}$	1.99E+13	6.62E+13	6.35E+14	6.62E+13	8.49E+13	6.62E+13
γ3	$1/s/Mg_{HM}$	1.32E+13	4.34E+13	1.74E+14	4.34E+13	5.97E+13	4.34E+13
γ4	$1/s/Mg_{HM}$	6.88E+11	1.95E+12	6.33E+12	1.95E+12	2.70E+12	1.95E+12
γ5	$1/s/Mg_{HM}$	8.78E+09	1.32E+10	1.34E+11	1.32E+10	1.81E+10	1.32E+10
γ6	$1/s/Mg_{HM}$	8.74E+08	1.10E+09	1.91E+10	1.10E+09	1.52E+09	1.10E+09
γ7	$1/s/Mg_{HM}$	6.15E+07	1.11E+08	2.59E+09	1.11E+08	2.32E+08	1.11E+08
Bottom End Fitting	1/s	4.82E+10	4.22E+11	2.43E+12	4.22E+11	5.35E+11	4.22E+11
Top End Fitting	1/s	1.11E+10	9.74E+10	5.94E+11	9.74E+10	1.31E+11	9.74E+10
Plenum Spring	1/s	1.04E+10	9.09E+10	5.89E+11	9.09E+10	1.30E+11	9.09E+10

Table 5.2-17 Bounding gamma source for TR3

Gamma Source for Thermal Requirement 3							
Position Group		A	B	C	D	E	F
Decay Heat, W		150	230	450	230	230	210
γ1	1/s/Mg_{HM}	1.95E+15	3.42E+15	6.00E+15	3.42E+15	3.42E+15	3.03E+15
γ2	1/s/Mg_{HM}	1.99E+13	1.72E+14	6.35E+14	1.72E+14	1.72E+14	8.56E+13
γ3	1/s/Mg_{HM}	1.32E+13	7.33E+13	1.74E+14	7.33E+13	7.33E+13	5.11E+13
γ4	1/s/Mg_{HM}	6.88E+11	2.98E+12	6.33E+12	2.98E+12	2.98E+12	2.23E+12
γ5	1/s/Mg_{HM}	8.78E+09	2.44E+10	1.34E+11	2.44E+10	2.44E+10	1.43E+10
γ6	1/s/Mg_{HM}	8.74E+08	2.34E+09	1.91E+10	2.34E+09	2.34E+09	1.09E+09
γ7	1/s/Mg_{HM}	6.15E+07	3.24E+08	2.59E+09	3.24E+08	3.24E+08	1.22E+08
Bottom End Fitting	1/s	4.82E+10	9.30E+11	2.43E+12	9.30E+11	9.30E+11	5.49E+11
Top End Fitting	1/s	1.11E+10	2.15E+11	5.94E+11	2.15E+11	2.15E+11	1.27E+11
Plenum Spring	1/s	1.04E+10	2.00E+11	5.89E+11	2.00E+11	2.00E+11	1.18E+11

Table 5.2-18 Bounding energy release rate per Mg heavy metal

Decay Heat, W		150	200	210	230	260	330	450
γ1	MeV/s/Mg_{HM}	1.12E+15	1.65E+15	1.74E+15	1.97E+15	2.24E+15	2.33E+15	3.45E+15
γ2	MeV/s/Mg_{HM}	1.69E+13	5.63E+13	7.28E+13	1.46E+14	2.98E+14	7.22E+13	5.40E+14
γ3	MeV/s/Mg_{HM}	1.64E+13	5.42E+13	6.39E+13	9.16E+13	1.27E+14	7.47E+13	2.18E+14
γ4	MeV/s/Mg_{HM}	1.20E+12	3.41E+12	3.90E+12	5.22E+12	6.70E+12	4.73E+12	1.11E+13
γ5	MeV/s/Mg_{HM}	1.98E+10	2.97E+10	3.22E+10	5.49E+10	2.36E+11	4.07E+10	3.02E+11
γ6	MeV/s/Mg_{HM}	2.40E+09	3.02E+09	3.00E+09	6.44E+09	3.82E+10	4.18E+09	5.25E+10
γ7	MeV/s/Mg_{HM}	2.15E+08	3.89E+08	4.27E+08	1.13E+09	6.30E+09	8.12E+08	9.07E+09

5.2.2 Neutron Source

The neutron sources are determined in an analogous way as the gamma ones. The two relevant neutron energy spectra – from spontaneous fission and from (α,n) reactions – exhibit different axial distributions due to the weaker burn-up towards the ends of the SNF (see Figure 5.2-2). It is checked, whether energy distributions of these two spectra could be realised by internal means of the MCNP code system (continuous energy distributions). While the energy spectrum from the spontaneous fission could be nicely described by the Watt spectrum from ^{244}Cm (parameters a = 0.902523 MeV, b = 3.72033 MeV^{-1}, see [4]), for the (α,n) energy spectrum no internal function has been found as it is rather a modified Maxwell distribution currently not implemented in the code. Finally, for (α,n)-neutrons a histogram function generated by ORIGAMI is utilised in the analysis.

The subcritical neutron multiplication is properly taken into account during particle transport with MCNP. [redacted]

[redacted]

Figure 5.2-2 Axial neutron source strength distributions

The nodal neutron source is determined in the same fashion (simultaneously) as the gamma one and is shown in Table 5.2-19 for spontaneous fission and in Table 5.2-20 for the (α,n)-reactions. The bounding neutron source for each loading pattern TR1 to TR3 is constructed from the maximum individual sources corresponding to the selected decay heat. The final sources used for the shielding analysis are reported in Table 5.2-21 for TR1, in Table 5.2-22 for TR2, and in Table 5.2-23 for TR3.

The total neutron sources for spontaneous fission and for (α,n)-reactions as a function of energy are displayed in Table 5.2-24 and Table 5.2-25, respectively.

[redacted]

Table 5.2-19 SNF type dependent neutron sources from spontaneous fission

[redacted]

Table 5.2-20 SNF type dependent neutron sources from (α,n)-reactions

[redacted]

Table 5.2-21 Bounding neutron source for TR1

Neutron Source for Thermal Requirement 1		
Position Group		**A to F**
Decay Heat, W		**260**
(α,n)-neutrons	$1/s/Mg_{HM}$	1.85E+07
spontaneous fission	$1/s/Mg_{HM}$	1.02E+09

Table 5.2-22 Bounding neutron source for TR2

Neutron Source for Thermal Requirement 2							
Position Group		**A**	**B**	**C**	**D**	**E**	**F**
Decay Heat, W		**150**	**200**	**450**	**200**	**330**	**200**
(α,n)-neutrons	$1/s/Mg_{HM}$	1.27E+07	1.53E+07	2.75E+07	1.53E+07	2.24E+07	1.53E+07
spontaneous fission	$1/s/Mg_{HM}$	4.26E+08	7.69E+08	2.47E+09	7.69E+08	1.60E+09	7.69E+08

Table 5.2-23 Bounding neutron source for TR3

Neutron Source for Thermal Requirement 3							
Position Group		**A**	**B**	**C**	**D**	**E**	**F**
Decay Heat, W		**150**	**230**	**450**	**230**	**230**	**210**
(α,n)-neutrons	$1/s/Mg_{HM}$	1.27E+07	1.69E+07	2.75E+07	1.69E+07	1.69E+07	1.58E+07
spontaneous fission	$1/s/Mg_{HM}$	4.26E+08	8.01E+08	2.47E+09	8.01E+08	8.01E+08	8.43E+08

Table 5.2-24 Bounding spontaneous fission neutron source as a function of energy

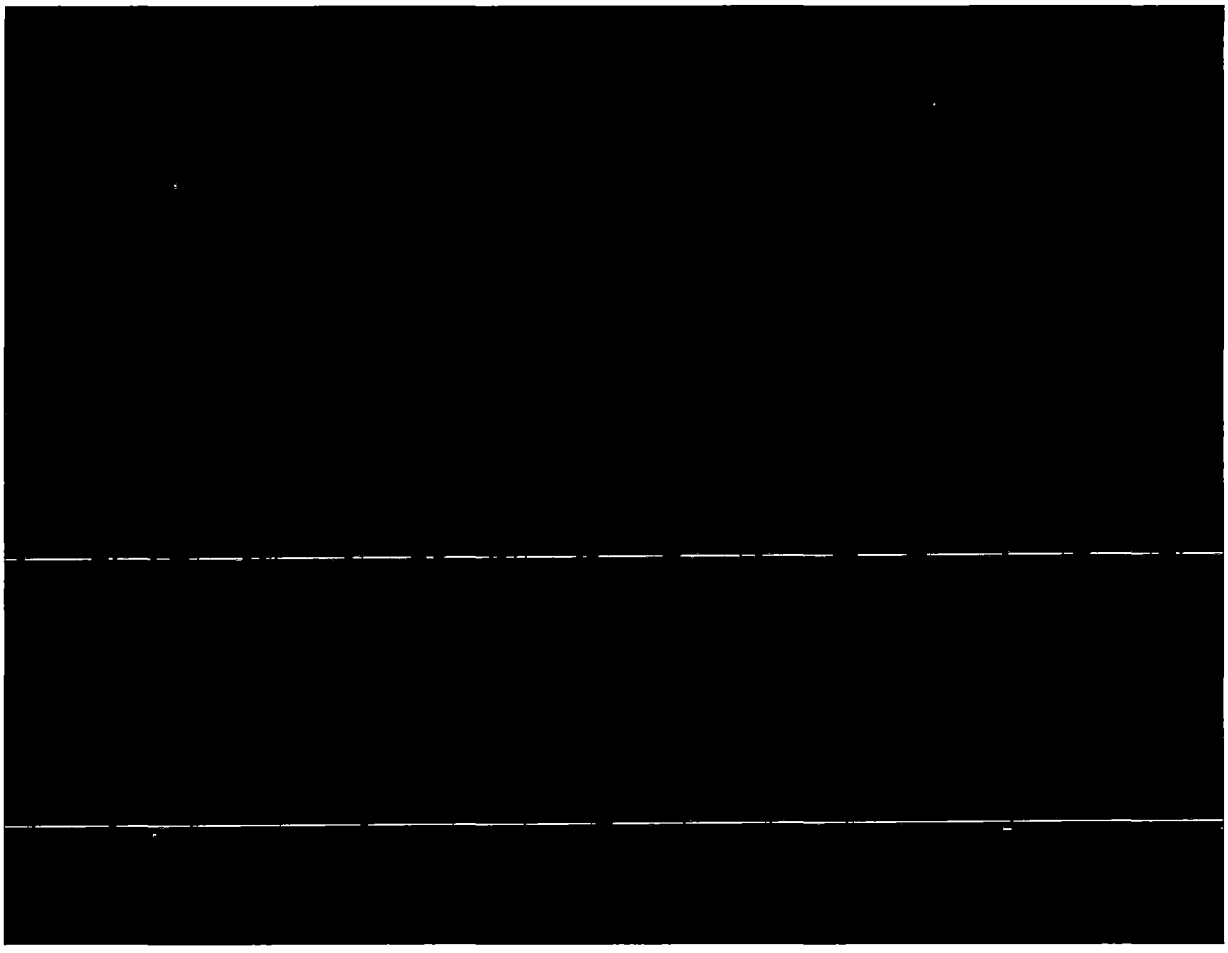

Table 5.2-25 Bounding (α,n)-reaction neutron source as a function of energy

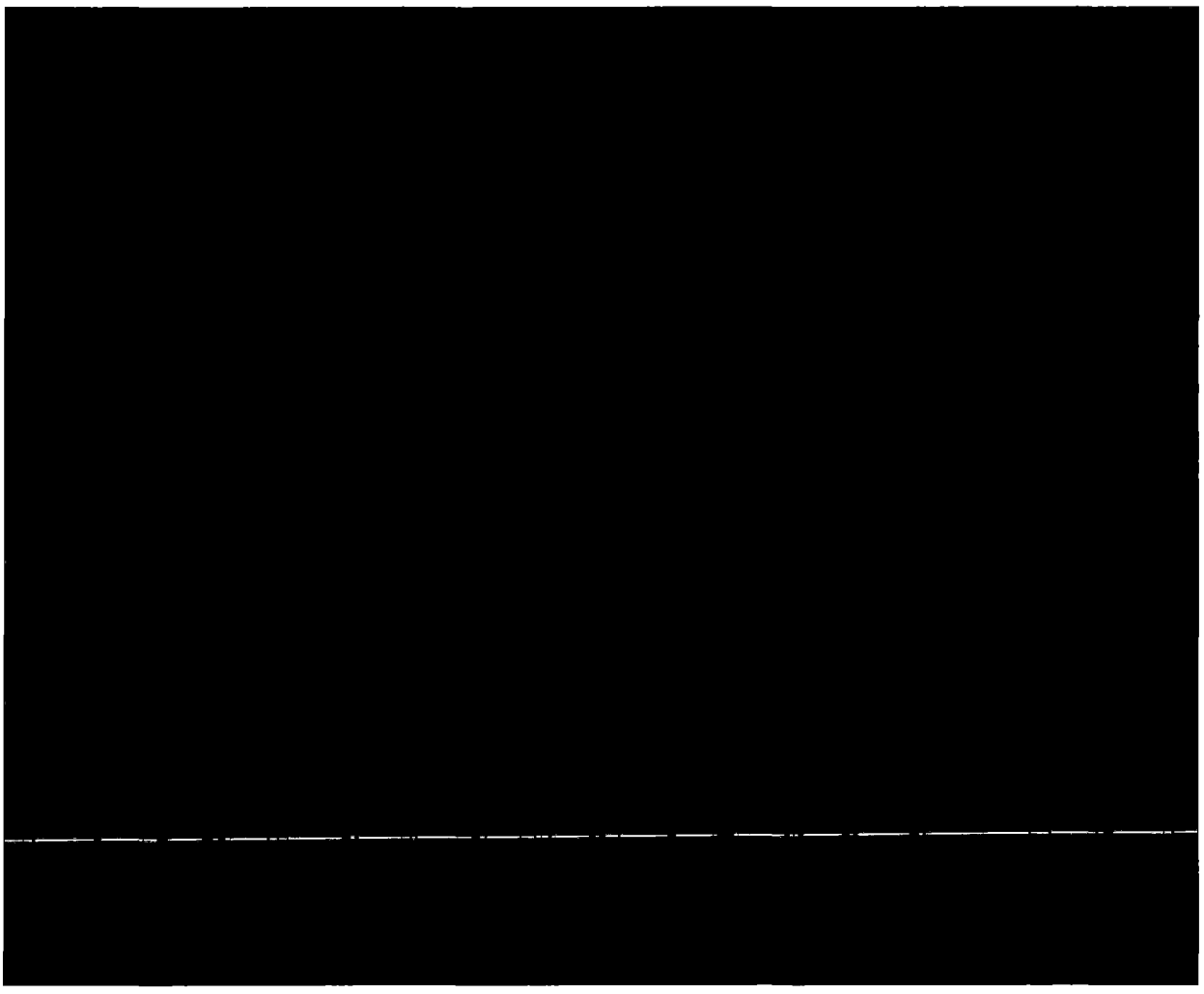

List of References

[1] NUREG/CR-7224, Axial Moderator Density Distributions, Control Blade Distributions, and Axial Burnup Distributions for Extended BWR Burnup Credit, ORNL/TM-2015/544

[2] CAL-DSU-NU-000005, Rev. 00A, CSNF Disposal Container, BWR Axial Profile, OCRWM, 2004

[3] PNL-6906 Vol. 1 to Vol. 3, UC-85, A. Luksic, Spent Fuel Assembly Hardware: Characterization and 10 CFR 61 Classification for Waste Disposal, 1989

[4] C.J. Werner (ed.), MCNP User's Manual - Code Version 6.2, LA-UR-17-29981, 2017

5.3 Shielding Model

	Name, Function	Date	Signature
Prepared	[redacted]		
Reviewed			

The shielding analysis of the CASTOR® geo69 is performed with MCNP6 2.0 (see Appendix 5-1). A separate MCNP calculation is performed for each position group A to F for every twelve sources (seven gamma groups from the fuel pellet stack, two neutron spectra, top end fittings, bottom end fittings, and plenum springs).

In this Section, the shielding models for NCT as well as for the HAC are discussed. The information about individual parts of the cask and the materials used in models are described.

5.3.1 Configuration of Source and Shielding

In total, seven shielding models of the package are analysed taking into account possible effect of the test of the packaging under different transport conditions. Especially under HAC there are two consequences affecting the shielding material. These are the changes to the moderator material as a result of the design basis fire, and damage of the impact limiters as a result of the 9 m drop. The shielding models evaluated are as follows:

Section 1.3 provides the drawings describing the CASTOR® geo69 package. These drawings are used to create the MCNP models used in the shielding calculations.

The elevation sections of the NCT and HAC models are presented in Figure 5.3-1. The axial null of the scale corresponds to the cask bottom edge (lower edge of the closure plate). Being of low relevance for the shielding analysis, the screws, compression springs and gaskets are not modelled. When appropriate they are substituted by air, e.g. the heads of the lid bolting or the top of the basket, or by surrounding material, e.g. inside the lid.

For the model with fuel reconfiguration under NCT an additional fuel region with 3 % of the source strength has been considered at the bottom of the canister (see Figure 5.3-2, left hand side) or close to its top in the region, where the shielding performance of the package is expected to be minimal [redacted]. The standard NCT sources attributed to the fuel pellet stack remain and contribute to the external dose rate with a strength of 97 %. The end fittings and plenum springs from the standard NCT model contribute with a full strength. The rubbleised mixture of fuel and cladding is relocated within the basket cell, the mass packing fraction for the rubble is 0.58 [1].

Under HAC, a similar approach is used. The difference is that a 100 % fuel failure is assumed. As no damage of the basket structures occurs (see section 2.7), the rubble consisting of fuel and cladding (the rest of the SNF structures is conservatively neglected) remains in the basket cell (see Figure 5.3-3).

The principal components of the shielding model are explained in the following subsections. The methods and main measurements are presented.

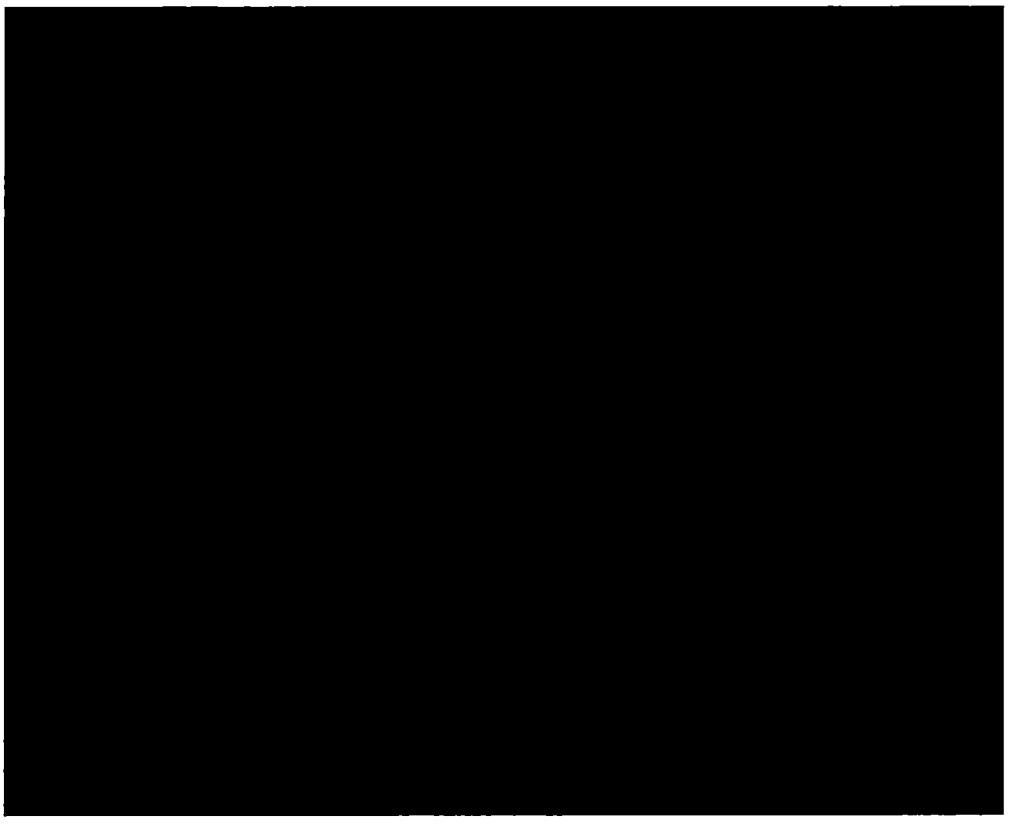

Figure 5.3-1 Elevation sections of NCT (left) and HAC (right) models in the trunnion plane

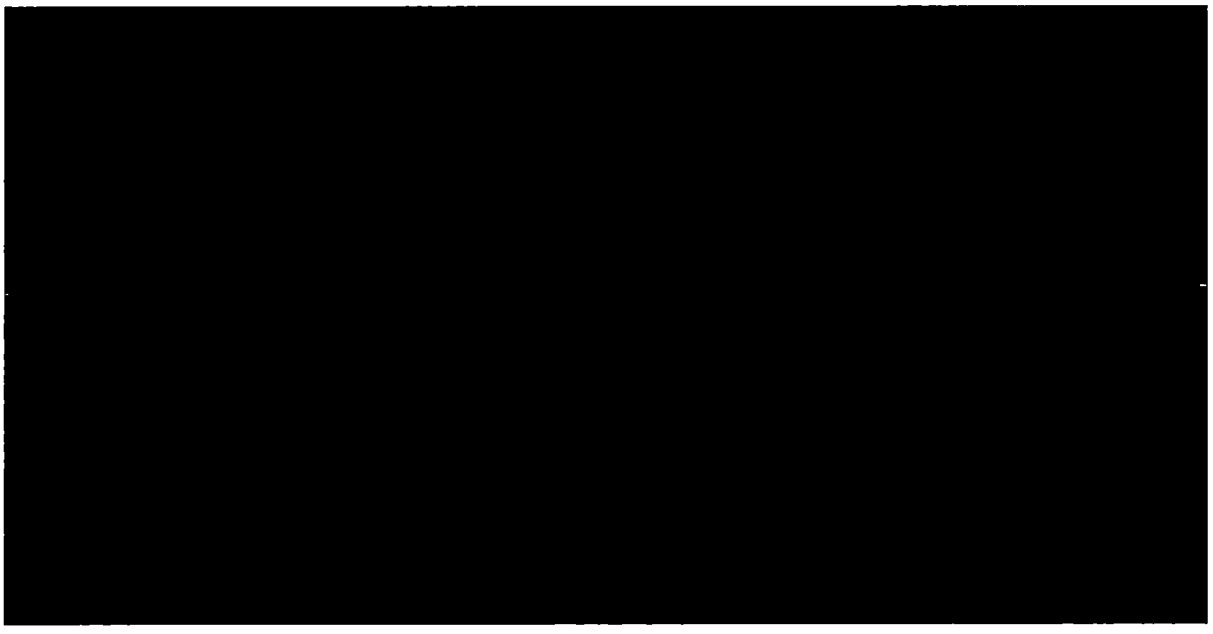

Figure 5.3-2 Source position in the NCT fuel failure model – at the bottom of the canister (left) and in the region with the expected minimum shielding performance (right)

Figure 5.3-3 HAC rubble at the bottom (left) and at the top (right) of the package

5.3.1.1 Spent Fuel

All 69 SNF are placed into the corresponding basket cells. Conservatively, Atrium-10A design is selected for the shielding model. The main reason for this is the lattice configuration. With the large water channel and part length rods the self-shielding effects are minimised. Additionally, this fuel design has the thinnest cladding and fuel channel thickness among other SNF.

The fuel rods including cladding are modelled individually. The cross section through the fuel model in its lower part, where all the rods are present, is presented in Figure 5.3-4.

It is assumed that the SNF are complete and do not contain dummy rods. Possible loss of self-shielding due to possible absence of fuel rods is overcompensated by the actual loss of source strength at this location.

The end fittings enter the calculations in a simplified fashion as tie plates only. This approach is justified, since the source strength is scaled with the full mass of the end fittings. The plenum springs are modelled homogenised as steel pieces with reduced density ( ).

Figure 5.3-4 Spent fuel model (dimensions in mm)

5.3.1.2 Basket

The basket in the shielding model (see Figure 5.1-1) consists of structure sheets made of NEXUS® 3000 material, outer sheets made of steel (SA-240 316L), and round segments made of aluminium (SB-209 5454). The mounting elements are left out and replaced by air. As discussed in section 5.1.1.1 and shown in Figure 5.3-1, the thicknesses of the sheets are minimised and the outer diameter of the round segments is reduced according to the design tolerances.

5.3.1.3 Shielding Elements

Shielding elements out of aluminium (SB-209 5454) are modelled as solid blocks (see Figure 5.3-5).

Figure 5.3-5 Shielding element

5.3.1.4 Canister

[redacted] The elevation view of the canister is presented in Figure 5.3-6.

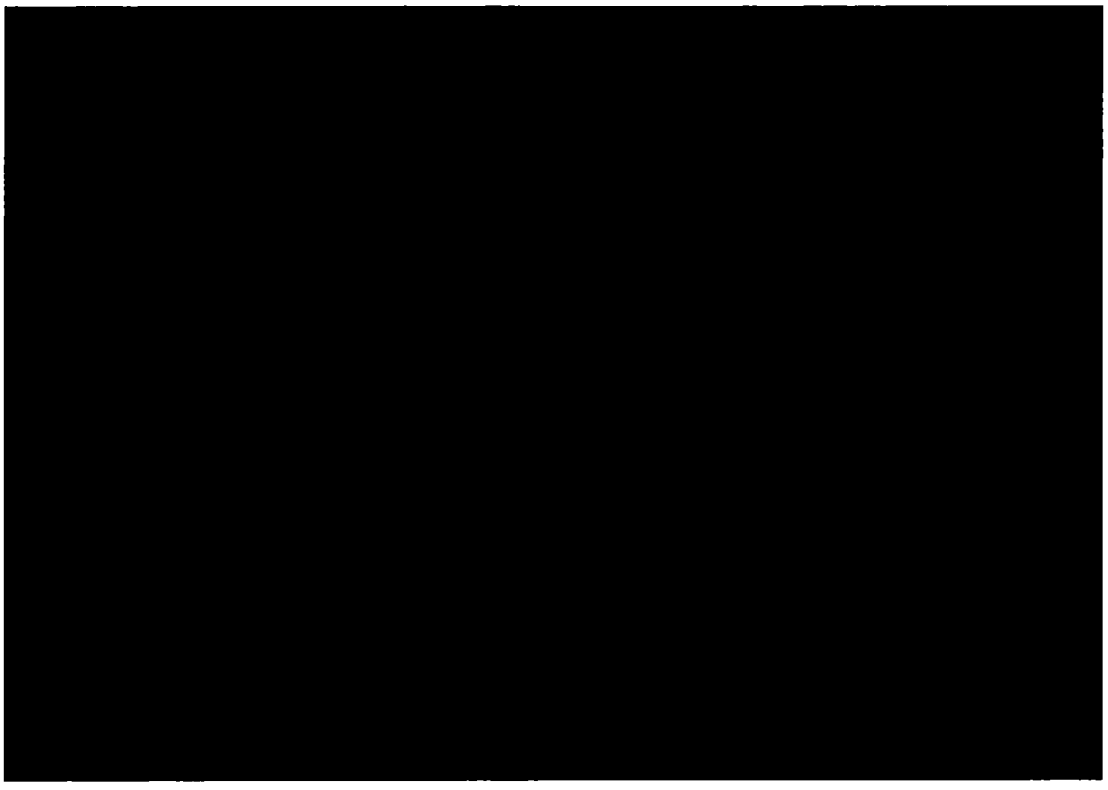

Figure 5.3-6 Canister elevation view (dimensions in mm)

5.3.1.5 Cask Body and Lid

The cask body with lid is modelled with the unfavourable combination of the tolerances in radial direction. Several so-called splitting levels (thin black lines in the model illustrations) are implemented into various components of the calculation model in order to increase its statistical performance using variance reduction techniques.

The trunnions are modelled as solid pieces made of steel (upper trunnions, SA-479M 414) or DCI (lower tilting studs), the corresponding flattenings of the cask body possess minimum dimensions.

The cask lid is modelled with the lid moderator plate mounted on its lower surface. The bolting of the lid is not modelled; the bolt heads are replaced with air.

5.3.1.6 Cooling Fins

The cooling fins are modelled explicitly (see Figure 5.3-7). It was found that homogenisation of this areas does not necessarily lead to conservative evaluation. [redacted]

Figure 5.3-7 Cooling fins (dimensions in mm)

5.3.1.7 Moderators

The moderator rods made of polyethylene ([redacted]) are modelled (NCT only) [redacted] They are analysed in two different configurations (when modelled at all), the design geometry representing the situation shortly after loading and the state of thermal equilibrium (see Figure 5.1-4 and Figure 5.1-5). Divergent from the design density of [redacted] the resulting polyethylene at equilibrium is conservatively reduced according to the maximum temperature over the entire length of the rod (no axial temperature profile is assumed, see section 2.2). For the moderator plates (bottom and lid ones) only the density is reduced in equilibrium state, no expansion is implemented.

5.3.1.8 Impact Limiters

Both impact limiters are modelled (NCT only) with their principal dimensions. The model includes (see Figure 5.1-2) foam filling [redacted], spacers and load distribution plate (aluminium EN AW-7020), [redacted] foam is assumed to fill the volume homogeneously. [redacted] This dimension is, however, not taken into account when discussing the distance of 1 m and 2 m from the outer surface of the package. The reference external surface of the package is assumed to coincide with the external surface of the cask at the fin tip.

[redacted]

5.3.1.9 Environment and Detectors

[redacted]

The information about particular dose rates is gained from detectors positioned all around the cask (see Figure 5.3-8). The information in each detector cell is readily available; this analysis however concentrates under NCT on an evaluation of the dose rates at the package surface, and at distances of 1m and of 2 m from the external surface of the package. For the HAC a distance of 1 m from the package surface is addressed. Besides this geometry-independent mesh of detectors, separate volumetric detectors are modelled in order to control the calculation process.

[redacted]

[redacted]

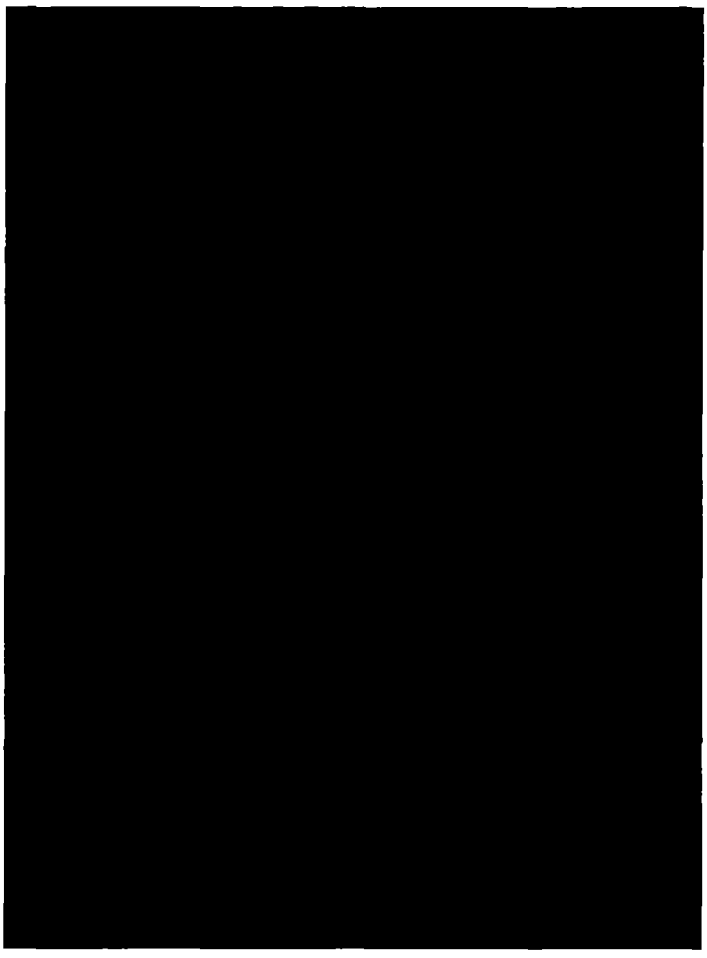

Figure 5.3-8 Detector raster (mesh tallying)

5.3.2 Material Properties

Compositions and densities of the materials used in the shielding model are presented in Table 5.3-1. For the moderator rods two densities are given, the nominal one for the shielding configuration shortly after loading, and the low one for the equilibrium configuration. The steel specification for the retention ring (SA-182M F316) is very similar to that of the SA-240M 316, for this reason no new material has been introduced.

The materials in Table 5.3-1 are arranged from inside to outside.

For the moderator material the temperature effects are studied as discussed in section 5.1.1.2.

[redacted]

The design basis for the material data is given in section 2.2.1.

Table 5.3-1 Material properties in the shielding model

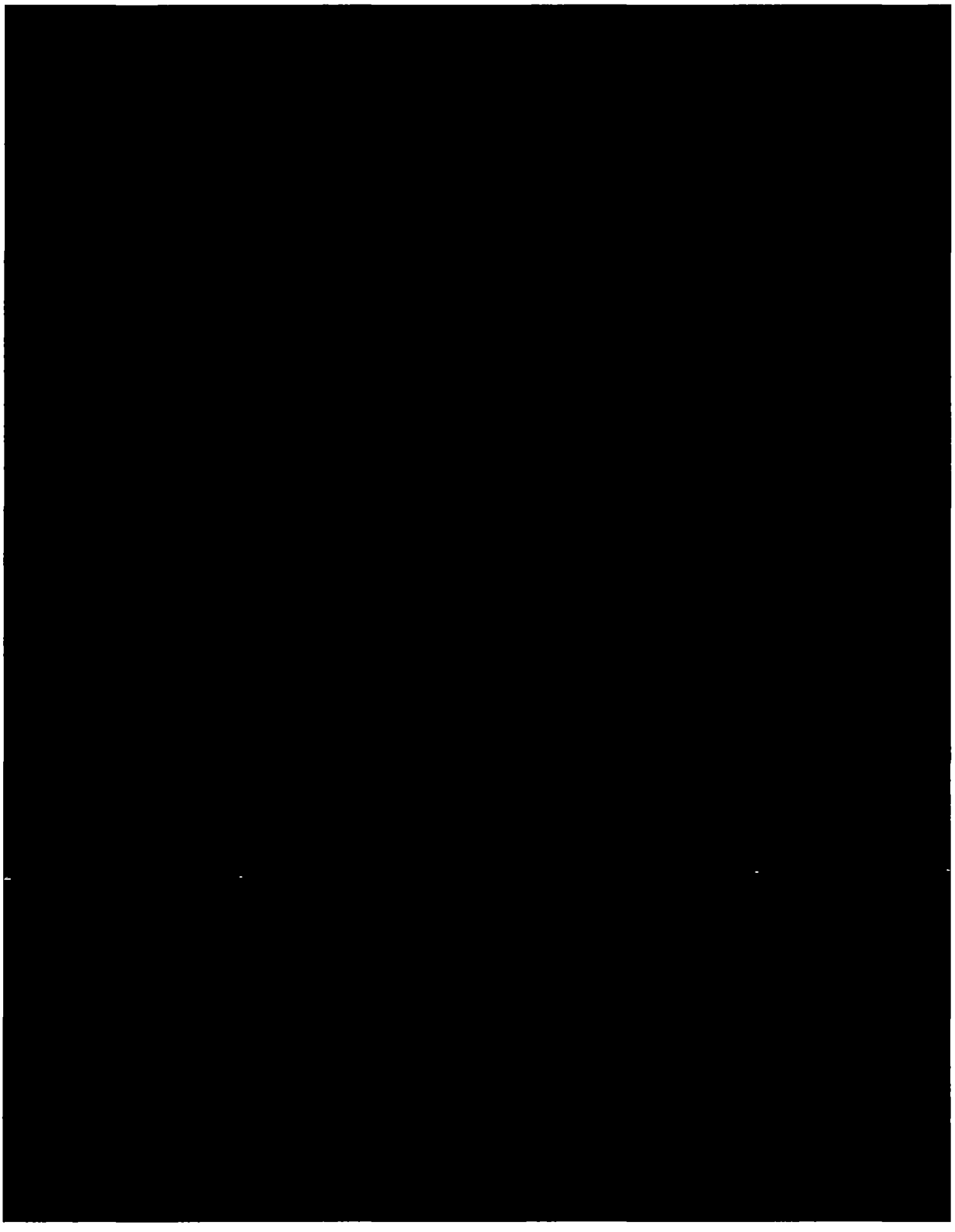

Table 5.3-1 Material properties in the shielding model (continued)

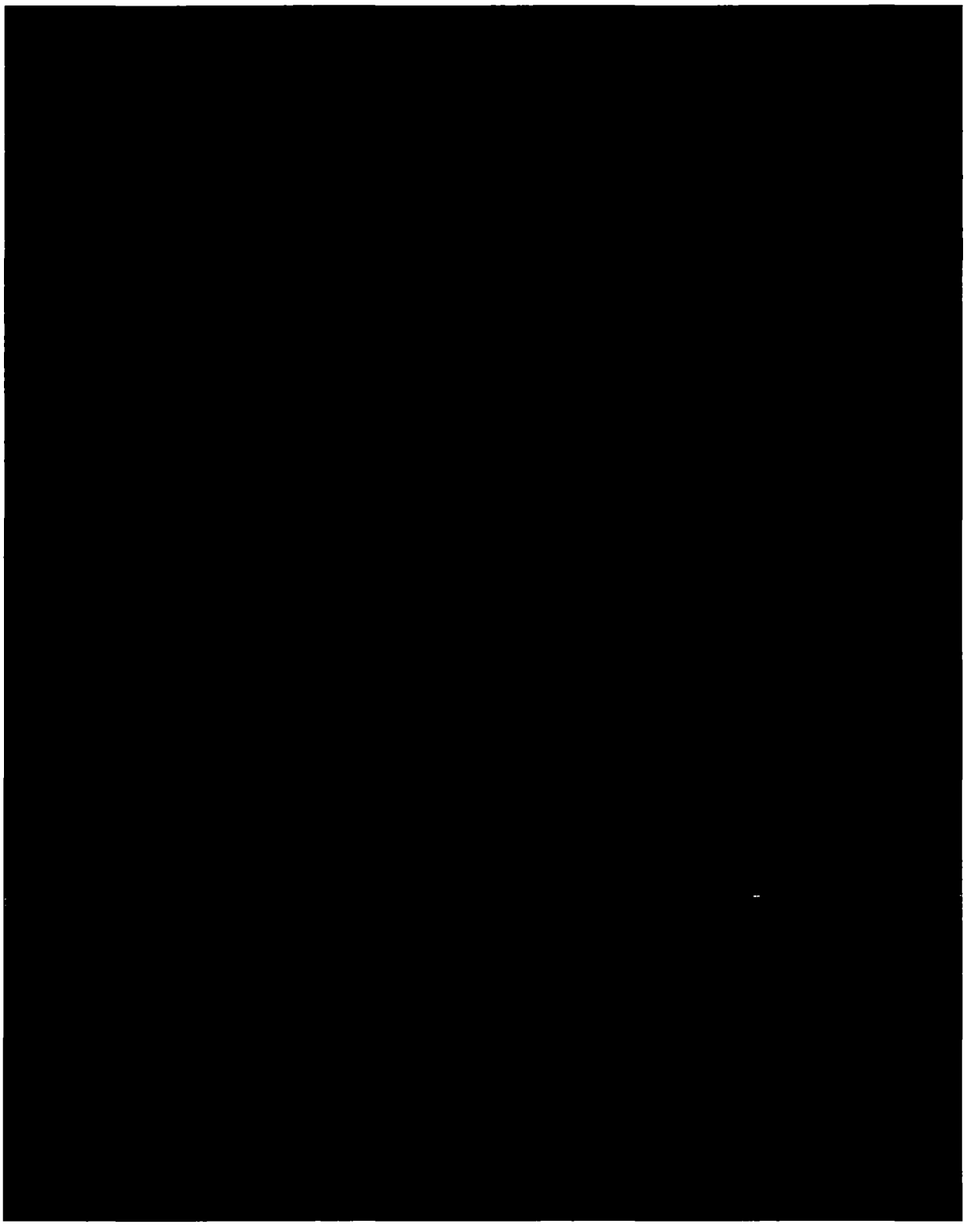

Table 5.3-1 Material properties in the shielding model (continued)

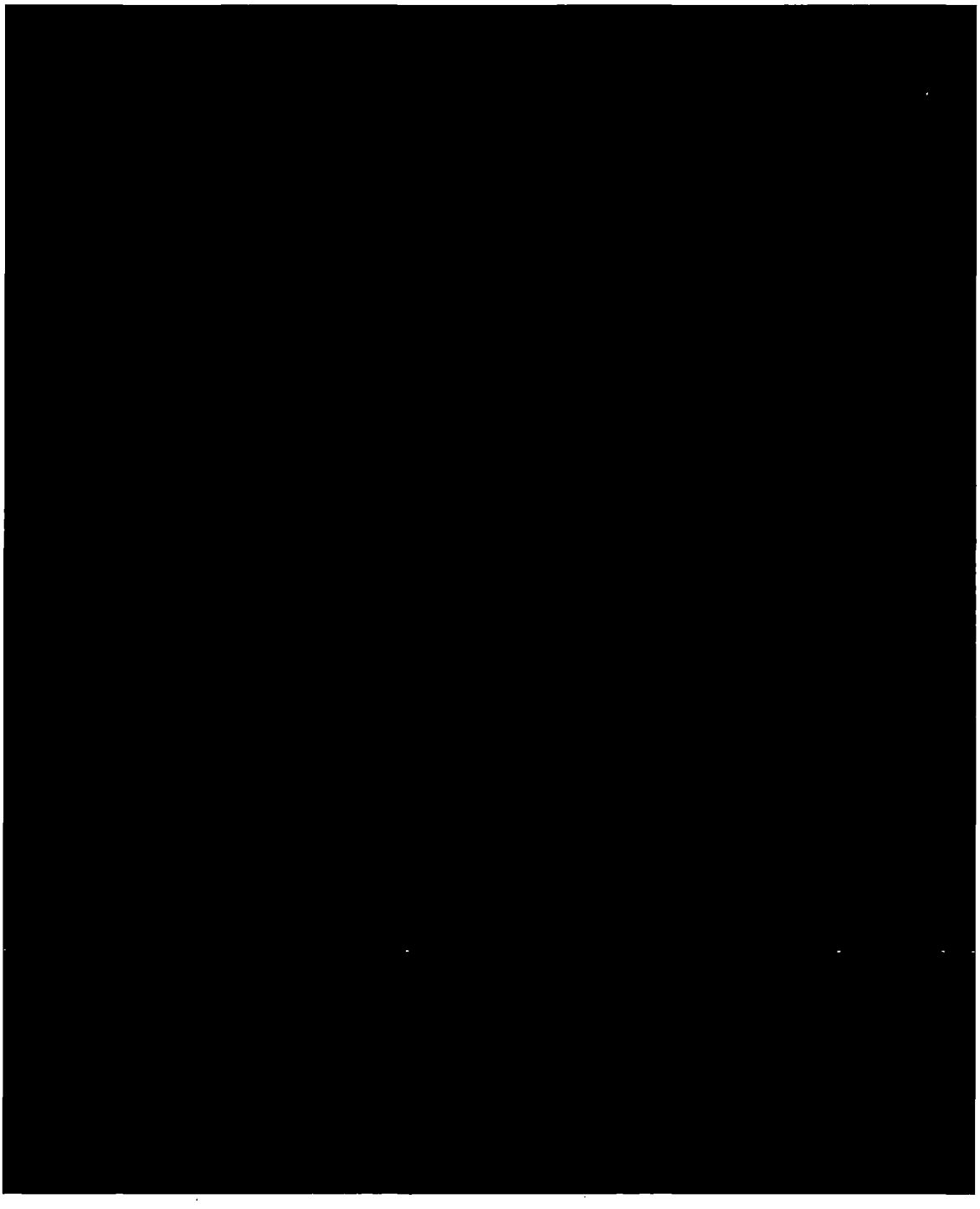

List of References

[1] NUREG-2224, Dry Storage and Transportation of High Burnup Spent Fuel (Draft for Comment), Washington, DC, July 2018

5.4 Shielding Evaluation

	Name, Function	Date	Signature
Prepared	[redacted]		
Reviewed			

5.4.1 Methods

As discussed in section 5.3 the MCNP6 code is used for the shielding analysis. The cross section data are based on ENDF/B-VII data. The MCNP code system is benchmarked against experimental data for a broad spectrum of gamma [1] and neutron [2] problems. Described shielding problems cover a wide range of energies and material compositions and involve both scattering and deep penetration. A good agreement between measured and calculated values has been demonstrated for all the validation scenarios.

The dose rates are calculated using volumetric mesh tallies (f4), multiplied by an appropriate flux-to-dose-rate conversion factor, heavy metal mass of the SNF in the shielding model (see section 5.3.1.1), and by the total source strength (per megagram heavy metal) for every radiation source term. Since the mesh is stretched around the entire geometry of the package, the locations of dose rate maxima are determined explicitly. Its use also allows for the evaluation of the wrapping dose rate distributions.

The NCT and HAC calculations are performed separately for six position groups introduced in Figure 5.0-1. The elementary external dose rates from different position groups, folded with corresponding sources and superposed, allow for the evaluation of an arbitrary loading pattern provided it consists of no more than six position groups. In this evaluation, the loading patterns TR1 to TR3 are assessed.

[redacted]

Each set of the MCNP calculations is foreseen with a message digest (md5) providing its unique identification.

5.4.2 Input and Output Data

Sample MCNP input files used to compute external dose rates, one for gamma radiation (NCT) und one for neutrons (HAC), are shown in Appendix 5-4. The output files being too large in size to be printed are presented in a shortened form (Appendix 5-5).

5.4.3 Flux-to-Dose-Rate Conversion

The conversion of the values calculated with MCNP for the spectral neutral and gamma flux density to the ambient equivalent dose is performed with the flux-to-dose-rate conversion factors according to ANSI/ANS-6.1.1-1977 [3]. The conversion factors are exhibited in Table 5.4-1 and Table 5.4-2 for gamma radiation and neutrons, respectively.

Table 5.4-1 Conversion factors for gamma radiation

Gamma Energy, MeV	Conversion Coefficient (Including Quality Factor), mSv/h/(γ/cm^2·s)	Gamma Energy, MeV	Conversion Coefficient (Including Quality Factor), mSv/h/(γ/cm^2·s)
0.01	3.96E-05	1.4	2.51E-05
0.03	5.82E-06	1.8	2.99E-05
0.05	2.90E-06	2.2	3.42E-05
0.07	2.58E-06	2.6	3.82E-05
0.1	2.83E-06	2.8	4.01E-05
0.15	3.79E-06	3.25	4.41E-05
0.2	5.01E-06	3.75	4.83E-05
0.25	6.31E-06	4.25	5.23E-05
0.3	7.59E-06	4.75	5.60E-05
0.35	8.78E-06	5	5.80E-05
0.4	9.85E-06	5.25	6.01E-05
0.45	1.08E-05	5.75	6.37E-05
0.5	1.17E-05	6.25	6.74E-05
0.55	1.27E-05	6.75	7.11E-05
0.6	1.36E-05	7.5	7.66E-05
0.65	1.44E-05	9	8.77E-05
0.7	1.52E-05	11	1.03E-04
0.8	1.68E-05	13	1.18E-04
1	1.98E-05	15	1.33E-04

Table 5.4-2 Conversion factors for neutrons

Neutron Energy, MeV	Conversion Coefficient (Including Quality Factor), mSv/h/(n/cm^2-s)
2.50E-08	3.67E-05
1.00E-07	3.67E-05
1.00E-06	4.46E-05
1.00E-05	4.54E-05
1.00E-04	4.18E-05
1.00E-03	3.76E-05
0.01	3.56E-05
0.1	2.17E-04
0.5	9.26E-04
1	1.32E-03
2.5	1.25E-03
5	1.56E-03
7	1.47E-03
10	1.47E-03
14	2.08E-03
20	2.27E-03

5.4.4 External Radiation Levels

The external radiation levels calculated with MCNP for each individual detector are modified by the corresponding statistical uncertainties provided by MCNP in the same tally. Thereby, instead of using a Gaussian error propagation, two standard deviations of MCNP are conservatively added to every single tallied value (penalising error propagation).

It is found that all the dose rates are below the regulatory limits assuming transport under exclusive use.

5.4.4.1 Normal Conditions of Transport

Table 5.4-3 through Table 5.4-5 provides the maximum external dose rates for three loading patterns assuming the packaging shortly after loading (cold model). The moderator material is at room temperature. The md5 of these calculations is 3ce64279a9e39bda7b877b207245d4a6. The uncertainties from the penalising error propagation are included. [redacted]

The dose rate limit at 1 m from the surface of the package is exceeded for all three loading patterns (bounding sources), which hints on the exclusiveness of the transportation. The dose rate

limit for all loading patterns is much more exploited at 2 m from the surface of the package compared to its surface.

[redacted]

The dose rate distributions on the surface of the package are shown in Figure 5.4-1. [redacted]

Assuming the radiation from fuel only, the maximum of the dose rate is observed close to the mid-plane of the package. [redacted] The dose rate distribution at 2 m from the surface of the package does not reveal any irregularities, and the maximum is observed as expected close to mid-plane of the package (see Figure 5.4-2).

During the calculations, we adjust the run time of the particle transport so that the resulting statistical uncertainties do not exceed 2 % at any point 2 m from the surface of the package. It is typically sufficient to guarantee a reasonable uncertainty on the surface of the package as well. Figure 5.4-3 displays fractional standard deviations of the calculated dose rates on the surface of package (see Figure 5.4-3, left) and in 2 m from the surface of the package (see Figure 5.4-3, right).

The dose rate distributions on the bottom and lid sides of the package (see Figure 5.4-4) exhibit a maximum on the middle axis of the cask (independent on the loading pattern). The absolute values are very low compared to the shell side of the package (a few µSv/h on the surface), so that the normally occupied location, e.g. by the vehicle driver, anticipated on the lid side of the package does not come in the nearness of the dose rate limit.

The dose rate distributions for other two loading patterns (TR2 and TR3) do not exhibit any particularities and are quite similar in shape (see Figure 5.4-5 for TR2 and Figure 5.4-6 for TR3).

Table 5.4-3 Maximum external dose rates for the cold shielding model under NCT (TR1)

Table 5.4-4 Maximum external dose rates for the cold shielding model under NCT (TR2)

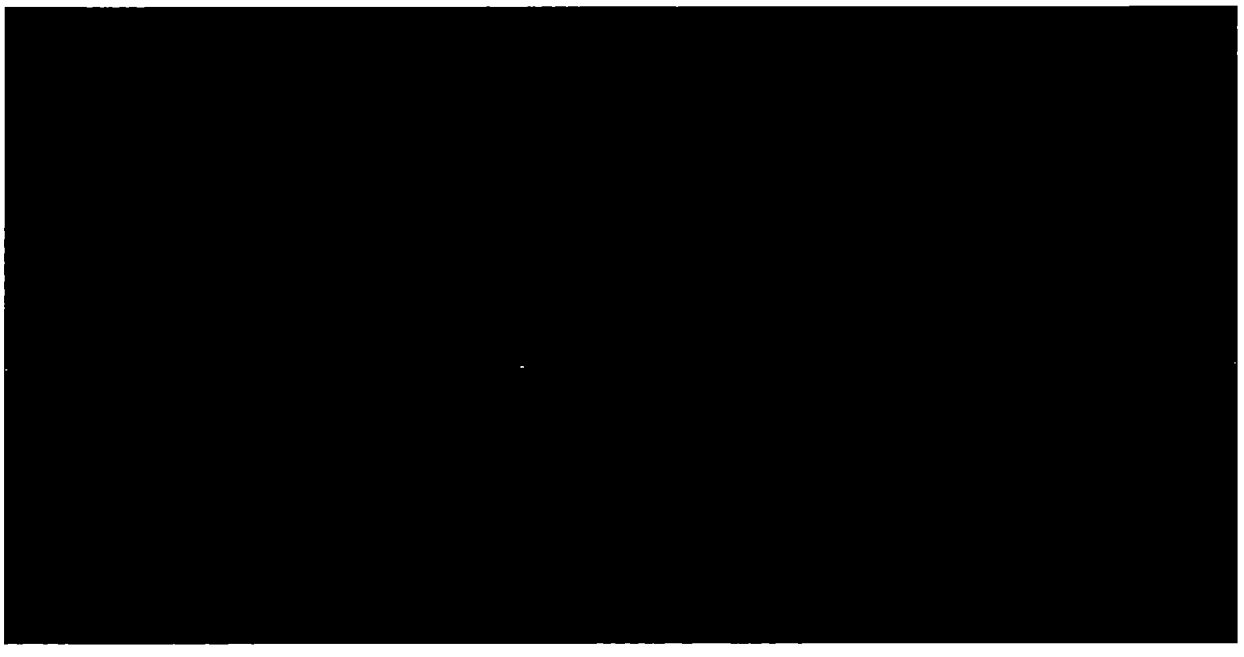

Table 5.4-5 Maximum external dose rates for the cold shielding model under NCT (TR3)

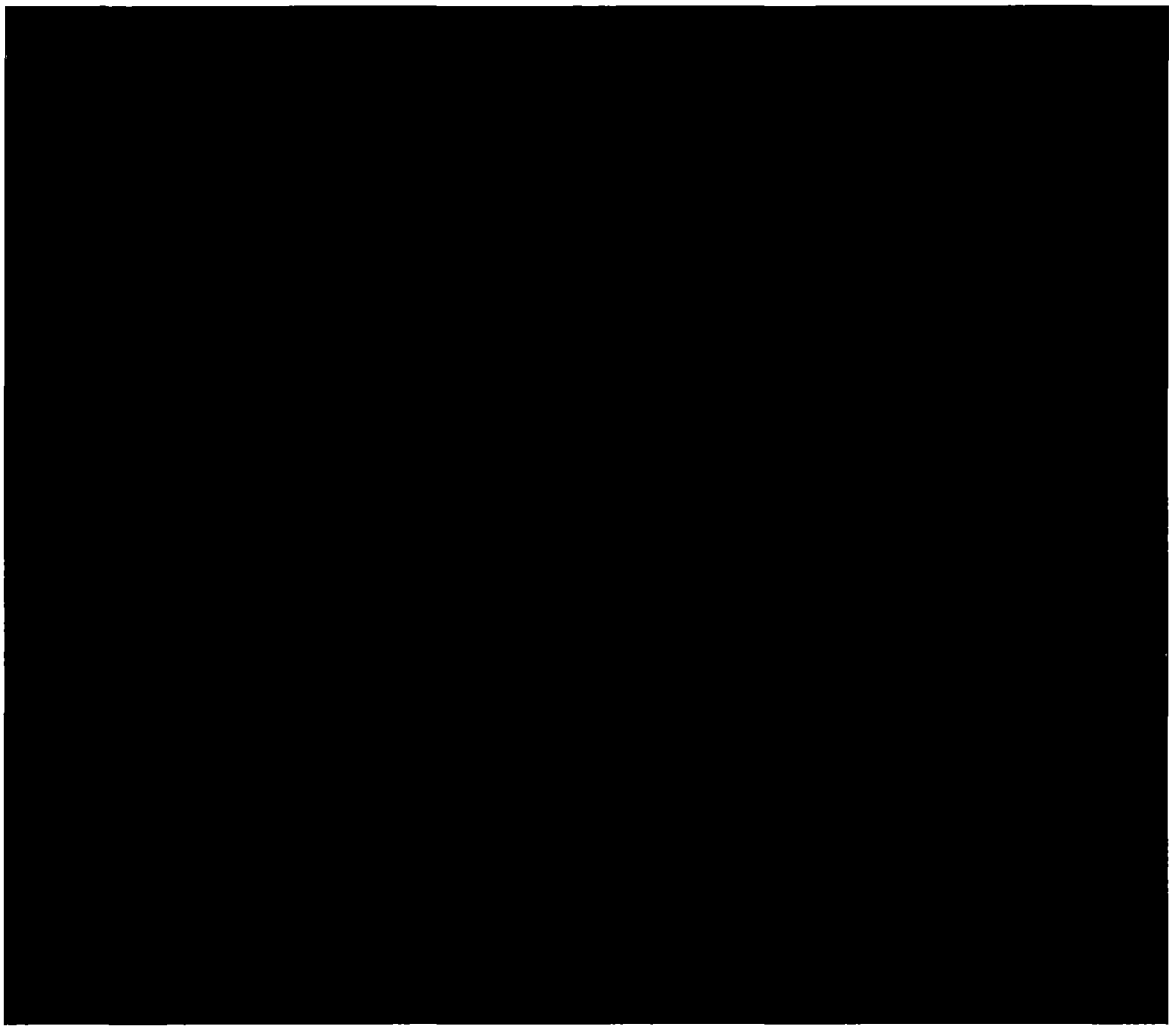

Figure 5.4-1 Dose rate distributions (TR1, cold model) at the surface of the package in mSv/h: total (top left), neutron (top right), fuel gamma (bottom left), and hardware gamma (bottom right)

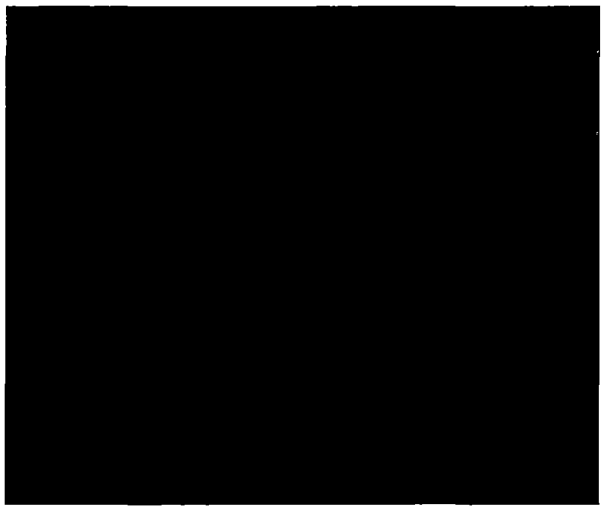

Figure 5.4-2 Dose rate distribution (TR1, cold model) at 2 m from the surface of the cask in mSv/h

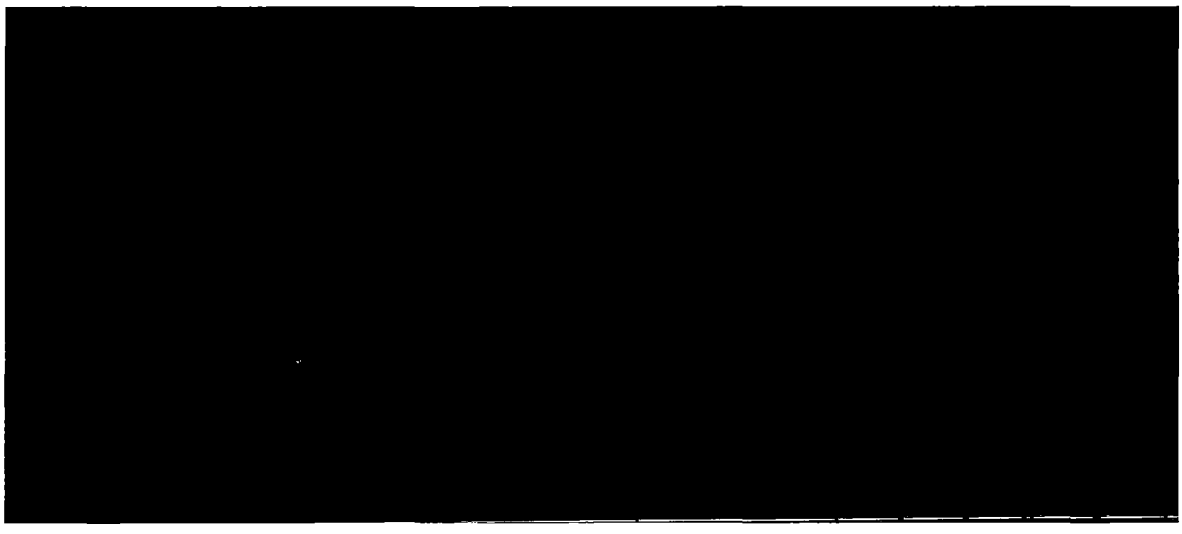

Figure 5.4-3 Fractional standard deviation distributions at the surface of the package (left) and in 2 m from the package surface (right) for the cold shielding model (TR1)

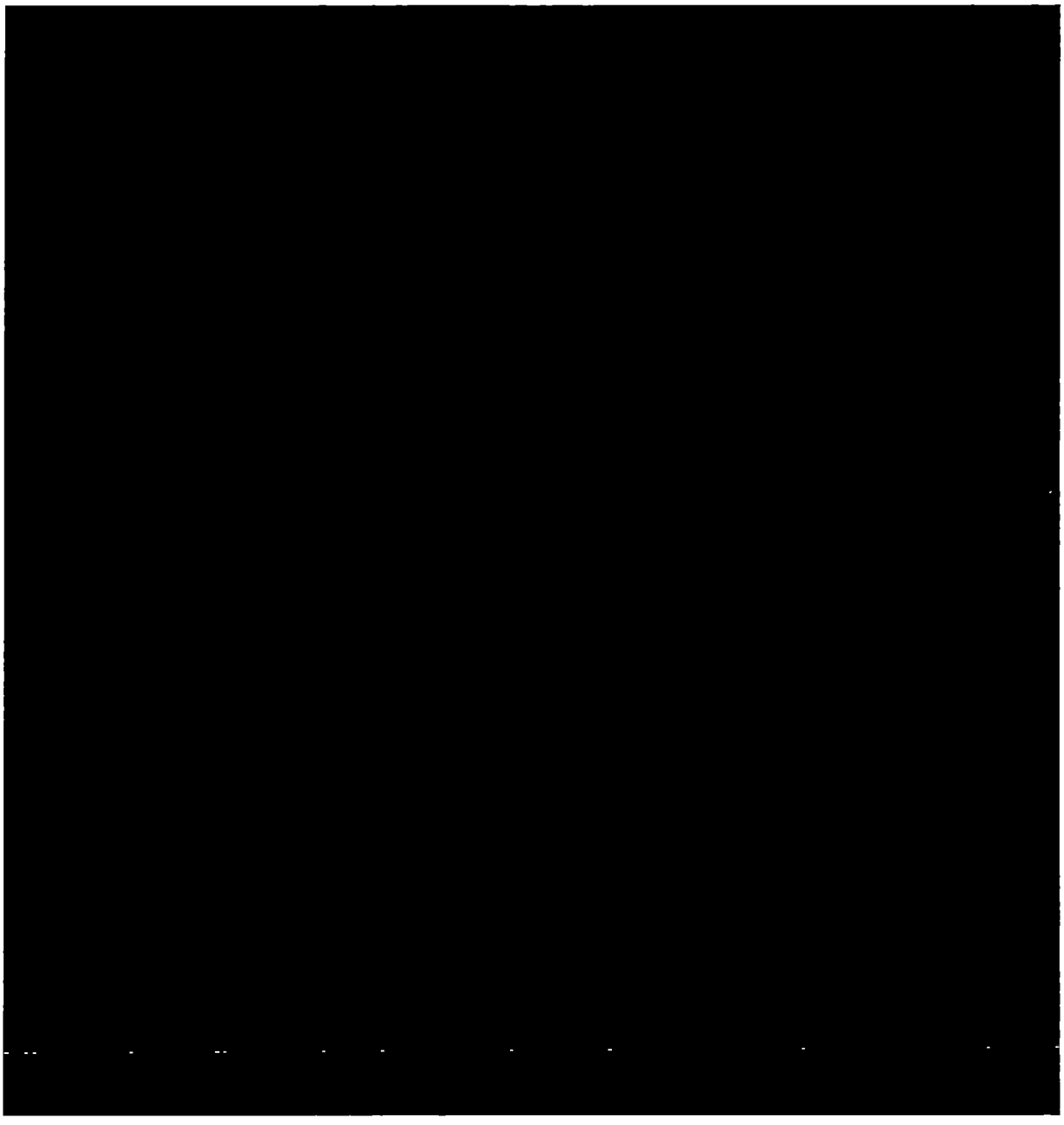

Figure 5.4-4 Dose rate distributions (TR1, cold model) for the axial ends of the package (the left column for bottom, the right one – for the lid side) at package surface (top), 1 m (middle), and 2 m (bottom) from the surface of the cask in mSv/h

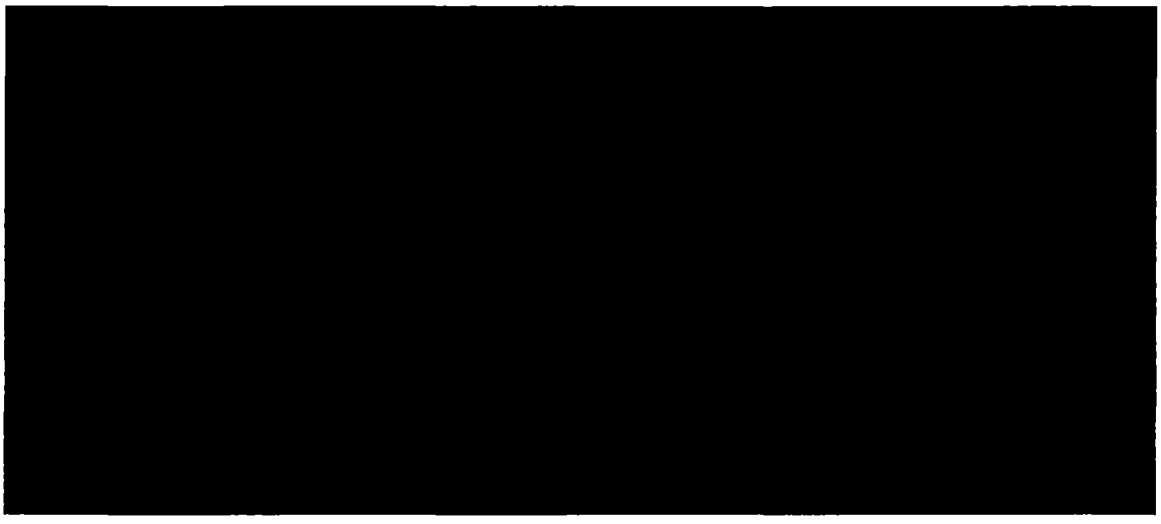

Figure 5.4-5 Dose rate distribution (TR2, cold model) at 2 m from the surface of the cask in mSv/h (left) and the corresponding fractional standard deviation (right)

Figure 5.4-6 Dose rate distribution (TR3, cold model) at 2 m from the surface of the cask in mSv/h (left) and the corresponding fractional standard deviation (right)

Table 5.4-6 through Table 5.4-8 provides the maximum external dose rates for the packaging under regular operating conditions with an attained thermal equilibrium (hot shielding model, md5: c8be18d5a42090e628472ac14ac9016e). The moderator material is at maximum temperature with corresponding reduced density and expanded dimensions. As previously, all the maximum dose rates are revealed on the shell side of the package.

As before, the TR1 generates the highest dose rates among all loading patterns.

[redacted]

The dose rate distributions from the hot shielding model are fairly similar to those from the cold one, and are therefore not presented here.

Table 5.4-6 Maximum external dose rates for the hot shielding model under NCT (TR1)

[redacted]

Table 5.4-7 Maximum external dose rates for the hot shielding model under NCT (TR2)

[redacted]

Table 5.4-8 Maximum external dose rates for the hot shielding model under NCT (TR3)

[redacted]

The fuel failure under NCT is evaluated for TR1 only, [redacted] Two cases are considered: the rubble at the canister bottom with weaker shielding capability of the package due to the bottom trunnion flattenings (md5: c8be18d5a42090e628472ac14ac9016e, see Table 5.4-9) and the rubble close to the canister lid also in an area with a weaker shielding performance – the rubble is positioned where the maximum effect is expected (md5: 5032019148e03514e5723435a22d2688, see Table 5.4-10). The relevant face side dose rates are given in brackets.

The reconfiguration is considered for transportation packages shipped after 20 years of storage [4], therefore the bounding source for this particular scenario is adjusted so that the minimum cooling time is not smaller than 20 years. [redacted]

The redistribution of the fuel does not affect the shell dose rate in a negative way. The maximum dose rates (at the surface of the package and 2 m from the surface of the package) are lower than those from the failure unaffected shielding models.

Contrary to this, the face sides of the package detect higher dose rates compared to the undisturbed model. [redacted]

Table 5.4-9 Maximum external dose rates for TR1 under NCT with 3 % fuel failure (bottom side)

Table 5.4-10 Maximum external dose rates for TR1 under NCT with 3 % fuel failure (lid side)

5.4.4.2 Hypothetical Accident Conditions

The calculated dose rates for the package under HAC are presented in Table 5.4-11 for all considered loading patterns (md5: 5032019148e03514e5723435a22d2688) as well as for the complete fuel failure gathered at the bottom of the canister md5: 7cd9c76b619a881b59e6352b81dd46dd)

and at its top (md5: 3a37d7a168848b7e9463f4dcebe8ad96). As for the NCT, the maximum dose rates for the model without fuel failure are revealed on the shell side of the package. For the models with the fully failed fuel, the dose rates are given for both the shell side and for the relevant face side (bracketed) of the package.

Despite of the missing impact limiters and moderator material, the exploitation of the dose rate limit is smaller compared to the NCT. [redacted]

Table 5.4-11 Maximum external dose rates under HAC

[redacted]

List of References

[1] Daniel J. Whalen, David E. Hollowell, and John S. Hendricks, Photon Benchmark Problems, LA-12196, Los Alamos National Laboratory, 1991

[2] Daniel J. Whalen, David A. Cardon, Jennifer L. Uhle, and John S. Hendricks, Neutron Benchmark Problems, LA-12212, Los Alamos National Laboratory, 1991

[3] American Nuclear Society. Working Group ANS-6.1.1; American National Standards Institute. American national standard neutron and gamma-ray flux-to-dose-rate factors, La Grange Park, Ill.: The Society, 1977

[4] NUREG-2224, Dry Storage and Transportation of High Burnup Spent Fuel (Draft for Comment), Washington, DC, July 2018

6.3 General Considerations

	Name, Function	Date	Signature
Prepared	[redacted]		
Reviewed			

This section addresses the assessment methodology used to evaluate criticality of the package.

The CASTOR® geo69 cask is designed for the accommodation of different types of BWR spent FA. To take a large number of relevant model parameters into account, for example the fabrication tolerances and the uncertainties in material compositions of FA or basket structures, the calculations of the neutron multiplication factors are performed using bounding models.

The analyzed FA represent square-pitched lattices of fuel rods. The qualitatively same impact of some model parameters on the system reactivity for all FA no. can be assumed. For example, the decrease of the moderator density or the increase of the absorber concentration in the fuel basket structures will reduce the reactivity of all FA no.

However, the distinctions of different FA no. lead to quantitative differences in reactivity impact of the same model parameter, i.e. the criticality calculations must be performed for each FA type and each cask loading pattern separately. For such calculations the same set of conservative model parameters can be applied.

Based on these assumptions, bounding calculation models (bounding models) for NCT and HAC are derived as described below and shown in Figure 6.3-1

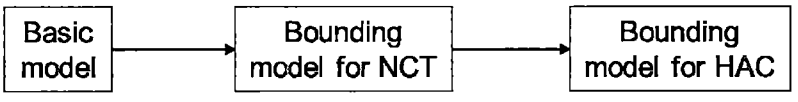

Figure 6.3-1 Development of bounding models

The bounding model for NCT is determined using sensitivity analyses based on a basic calculation model (basic model), as described in section 6.3.4.1. The basic model is based on the package and content descriptions from section 1.2.1 and 1.2.2 and contains either nominal, representative or expected to be bounding values for geometry, material compositions and densities of the cask, fuel basket and inventory.

Based on this basic model sensitivity analyses are performed for a full homogeneous cask loading with a reference FA (ATRIUM-10A) only, as described in section . 6.3.4.1 The sensitivity analyses bound all fabrication tolerances, uncertainties in material compositions, axial and radial FA displacements within the basket receptacles as well as optimal moderation conditions. The effect of a variation of a certain parameter is described as a deviation (Δk in pcm, i.e. 10^{-5}) of the calculated k-value to the k-value of the basic model. If the variation of a certain parameter leads for the reference FA to an increase in reactivity, the same behavior can be expected for all the other FA no.

The corresponding basic model of each FA no. is then adapted according to the possible tolerance range of this parameter.

With the above mentioned approach a bounding model for NCT for each FA no. is developed. The bounding model for NCT is described in sections 6.3.1 and 6.3.2.

On the basis of this bounding model for NCT additional proof of its conservativity as well as analyses concerning the package behavior under HAC are usually performed leading for each FA no. to a bounding model for HAC. The proof of the conservativity of the bounding model for NCT is provided in section 6.3.6. As the damage of the cask wall and bottom as well as the loose of integrity of the cask and canister lid systems under HAC are excluded, as shown in [1] and section 2.7 the bounding model for HAC is identical (except for inner moderation condition) to the bounding model for NCT, described in sections 6.3.1 and 6.3.2.

Based on the bounding model for NCT the compliance with the requirements of § 71.55 and § 71.59 is demonstrated in sections 6.4 through 6.7.

Every possible mixed loading of the cask with FA no. for which safe subcriticality can be demonstrated is bounded by the maximum effective neutron multiplication factor k of a full homogeneous cask loading with one of these FA no.

6.3.1 Model Configuration

In the bounding calculation model for NCT the cylindrical canister and cask body with the corresponding bottom and top (lid system) structures are considered. The model represents an infinite array of densely packed and fully flooded casks. The volume outside the casks is filled with void.

The calculation model does not include an explicit consideration of neither the sealing system nor other outer parts, e. g. moderator rods inside the cask body, cooling fins, trunnions or impact limiters, as well as the axial gaps between the canister and the cask.

The radial and axial cross sections of the bounding model for NCT are shown in Figure 6.3-2 and Figure 6.3-3.

Figure 6.3-2 Radial cross section of the bounding model for NCT

Figure 6.3-3 Axial cross section of the bounding model for NCT

[redacted]

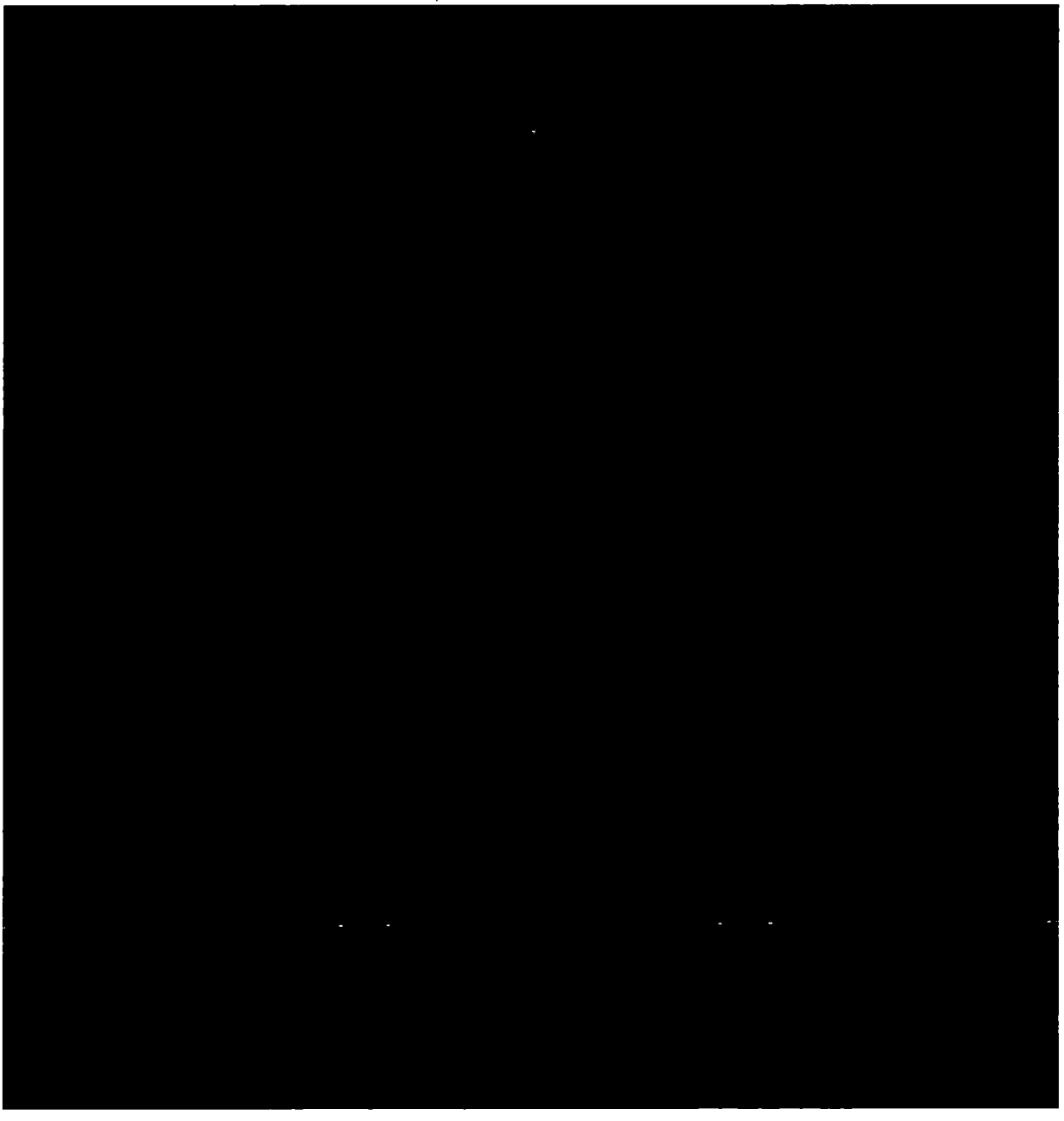

Figure 6.3-4 Cross sections of the analyzed FA

Figure 6.3-5 Radial cross section of the bounding model for NCT for a homogeneous full cask loading with ATRIUM-10A

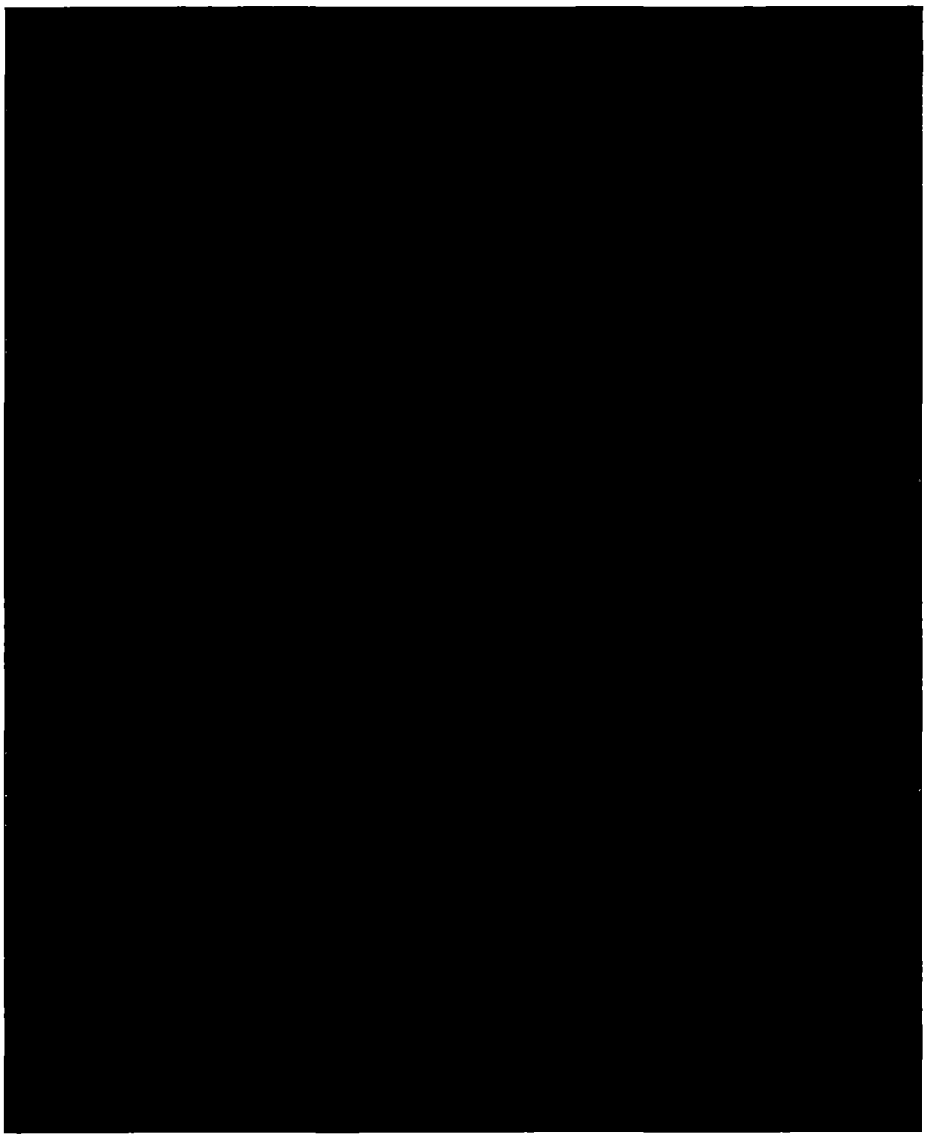

Figure 6.3-6 Axial cross section of the bounding model for NCT for a homogeneous full cask loading with the ATRIUM-10A

Comparing to the basic model used as a starting point for the development of the bounding model for NCT, as described in section 6.3.4.1, the following modifications are incorporated in the bounding model for NCT (cf. section 6.3.5):

- bounding material densities and compositions,
- maximum clad inner diameter,
- minimum clad outer diameter,
- minimum inner dimension of basket receptacles,

radial displacement of all FA towards the center of the fuel basket.

6.3.2 Material Properties

The bounding material densities and compositions are determined using the sensitivity analysis, as described in section 6.3.4.1, and are listed in Table 6.3-1 and Table 6.3-2.

The fuel basket contains fixed neutron absorbing structures (boronated basket sheets). The presence and the proper distribution of boron in the basket sheets at time of fabrication are ensured by quality measures. Loss of absorber material as a result of physical, chemical and corrosive mechanisms can be excluded according to chapter 2.

The Loss of absorber material through direct neutron absorption (and, thus, transmutation to a non-absorbing isotope) is inconsequential because any measurable depletion would take millions of years of routine operation as a result of the extremely low neutron flux levels in a subcritical system.

[redacted]

6.3.3 Computer Code and Cross-Section Libraries

The criticality calculations for the CASTOR® geo69 are performed using the 3-dimensional Monte-Carlo program KENO-VI from the SCALE 6.2 code package [2]. The neutron multiplication factors are calculated using the 252-group neutron cross sections based on the ENDF/B-VII.1 evaluation (V7.1-252n, T = 293 K).

[redacted]

In the criticality calculations the number of neutron generations with 20,000 neutrons per generation as well as the number of first neutron generations to be skipped is chosen in such a way, that the standard deviation of the calculated neutron multiplication factors is below 20 pcm.

[redacted]

The criticality safety analysis as well as the validation of the used calculation system, i.e. the Monte-Carlo program together with the cross-section library, is performed under the same or comparable boundary conditions.

6.3.4 Demonstration of Maximum Reactivity

Based on the basic model, the sensitivity analysis for the full cask loading with the most reactive FA type (ATRIUM-10A) is performed and bounding models for NCT and HAC are derived, as described in section 6.3.

6.3.4.1 Development of Bounding Model for NCT

The sensitivity analysis for the development of the bounding model for NCT includes the following evaluations:

- material densities and compositions,
- pellet diameter,
- length of active zone,
- clad inner and outer diameter,
- thickness of FA internals,
- inner and outer dimensions of FA channel,
- axial and radial displacement (including clustering) of FA,
- axial position of part-length fuel rods,
- FA orientation within basket receptacles,
- temperature,
- dimension of basket receptacles,
- thickness of basket sheets,
- thickness of outer sheets,
- canister dimensions,
- radial displacement of canister within the cask cavity,
- outer boundary conditions for the cask,
- partial vertical and horizontal flooding of the cask cavity,
- moderator rod material in the cask wall,

- shielding element structure.

The results of the analysis are presented in sections 6.3.4.1.1 to 6.3.4.1.22.

6.3.4.1.1 Material Densities and Compositions

[redacted]

Table 6.3-1 Determination of material densities for bounding model

Table 6.3-2 Determination of material compositions for bounding model

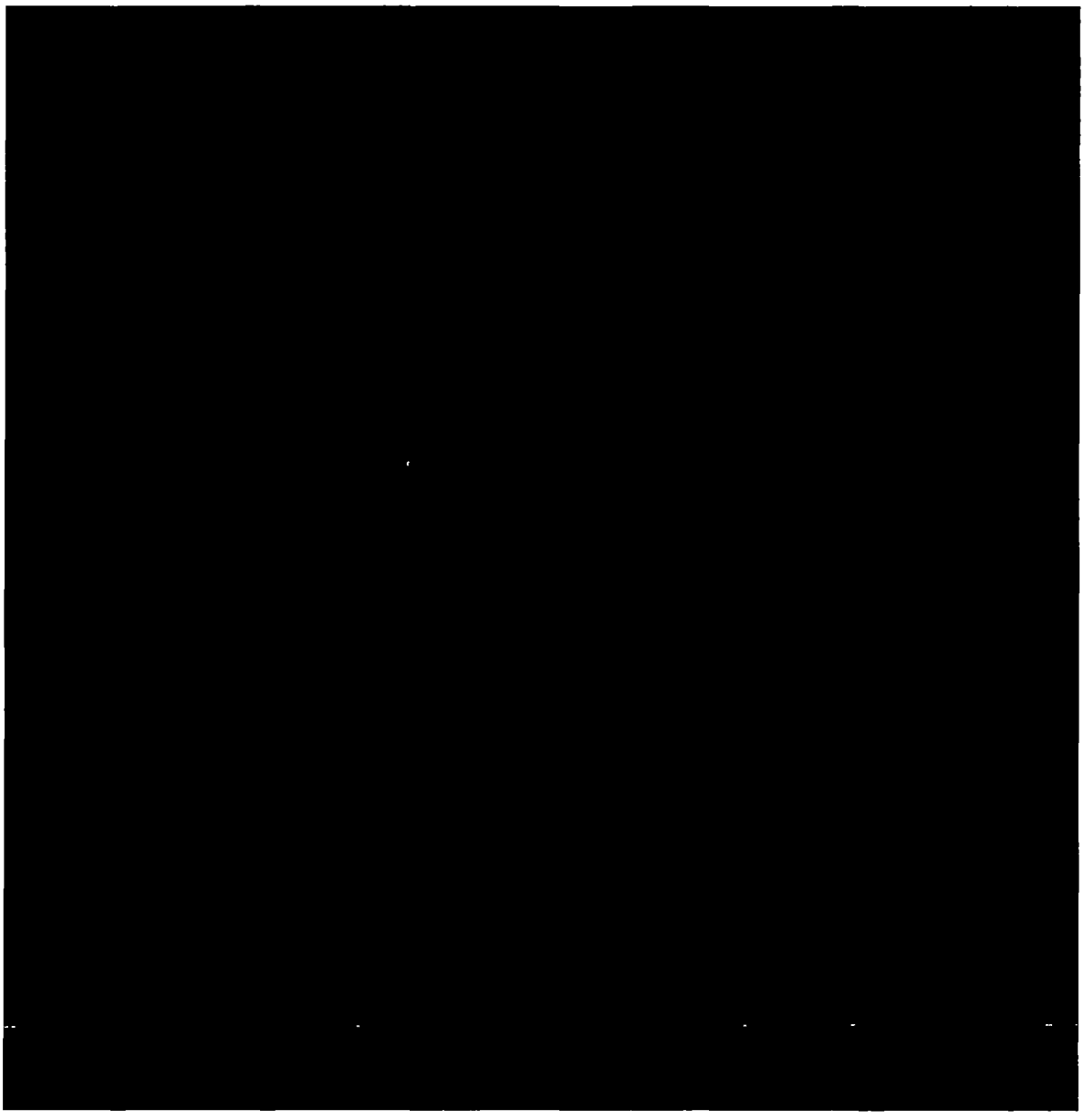

6.3.4.1.2 Pellet Diameter

The pellet diameter is parametrically varied within a range of -200 µm/+150 µm at a fixed fuel density of [redacted] The results given in Table 6.3-3 and Figure 6.3-9 show no statistically significant influence of this parameter on the reactivity.

As a result, no changes need to be considered in the bounding model.

6.3.4.1.3 Length of Active Zone

The length of the active zone is parametrically varied between ±20 mm, that corresponds to a height of about two single fuel pellets. The results provided in Table 6.3-3 and Figure 6.3-9 show no statistically significant influence of this parameter on the reactivity.

As a result, no changes need to be considered in the bounding model.

6.3.4.1.4 Clad Inner and Outer Diameter

The clad inner diameter is varied between -150 µm/+200 µm; the clad outer diameter between ±200 µm. The results for both variations are given in Table 6.3-3 and Figure 6.3-9. It can be seen that the clad thickness has a significant influence on the reactivity.

As a result, the maximum inner and minimum outer clad diameters are considered in the bounding model.

6.3.4.1.5 Thickness of Water Channel

The thickness of the water channel of the reference FA (ATRIUM-10A) is parametrically varied by the variation of the outer channel dimension between ±200 µm at a fixed inner channel dimension. The results given in Table 6.3-3 and Figure 6.3-9 show a significant increase of reactivity at smaller thicknesses of the water channel.

As a result, the minimum thicknesses of the FA internals, as already implemented in the basic model, are considered in the bounding model.

6.3.4.1.6 Inner and Outer Dimensions of FA Channel

The inner and outer dimensions of the FA channel are separately varied between ±200 µm, resulting in a variation of the wall thickness of the FA channel. The results of criticality calculations are given in Table 6.3-3 and Figure 6.3-9. It can be seen that the wall thickness of the FA channel has no statistically significant influence of the reactivity.

As a result, no changes need to be considered in the bounding model.

6.3.4.1.7 Axial Displacement of FA

The axial displacement of the FA is varied between ±40 mm. The results provided in Table 6.3-3 and Figure 6.3-9 show no significant influence on reactivity.

As a result, no changes need to be considered in the bounding model.

6.3.4.1.8 Radial Displacement of FA

The reactivity impact of the radial displacement of the FA within the fuel basket is parametrically investigated via simultaneous shift of all FA towards the basket center [redacted] or towards the basket periphery [redacted]. The results of these calculations are shown in Table 6.3-3 and Figure 6.3-9. It can be seen that the displacement towards the basket center leads to significant increase of reactivity.

As a result, the maximum possible displacements of the FA towards the basket center are considered in the bounding model.

6.3.4.1.9 Clustering

Additionally to the radial displacement of all FA towards the basket center or the basket periphery, as discussed in section 6.3.4.1.8, the building of FA conglomerates (clustering) within the fuel basket is investigated. The selected configuration is shown in Figure 6.3-7 and results in the significant decrease of reactivity (see Table 6.3-3) comparing to the reference (basic) model with FA centered within the basket receptacles.

As a result, the maximum possible displacements of the FA towards the basket center are considered in the bounding model, as discussed in section 6.3.4.1.8.

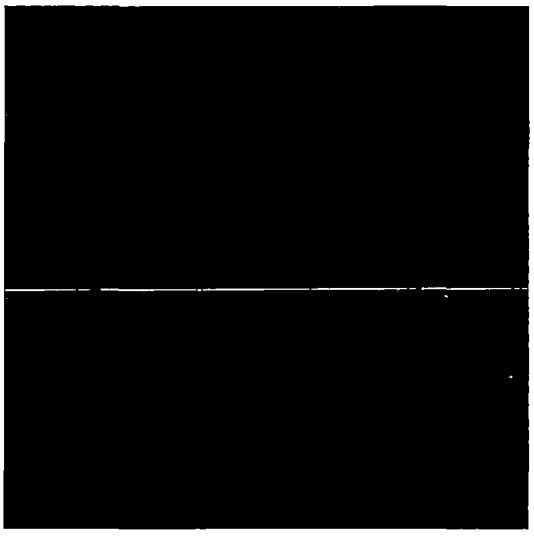

Figure 6.3-7 FA clustering

6.3.4.1.10 Axial Position of Part-Length Fuel Rods

The axial position of the part-length fuel rods is varied up to 40 mm beginning at the lower edge of the full-length fuel rods. The results presented in Table 6.3-3 and Figure 6.3-9 indicate the reactivity decrease by the axial shift of the part-length fuel rods towards the center of the active zone.

As a result, no axial displacement of the part-length fuel rods, as already implemented in the basic model, is considered in the bounding model.

6.3.4.1.11 FA Orientation within Basket Receptacles

During the basket loading with FA different orientations of FA internals (water rods/channel) relative to the neighboring FA are possible. This effect is investigated via the fuel lattice rotation of 90°, 180° and 270° for exemplary selected FA in the calculation model. The investigated configuration is presented in Figure 6.3-8 and shows no statistically significant influence (see Table 6.3-3) of the FA orientation within the basket receptacles on the reactivity.

As a result, the same orientation of all FA, as already implemented in the basic model, is considered in the bounding model.

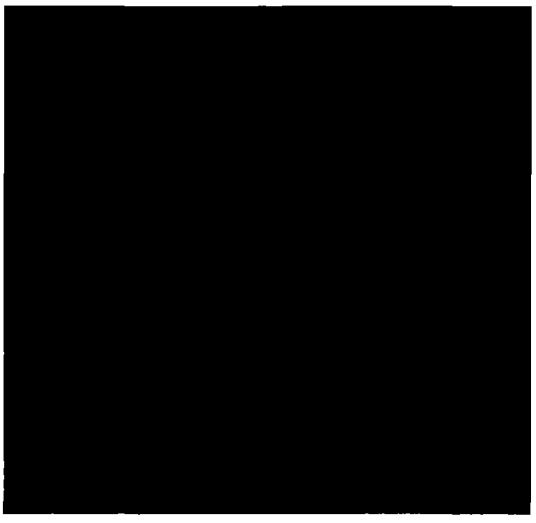

Figure 6.3-8 FA orientation

6.3.4.1.12 Temperature

The temperature of structure materials is parametrically varied between 0 °C and 170 °C. The results presented in Table 6.3-3 and Figure 6.3-9 confirm the reactivity decrease by increased temperature due to the Doppler broadening.

As a result, the room temperature (20 °C), as already implemented in the basic model, is considered in the bounding model.

6.3.4.1.13 Dimension of Basket Receptacles

The inner dimension of the basket receptacles is parametrically varied within the possible tolerance range between [redacted] at a fixed thickness of the basket sheets. The results provided in Table 6.3-3 and Figure 6.3-9 show significant reactivity increase by decreased basket receptacles.

As a result, the minimum possible inner dimension is applied to all basket receptacles in the bounding model.

6.3.4.1.14 Thickness of Basket Sheets

The thickness of borated aluminium sheets of the basket is parametrically increased up to [redacted]. As shown in Table 6.3-3 and Figure 6.3-9, increased thickness of the basket sheets leads to the significant decrease of reactivity.

As a result, the minimum possible thickness of the basket sheets, as already implemented in the basic model, is considered in the bounding model.

6.3.4.1.15 Thickness of Outer Sheets

The thickness of the outer basket sheets is parametrically increased up to [redacted]. The results given in Table 6.3-3 and Figure 6.3-9 show no statistically significant influence of this parameter on the reactivity.

As a result, no changes need to be considered in the bounding model.

6.3.4.1.16 Canister Dimensions

The reactivity impact of the canister dimensions, such as inner and outer diameter (I.D. and O.D.) as well as the wall thickness (T), is investigated via calculations for all possible combinations of minimum and maximum parameter values. The results are provided in Table 6.3-3 and confirm that the parameter set implemented in the basic model (maximum O.D. and T) is conservative.

As a result, no changes need to be considered in the bounding model.

6.3.4.1.17 Radial Displacement of Canister

The radial displacement of the canister within the cask cavity is investigated via canister shift towards the cask wall. The result is provided in Table 6.3-3 and shows no influence of the radial canister position on the reactivity.

As a result, the canister centered within the cask cavity, as already implemented in the basic model, is considered in the bounding model.

6.3.4.1.18 Outer Boundary Conditions

The outer boundary conditions, such as external moderation and reflection, are evaluated for a single cask as well as for an infinite array of similar densely packed casks. For a single cask, the full reflection is achieved by surrounding the cask with 20 cm water reflector. The results of the investigations with and without external moderation (water or void) are shown in Table 6.3-3. It can be seen that the external moderation has no impact on the reactivity due to the thick cask wall.

As a result, an infinite array of similar, densely packed casks without external moderator, as already implemented in the basic model, is considered in the bounding model.

6.3.4.1.19 Partial Flooding of the Cask

The partial flooding of the cask is investigated for the vertical and horizontal orientations of the cask. The results for both orientations are given in Table 6.3-3 and Figure 6.3-9 and indicate that the fully flooded condition is most conservative.

As a result, the fully flooded cask cavity with water (ρ = 1.0 g/cm^3), as already implemented in the basic model, is considered in the bounding model.

6.3.4.1.20 Moderator Rod Material

The impact of the moderator rod material as well as of the corresponding boreholes on the reactivity is investigated. The results are given in Table 6.3-3 and indicate that the neglecting the moderator material and replacing it by the material of the cask body (cast iron) is most conservative.

As a result, no changes need to be considered in the bounding model.

6.3.4.1.21 Shielding Element Structure

The reactivity impact of the drain support in one shielding element is investigated. The results are given in Table 6.3-3 and indicate that the neglecting the drain support and replacing it by the material of the shielding element (aluminium) is most conservative.

As a result, no changes need to be considered in the bounding model.

6.3.4.1.22 Summary Results of Sensitivity Analysis

The results of the sensitivity calculations described in the previous sections are summarized in Table 6.3-3 and presented in Figure 6.3-9.

Table 6.3-3 Summary results of the sensitivity analysis

	FA no. 6	
k-value for basic model	0.92065	20dr09cc03
variation	**Δk, pcm**	**calc. ID**
Pellet diameter, Δ in μm		
-200	-75	20ln09oF03
-150	-30	20un09uS03
-100	-41	20WZ09nh03
-50	-15	20ai09fw03
0	0	20Sx09iF03
50	12	20Rm09fs03
100	-9	20Xv09ra03
150	36	20xK09Vg03
Length of active zone, Δ in mm		
-20	8	20Dt09zS03
-15	10	20WF09aQ03
-10	-2	20cH09Cy03
-5	-34	20mw09cw03
0	0	20hr09qH03
5	-6	20aQ09do03
10	3	20MU09hO03
15	-21	20yX09zr03
20	-31	20So09UA03
Clad inner diameter, Δ in μm		
-150	-452	20YL09eg03
-100	-339	20Pk09nU03
-50	-170	20MR09KC03
0	0	20Gz09tK03
50	168	20yt09Ow03
100	272	20gT09vt03
150	474	20hd09Py03
200	625	20xU09cC03
Clad outer diameter, Δ in μm		
-200	759	20GE09hl03
-150	583	20vO09xi03
-100	333	20nR09ZP03
-50	222	20OQ09kK03
0	0	20ES09hD03
50	-207	20Sn09oe03
100	-370	20Ww09qY03
150	-613	20aG09kN03
200	-760	20XV09iY03

	FA no. 6	
k-value for basic model	0.92065	20dr09cc03
variation	**Δk, pcm**	**calc. ID**
Thickness of water channel, Δ in μm		
-200	66	20BC09Zb03
-150	64	20ZW09cK03
-100	13	20vx09FJ03
-50	13	20TC09LA03
0	0	20rJ09Jb03
50	-46	20Yj09vu03
100	-51	20RM09rZ03
150	-71	20ho09Py03
200	-86	20yJ09Fb03
Inner dimension of FA channel, Δ in μm		
-200	-28	20HW09KZ03
-150	1	20ee09xg03
-100	15	20RN09vw03
-50	-36	20kO09QD03
0	0	20Sz09vW03
50	-5	20AZ09tW03
100	-14	20Fl09qe03
150	-39	20Ml09mK03
200	-29	20JT09PF03
Outer dimension of FA channel, Δ in μm		
-200	-22	20DO09FD03
-150	-25	20Vz09ap03
-100	-6	20yW09yN03
-50	21	20Cf09CN03
0	0	20vJ09Al03
50	37	20Ut09wv03
100	31	20Rz09Fl03
150	-1	20yB09bg03
200	-5	20EB09cR03
Axial displacement of FA, Δ in mm		
-40	-6	20xD09kv03
-30	-17	20wM09EO03
-20	12	20jx09yn03
-10	-30	20yD09HL03
0	0	20oW09RI03
10	-20	20lI09TN03
20	-47	20pX09qY03
30	15	20fW09Bo03
40	9	20aZ09XJ03

Table 6.3-3 Summary results of the sensitivity analysis (continued)

Radial displacement of FA, Δ in mm		
	510	20sO09Bl03
	459	20XO09Xb03
	413	20jJ09Yw03
	354	20Jz09Oo03
	273	20mu09jy03
	152	20vz09EF03
	0	20hd09rU03
	-135	20el09ST03
	-336	20Ee09Pg03
	-519	20Nn09fU03
	-739	20xe09uW03
	-967	20HE09KN03
	-1359	20tq09jA03
Axial position of part-length fuel rods, Δ in mm		
0	0	20Ri09vC03
5	-7	20Py09oN03
10	-33	20uF09Jx03
15	-70	20lo09BY03
20	-78	20rZ09Au03
25	-85	20ly09pr03
30	-145	20GX09LP03
35	-118	20is09cK03
40	-120	20JH09eK03
FA orientation within basket receptacles		
Clustering	-235	20ek09Fc03
Rotation	19	20SY09XK03
Material temperature, °C		
0	-12	20nN09Et03
10	-36	20Jx09CU03
20	0	20lJ09Xw03
30	-124	20xv09pr03
40	-253	20oR09DF03
70	-483	20MH09BO03
120	-1034	20Gr09xg03
170	-1490	20Fq09vG03
Dimension of basket receptacles, Δ in mm		
	179	20SD09Wf03
	0	20oK09za03
	-214	20rn09KB03
	-368	20WN09UL03
	-563	20ZY09dL03
Thickness of basket sheets, Δ in mm		
	0	20EZ09ED03
	-136	20Rm09NM03
	-224	20ar09Dj03
	-315	20Xv09jv03
	-488	20Gi09Ao03
	-551	20FM09DC03

Thickness of outer sheets, Δ in mm		
	0	20ut09la03
	-4	20Rt09xV03
	7	20sY09rg03
	-2	20bF09LL03
	-27	20mJ09yW03
	5	20lu09oH03
Canister dimensions, mm		
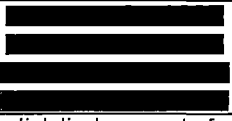	-248	20zE09by03
	-47	20jv09Ba03
	26	20ih09lf03
	0	20Jv09pj03
Radial displacement of canister		
to the cask wall	-24	20aL09cq03
Outer boundary conditions		
Array, ext. mod. 0 %	0	20wm09SY03
Array, ext. mod. 100 %	4	20Wi09TH03
Single, ext. mod. 100 %	-8	20Mr09LJ03
Single, ext. mod. 0 %	-39	20pE09xn03
Partial flooding (vertical), Δ in cm		
-200	-619	20UM09uz03
-150	-405	20Pb09Kz03
-100	-193	20zN09RC03
-90	-164	20Yo09nW03
-80	-80	20Hd09Uc03
-70	-23	20qo09Jv03
-60	29	20lA09eP03
-50	5	20VA09ro03
-40	-32	20jd09sj03
-30	17	20SR09OW03
-20	31	20ab09at03
-10	0	20cd09aw03
0	0	20rt09gh03
Partial flooding (horizontal), number of dry FA rows		
0	0	20kO09BF03
1	-230	20jx09MZ03
2	-474	20OH09eX03
3	-918	20Fy09Vy03
4	-1523	20yt09LW03
5	-2463	20sR09TV03
Moderator rod material		
Neglected	0	20JQ09jh03
PE	-189	20Fc09va03
Void	12	20li09CF03
Water	-236	20hl09FS03
Shielding element structure		
Drain support	-61	20Jl09UQ03

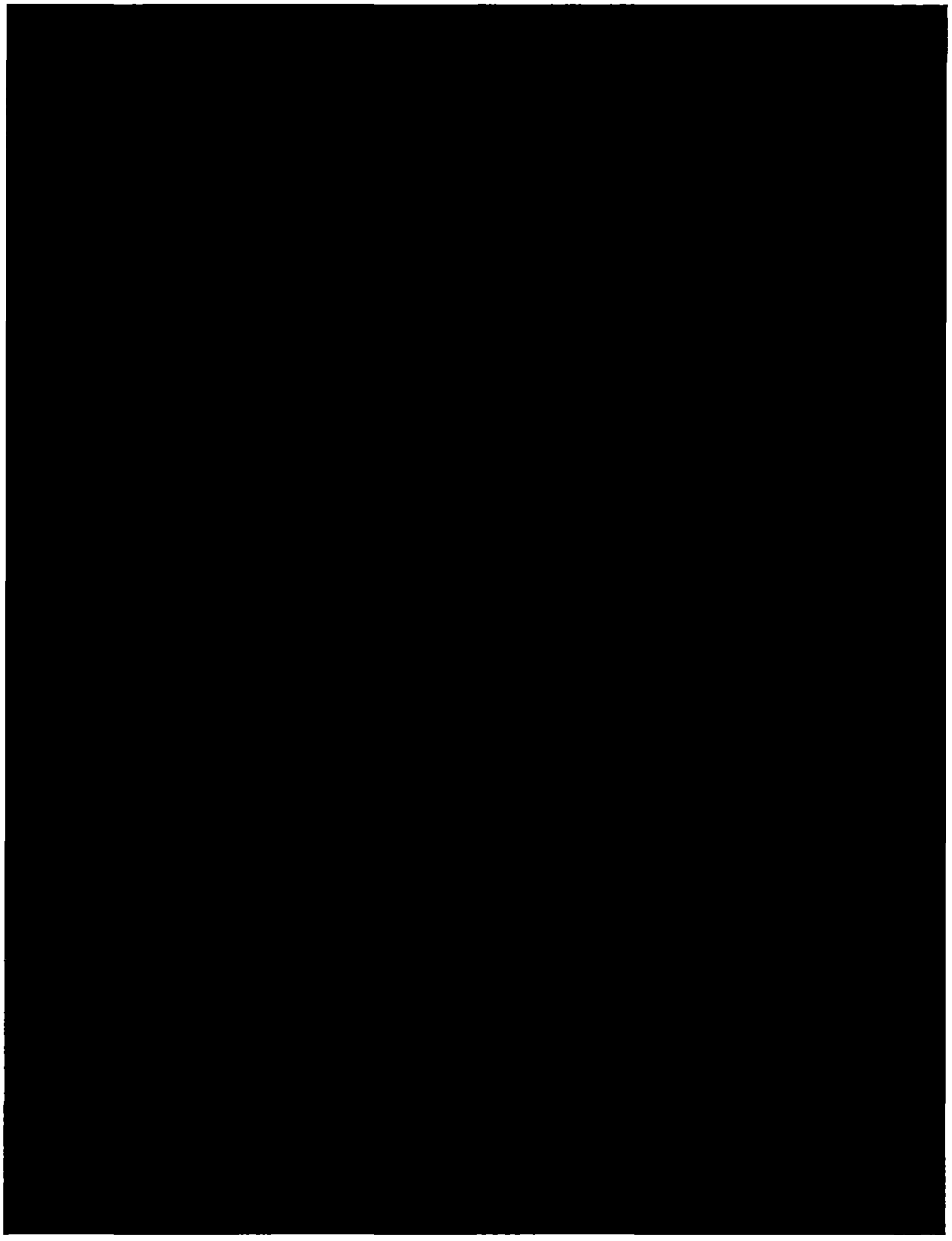

Figure 6.3-9 Graphical representation of the summary results

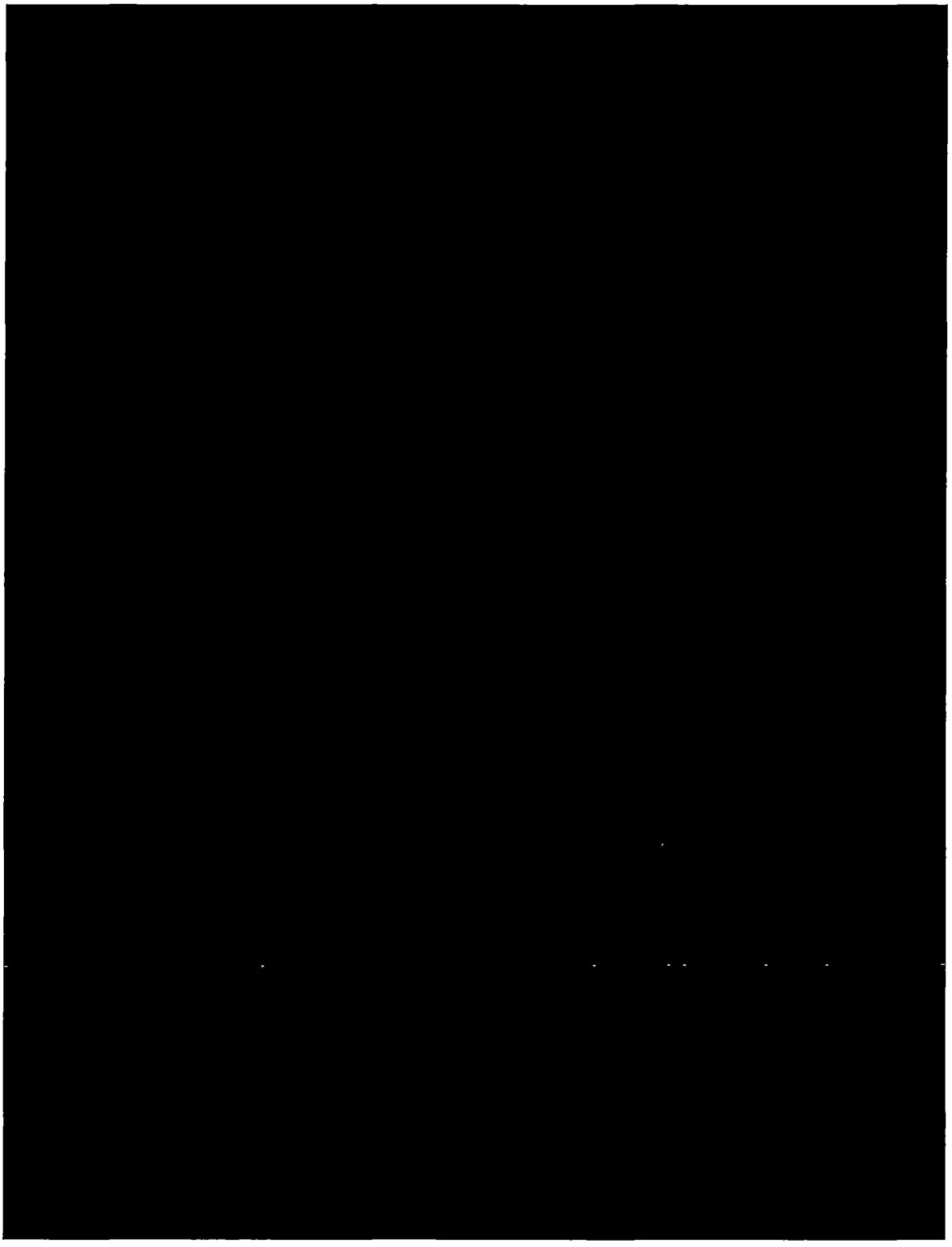

Figure 6.3-9 Graphical representation of the summary results (continued)

6.3.5 Results for Bounding Model for NCT

As discussed in section 6.3.4, the following conservative assumptions for the basic model are confirmed:

- fully flooded gap between fuel pellet and clad,
- nominal pellet diameter,
- nominal length of the active zone,
- minimum thickness of FA internal structures,
- nominal dimensions of FA channel,
- nominal axial position of FA,
- axial position of part-length fuel rods beginning at the lower edge of the active zone,
- same orientation of all FA within the basket receptacles,
- nominal temperature,
- nominal thickness of basket sheets,
- nominal thickness of outer sheets,
- maximum canister outer diameter with maximum wall thickness,
- no radial displacement of canister within the cask,
- void outside the cask (external moderation 0 %),
- infinite array of densely packed casks,
- fully flooded cask (internal moderation 100 %),
- neglected moderator rods and sheets,
- neglected drain support in the shielding element.

Based on the sensitivity analysis in section 6.3.4, the following changes are applied to the basic model to develop the bounding model for NCT:

- bounding material densities and compositions,
- maximum clad inner diameter,
- minimum clad outer diameter,
- minimum inner dimension of basket receptacles,
- radial displacement of all FA towards the center of the fuel basket.

The criticality calculations using the bounding model for NCT are performed for all analyzed FA. The results are summarized in Table 6.3-4 and include the maximum effective neutron multiplication factors k and the calculational bias with its uncertainty Δk_U. All contributions to the final results are determined with a 95 % probability at a 95 % confidence level, as discussed in section 6.8.2 and Appendix 6-1

A sample input file for the bounding model for NCT with the FA of type ATRIUM-10A is provided in Appendix 6-2.

Table 6.3-4 Results for the bounding model for NCT

FA no.	Case	Infinite array of flooded packages (bounding model for NCT)	
	Internal moderation	100%	
	External moderation	0%	
	Fuel type	$k + \Delta k_U$	calc. ID
1	GE 8x8-1	0.84386	20tZ09ny02
2	GE 8x8-2	0.85061	20da09vS02
3	SPC 8x8-2	0.84625	20rq09Tj02
4	GE9B 8x8	0.88137	20ll09Vo02
5	GE12 LUA	0.90514	20Xb09ei02
6	ATRIUM-10A	0.93729	20nS09hZ02

6.3.6 Proof of Conservativity of the Bounding Model for NCT

Additional evaluations as a proof the conservativity of the bounding model for NCT is based on this model and includes:

- partial cask loading,
- planar fuel enrichment,
- fuel basket deformations.

The results of the analysis are presented in sections 6.3.6.1 through 6.3.6.3.

6.3.6.1 Partial Cask Loading

The impact of different empty basket positions on the reactivity is evaluated. The investigated single empty basket positions (No. 6, 9, 32, 49, 51, 63, 64 and 69) are radially distributed within the fuel basket, as shown in Figure 6.3-10. The results of these different calculations are given in Table 6.3-5 and Figure 6.3-11 and confirm that the full cask loading is conservative.

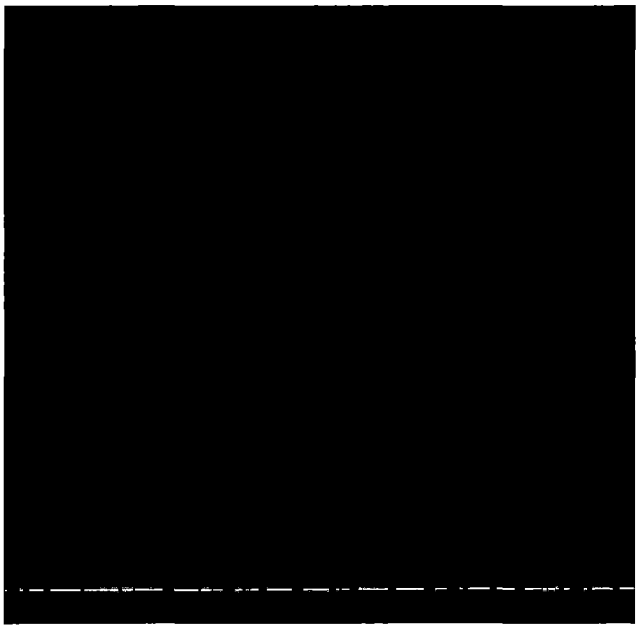

Figure 6.3-10 Evaluated empty basket positions

Table 6.3-5 Evaluation results for the partial cask loading

	FA no. 6	
k-value for NCT model	0.93032	20Xg09mz04
variation	**Δk, pcm**	**calc. ID**
Number of empty basket position		
6	-93	20In09oF03
49	-409	20un09uS03
63	-1002	20WZ09nh03
69	-1463	20ai09fw03
64	-1197	20Sx09iF03
51	-741	20Rm09fs03
32	-415	20Xv09ra03
9	-168	20xK09Vg03

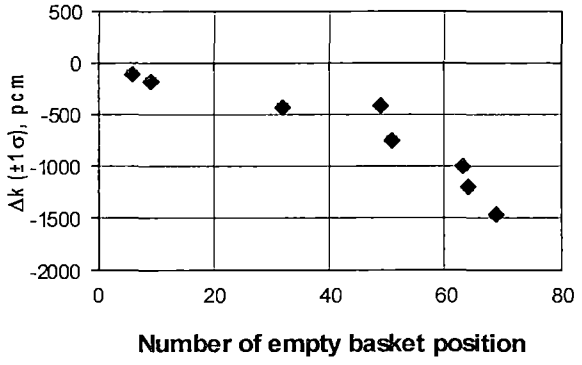

Figure 6.3-11 Graphical representation of results for the partial cask loading

6.3.6.2 Planar Fuel Enrichment

[redacted]

Figure 6.3-12 Cross section of the fuel lattice and the group numbers (Group no.) with different enrichments in the generic model

Table 6.3-6 Investigated enrichment distributions

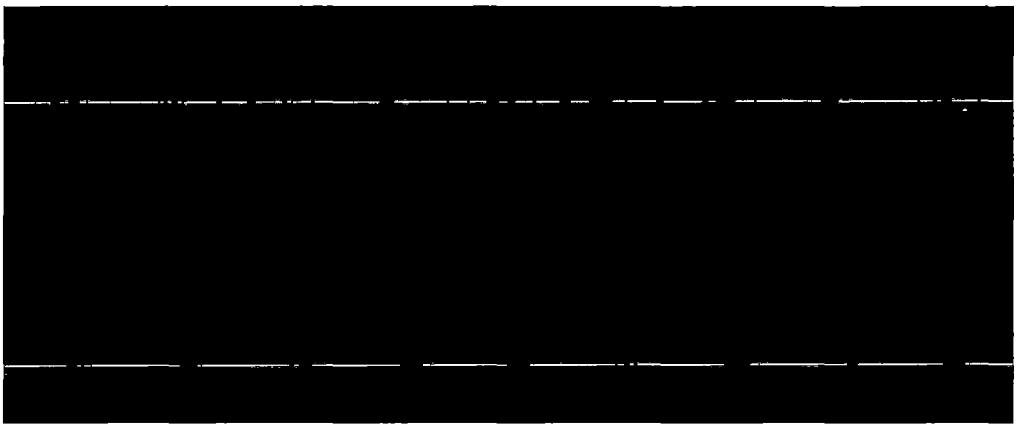

The results of criticality calculations given in Table 6.3-7 and Figure 6.3-13 and confirm that the use of the planar-averaged uniform enrichment is conservative.

Table 6.3-7 Evaluation results for the planar fuel enrichment

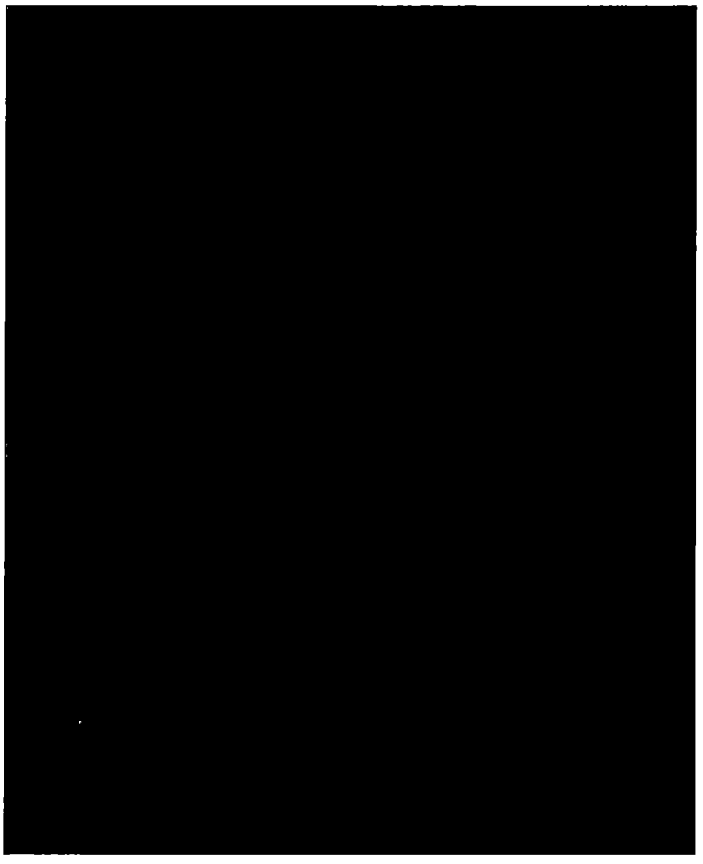

Figure 6.3-13 Graphical representation of results for the planar fuel enrichment

6.3.6.3 Fuel Basket Deformations

The criticality safety analysis is performed with the assumption that the borated MMC plates will retain their geometric shape and dimensions under NCT and HAC, and that the FA are radially displaced towards the center of the fuel basket, as described in sections 6.3.1 and 6.3.5. This conservative assumption is based on the following considerations.

The structural analysis of the fuel basket in Appendix 2-2 shows that

- the FA are displaced in the direction of the drop orientation and
- the relative displacement of the neighboring borated MMC plates under NCT is well below 1 mm for all investigated drop orientations.

As can be seen from the sensitivity analysis in sections 6.3.4.1.8 and 6.3.4.1.13,

- the maximum possible radial displacement of all FA towards the center of the fuel basket, as implemented in the bounding model for NCT, corresponds to the reactivity increase of Δk = 510 pcm (Calc. ID: 20sO09Bl03) and
- the decrease of the inner dimension of all basket receptacles by 1 mm leads to the reactivity increase of Δk = 179 pcm (Calc. ID: 20SD09Wf03).

The bounding model for NCT, as described in section 6.3.5, which conservatively takes into account the radial displacement of all FA towards the center of the fuel basket, can consequently be considered as bounding for the fuel basket deformations under NCT.

The leak-tightness of the cask and canister lids under HAC is demonstrated in section 2.7. The structural analysis of the cask and canister as well as of the fuel basket under HAC is provided in Appendix 2-1 and Appendix 2-2, respectively.

As the damage of the cask wall and bottom as well as the loss of integrity of the cask and canister lid systems under HAC are excluded, the reactivity of the credible fuel basket configurations under dry conditions is bounded by the fully flooded cask configuration, as provided by the bounding model for NCT. Thus, the separate analysis of the basket deformations under HAC is not necessary.

List of References

[1] ANSI/ANS-8.1-2014: Nuclear Criticality Safety in Operations with Fissile Material Outside Reactors.

[2] B. T. Rearden and M. A. Jessee, Eds.
SCALE Code System, ORNL/TM-2005/39, Version 6.2.2
Oak Ridge National Laboratory, Oak Ridge, Tennessee (2017)
Available from Radiation Safety Information Computational Center as CCC-834

7 Package Operations

7.0 Overview

	Name, Function	Date	Signature
Prepared	[redacted]		
Reviewed			

This document provides a description of all designated essential package operations with the CASTOR® geo69 transport and storage cask acc. to RG 7.9 [1], comprising sufficient details regarding preparation for package loading, package loading, preparation for transport, package unloading, preparation of empty package for transport and other applicable operations. The operations shall ensure the performance of the packaging and that it is operated in a manner consistent with the conditions assumed in the evaluation in the SAR acc. to 10 CFR 71.

All operations shall be performed according to detailed written and approved procedures and shall comply with the content of this document, the applicable codes and standards and the CoC. The preparation of these procedures is the responsibility of the user, they are thus site-specific. The results from tests to be performed within the scope of the operations (e.g. leakage tests) shall be documented and become part of the quality documentation of the packaging.

The package operations have to be consistent with maintaining occupational radiation exposures as low as reasonably achievable (ALARA) as required by 10 CFR 20.1101(b) [2].

In general, even if not explicitly mentioned, all components shall be subject to visual inspections prior to handling to ensure they are in proper condition.

The mentioned components and items (except for equipment) are consistent with the package description in section 1.2 and the corresponding drawings and parts lists according to the Appendix 1.3 of Chapter 1.

List of References

[1] Regulatory Guide 7.9, Rev. 2, March 2005
Standard Format and Content of Part 71 Applications for Approval of Packages for Radioactive Material
U.S. Nuclear Regulatory Commission, Office of Nuclear Regulatory Research

[2] Title 10 CFR Part 20
Standards for Protection Against Radiation
U.S. Nuclear Regulatory Commission

7.1 Package Loading

	Name, Function	Date	Signature
Prepared	[redacted]		
Reviewed			

The CASTOR® geo69 is designated as transport and storage cask. The applicable loading-related preparations, tests, and inspections of the package described in the following comply with the transportation regulations 10 CFR 71 and the CoC. The description include inspections made before loading to determine that the package is not damaged and radiation and surface contamination levels are within allowable regulatory limits. Casks loaded to be directly stored on-site, must also comply with 10 CFR 72 [1]. Casks deployed at a storage facility must be confirmed to meet all conditions of the 10 CFR 71 CoC prior to transport on public routes. Instances in which the conditions of approval in the CoC were not observed in making a shipment shall be reported to the NRC.

The package is loaded and closed in accordance with detailed written and approved procedures, including procedures for the preservation of screws with lubricant where necessary and tightening methods for the installation of all lids. Each screw is installed with either a nominal tightening torque or a nominal preload. Table 7.1-1, Table 7.1-2 and Table 7.1-3 summarize the operations for preparation for loading, loading of contents and preparation for transport, respectively.

7.1.1 Preparation for Loading

It is assumed that the transfer cask is already in the reactor hall and that the transfer lock and further equipment necessary for the transhipment of the canister from the transfer cask into the CASTOR® geo69 cask is available. Further, it is assured that all components of the CASTOR® geo69 CLU-System are in proper condition and ready for usage.

Table 7.1-1 Operations for preparation of loading

Step	*Description*	*Requirement*
A	**Acceptance of the empty packaging.**	
A1	**Delivery of the transport unit including the documents accompanying transport.**	
A2	**Check of the validity of the CoC for the cask.**	Cask logbook
A3	**Visual inspection of the packaging for proper condition, deformation, wear and corrosion.**	
A4	**Removal of impact limiters and [redacted] if installed on cask when accepted.**	
A5	**If the cask has previously been used with SNF: Contamination control, decontamination in case of any issues.**	**49 CFR 173.443 [2]**
A6	**If the cask has previously been used with SNF: External dose rate measurement.**	**10 CFR 71.47**
A7	**Visual inspection of the empty packaging**	
A7.1	Visual inspection of the outer surface coating of the cask.	
A7.2	Visual inspection of cask lid, blind flange and protection cap in installed condition, as far as accessible.	

Step	*Description*	*Requirement*
A7.3	Visual inspection of the trunnions in installed condition, as far as accessible.	
A7.4 [1]	Visual inspection of tilting studs and wear protection in installed condition, as far as accessible.	
A7.5	Visual inspection of the preservation on wear protection and of the hexagon screws.	
A7.6 [3]	Leak-tightness test of the wear protection.	
A7.7 [2]	Visual inspection of closure plate, hexagon head screws, sealing screws and seal plug in installed condition, as far as accessible.	
A7.8	Visual inspection of the preservation of the closure plate, hexagon head screws and seal plug.	
A7.9 [3]	Leak-tightness test of the closure plate and the sealing screws.	
A8	**Transfer of the cask to handling position in the truck lock.**	
A8.1	Load attachment on the trunnions, tilting of the cask into the vertical orientation and subsequent lifting.	
A8.2	Placement of the cask in the lock wagon.	
A8.3	Transfer of the lock wagon to the handling position in the truck lock and closing of the service platform around the cask.	
B	**Preparation of the empty cask for accepting the canister.**	
B1	**Removal of the cask lid.**	
B1.1	Visual inspection of the six threaded holes for the load attachment on top of the cask lid.	
B1.2	Remove hexagonal screws and hexagon head screws for sealing: - Removal of the three hexagon screws at marked positions (see numbering on the cask lid), - Visual inspection of the respective threaded holes in the cask body, as far as accessible, - Visual inspection of threads of the three guide bolts, - Installation of the three guide bolts in the corresponding threaded holes in the cask body, - Installation of the lifting pintle on the cask lid, - Removal of the remaining hexagonal screws and hexagon head screws for sealing.	
B1.3	Removal of the cask lid. The lifting pintle remains installed on the cask lid.	
B1.4	Removal of the three guide bolts.	
B1.5	Visual inspection after removing the cask lid: - Cask lid as a whole, - Sealing groove for metal gasket in the cask lid after removal of the metal gasket, - Sealing surface for metal gasket on the cask body, - Hexagonal screws and hexagon head screws for sealing, - Threaded holes for screws in cask body.	
B1.6	Visual inspection of sealing surface protection of cask lid fit for impurities and damage. Installation of in lid fit.	
B2	**Removal of blind flange from cask lid.**	
B2.1	Removal of the cap screws.	
B2.2	Removal of blind flange via the LAP located in the centre.	

Step	*Description*	*Requirement*
B2.3	Visual inspection after removing the blind flange: - Blind flange as a whole, - Sealing groove for metal gasket in the blind flange after removal of the metal gasket, - Sealing surface for metal gasket on the cask lid, - Cap screws, - Threaded holes for cap screws in the cask lid.	
B3	**Removal of protection cap from cask lid.**	
B3.1	Removal of the cap screws.	
B3.2	Removal of protection cap via the two LAPs.	
B3.3	Visual inspection after removing the protection cap: - Protection cap as a whole, - Sealing groove for metal gasket in the protection cap after removal of the metal gasket, - Sealing surface for metal gasket on the cask lid, - Cap screws, - Threaded holes for cap screws in the cask lid.	
B4	**Disassembly of the retention ring.**	
B4.1	[redacted]	
B4.2	[redacted]	
B5	**Installation of the lifting pintle on the canister lid.**	
B6	**Positioning of the transfer lock on top of the cask.**	
C	**Canister transfer into transfer cask.**	
C1	**Positioning of transfer cask on top of the CASTOR® geo69 cask.**	
C1.1	Load attachment on the trunnions of the transfer cask and vertical crane transfer to the handling position in the truck lock.	
C1.2	Positioning of the transfer cask on the transfer lock on top of the CASTOR® geo69. Two centre bolts provide adjustment. The trunnions of the transfer cask remain attached to the traverse during the entire transhipment.	
C2	**Transfer of the canister into the transfer cask.**	
C2.1	Opening of the bottom lid of the transfer cask via the transfer lock.	
C2.2	Attachment of the lifting pintle on the canister lid.	
C2.3	Lifting of the canister from the CASTOR® geo69 into the transfer cask.	
C2.4	Closure of the bottom lid of the transfer cask via the transfer lock.	
C2.5	Settling of the canister on the bottom lid of the transfer cask and strike off from the crane.	
C2.6	Transfer of the transfer cask with canister to the service position in the reactor hall.	
C2.7	Closing of the platform around the transfer cask and disassembly of the crane traverse.	
D	**Preparation of canister and transfer cask for loading.**	
D1	**Preparation of the canister in the transfer cask.**	

Step	*Description*	*Requirement*
D1.1	[redacted]	
D1.2	[redacted]	
D1.3	[redacted]	
D1.4	[redacted]	
D1.5	[redacted]	
D1.6	[redacted]	
D1.7	[redacted]	
D1.8	[redacted]	
D1.9	[redacted]	
D2	**Preparation of the transfer cask.**	
D2.1	[redacted]	
D2.2	[redacted]	
D2.3	[redacted]	
D2.4	[redacted]	
D2.5	[redacted]	
D2.6	[redacted]	
D2.7	[redacted]	

1 Removal of the sealing compound and removal of the hexagon screws not required
2 Removal of the sealing compound not required
3 A leak-tightness test is not required if the result of visual inspection of the preservation of the wear protection in step A7.5 and of closure plate in step A7.7 demonstrates condition according to specification.
4 In case the transfer cask lid is mounted

7.1.2 Loading of Contents

This chapter describes the loading process of the canister after its transfer inside the transfer cask to the underwater FA loading position on ground the spent fuel pool. Cask and canister loaded and closed in accordance with detailed written and approved procedures, including procedures for the preservation of screws with lubricant where necessary and tightening methods for the installation of all lids. Each screw is installed with either a nominal tightening torque or a nominal preload.

Both, canister as well as cask cavities are vacuum dried by adjusting and maintaining a vacuum pressure of [redacted]. After a sufficient drying period the interior is disconnected from the vacuum pump. [redacted] After successful completion of drying, the cavities is filled with inert gas.

In accordance with the thermal evaluation in Chapter 3 some constraints apply to the loading operations to ensure compliance with temperature limits of both, cask components and fuel rod cladding and to prevent the water inside the canister from boiling:

[redacted]

Table 7.1-2 Operations for loading of contents

Step	*Description*	*Requirement*
E	**Loading of the canister in the FA storage pool.**	
E1	**Loading of fuel assemblies.**	
E1.1	Only the inventory defined in the valid CoC is permitted to be loaded. An approved corresponding loading plan in compliance with the CoC is required before loading to prove conformity between loading plan and transport licence.	CoC, Loading plan

Step	*Description*	*Requirement*
E1.2	Placing of fuel assemblies into the specified loading positions in compliance with the specified loading plan. Before and after the loading of each individual fuel assembly, comparison of the fuel assembly number and the planned/implemented loading position. To be recorded in the loading plan.	Loading plan
E1.3	Final loading inspection of the canister by comparing the loading plan with the actual loading configuration, following the "four-eye principle". To be recorded in the loading plan.	Loading plan
E2	**Removal of transfer cask with canister from the FA storage pool.**	
E2.1	Visual inspection of a new metal gasket and the sealing ring in the sealing groove of the canister lid. Assembly of the metal gasket. Recording of the metal gasket identification in the cask logbook.	Cask logbook
E2.2	Underwater removing of sealing surface protection from the lid fit in the canister body.	
E2.3	Underwater positioning of canister lid. Visual check for proper installation.	
E2.4	[redacted]	[redacted]
E2.5	[redacted]	
E2.6	[redacted]	
E2.7	[redacted]	
E2.8	[redacted]	[redacted]
E2.9	[redacted]	[redacted]
E2.10	[redacted]	
E2.11	Lifting of the transfer cask (incl. canister) above the water surface of the FA storage pool. Decontamination of the outer surface of the transfer cask with deionized water.	
E2.12	Placement of transfer cask in the platform in the reactor hall and closure of the platform. Removal of the traverse from the transfer cask trunnions.	
E2.13	Dewatering and drying of annulus between canister and transfer cask cavity.	
F	**Preparation of canister and transfer cask before loading of canister into CASTOR® geo69 cask.**	
F1	**Installation of the additional temporary neutron and gamma shielding.**	
F2	**Work and tests on the canister lid.**	
F2.1	[redacted]	
F2.2	[redacted]	
F2.3	Check for proper installation of the canister lid	
F2.4	Disassembly of the lifting pintle from the canister lid.	
F2.5	Installation of the shielding plate (part of multi-equipment) on the canister lid.	

Step	*Description*	*Requirement*
F2.6	Vacuum drying (at vacuum pressure p_v) of canister cavity and verification of the [redacted]	[redacted]
F2.7	Setting of the blind plug and mounting of the quick connect incl. bonded seal.	
F2.8	Evacuation and helium filling of the canister via quick connect.	[redacted]
F2.9	[redacted]	[redacted]
F2.10	Visual inspection of a new Metal gasket.	
F2.11	Installation of new metal gasket, tightening plug and pressure nut and tightening with nominal torque. Recording of the metal gasket identification in the cask logbook.	
F2.12	Leakage test of the metal gaskets of the canister lid system.	ANSI N14.5 [3]
F3	**Disassembly of the temporary additional shielding.**	
F4	**Installation of the lifting pintle on the canister lid.**	
G	**Loading of the CASTOR® geo69 cask.**	
G1	**Transfer of the canister into CASTOR® geo69 cask.**	
G1.1	Load attachment on the trunnions of the transfer cask and vertical crane transfer from the platform in the reactor hall to the handling position in the truck lock.	
G1.2	Positioning of the transfer cask on the transfer lock on top of the CASTOR® geo69 cask. Two centre bolts provide adjustment. The trunnions of the transfer cask remain attached to the traverse during the entire transhipment.	
G1.3	Load attachment to the lifting pintle on the canister lid and slight lifting of the canister.	
G1.4	Opening of the bottom lid of the transfer cask via the transfer lock.	
G1.5	Lowering of the canister into the CASTOR® geo69.	
G1.6	Closure of the bottom lid of the transfer cask via the transfer lock.	
G1.7	Transfer of the transfer cask to the platform in the reactor hall.	
G1.8	Disassembly of the transfer lock. Installation of the temporary additional shielding and disassembly of the lifting pintle from the canister lid.	
G2	**Assembly of the retention ring.**	
G2.1	[redacted]	
G3	**Closure of the transport cask.**	
G3.1	Removal of the sealing surface protection from the cask lid fit and installation of the guide bolts.	
G3.2	Visual inspection of a new metal gasket.	
G3.3	Installation of blind flange with the new metal gasket and cap screws in the cask lid. Tightening of the cap screws with nominal torque. Recording of the metal gasket identification in the cask logbook.	
G3.4	Check for proper installation of the blind flange.	
G3.5	Visual inspection and installation of a new metal gasket with clips in the cask lid. Recording of the metal gasket identification in the cask logbook.	

Step	*Description*	*Requirement*
G3.6	Lifting of the cask lid via the installed lifting pintle. Visual Inspection of the proper installation and condition of the moderator plate, as far as accessible. Placement of the cask lid on the cask.	
G3.7	Installation of the hexagonal screws and removal of the guide bolts. Installation of the three hexagon head screws for sealing. Tightening with nominal torque.	
G3.8	Check for proper installation of the cask lid.	
G3.9	Vacuum drying (at vacuum pressure p_v) of cask cavity and verification of the [redacted]	[redacted]
G3.10	Filling cask interior with helium using the quick connect. Adjustment of the helium pressure in the cask.	[redacted]
G3.11	Visual inspection of a new metal gasket.	
G3.12	Installation of protection cap with metal gasket and cap screws in the cask lid. Tightening of the cap screws with nominal torque. Recording of the metal gasket identification in the cask logbook.	
G3.13	Check for proper installation of the protection cap.	
G3.14	Leakage test of the metal gaskets of the cask lid system.	ANSI N14.5
G3.15	Disassembly of the temporary additional shielding.	

7.1.3 Preparation for Transport

Table 7.1-3 Operations for preparation for transport

Step	*Description*	*Requirement*
H	**Work and measurements on the CASTOR® geo69 transport cask**	
H1	**Contamination measurement on the cask.**	49 CFR 173.443
H2	**Dose rate measurement on the cask.**	10 CFR 71.47
H3	**Visual inspection of the cask.**	
H3.1	Visual inspection of the surface coating; as far as accessible.	
H3.2	Visual inspection of the trunnions in installed condition, as far as accessible.	
H3.3	Visual inspection of tilting studs and wear protection in installed condition, as far as accessible.	
H4	**Placement of transport cask on the trailer.**	
H4.1	Opening of the platform. Transfer of the cask via lock wagon out of the truck lock.	
H4.2	Load attachment on the trunnions of the cask. Lifting of the cask and placement on the turning support of the transport frame on the trailer.	
H4.3	Lowering of the cask into the horizontal orientation.	
H4.4	Visual inspection of closure plate, hexagon head screws and seal plug in installed condition, where accessible.	
J	**Preparation of package for transport.**	
J1	**Replacing the sealing screws and O-rings in the closure plate with the sealing screws with valve.**	

Step	*Description*	*Requirement*
J1.1	Visual check of the two sealing screws with valve for integrity.	
J1.2	Removal of the two sealing screws and O-rings in the closure plate; installation of sealing screws with valve and tightening with nominal torque.	
J2	**Preservation of cask according to requirements for "transport configuration".**	
J3	**Installation of lid and bottom impact limiter.**	
J3.1	Visual check of the surface coating of the impact limiters. Check of other surfaces and seals for visible damages i.e. dents or scratches.	
J3.2	[redacted]	
J3.3	Positioning of the impact limiters on the cask; visual check for proper seating, mounting of cap screws and washers and tightening with nominal torque.	
J4 [1]	**Dose rate measurement on package.**	10 CFR 71.47
J5	**Temperature measurement on package.**	10 CFR 71.43(g)
J6	**Preservation of impact limiters according to requirements for "transport configuration".**	
J7 [1]	**Dose rate measurement on the transport unit.**	10 CFR 71.47
J8	**Temperature measurement on the transport unit.**	10 CFR 71.43(g)
J9	**Labelling of the transport unit taking into account the measured dose rate (transport index TI) and the criticality safety index (CSI) in compliance with the certificate of approval.**	10 CFR 71.5(ii)
J10	**Complete the transport documentation and give clearance for departure.**	

[1] The dose rate measurements can be omitted, provided that the results of the dose rate measurement in step H2 was already in compliance with the requirements for transport on public routes.

List of References

[1] Title 10 CFR Part 72
Licensing Requirements for the Independent Storage of Spent Nuclear Fuel, High-Level Radioactive Waste, and Reactor-Related greater than Class C Waste
U.S. Nuclear Regulatory Commission

[2] Title 49 CFR Part 173
Shippers – General Requirements for Shipments and Packagings
U.S. Nuclear Regulatory Commission

[3] ANSI N14.5-2014
American National Standard for Radioactive Materials –
Leakage Tests on Packages for Shipment

7.2 Package Unloading

	Name, Function	Date	Signature
Prepared	[redacted]		
Reviewed			

The package is opened and unloaded in accordance with detailed written and approved procedures. Table 7.2-1 summarizes the operations during receipt of package from carrier. Table 7.2-2 and Table 7.2-3 summarize the operations during removal of contents.

7.2.1 Receipt of Package from Carrier

The operations performed after receiving the package from carrier are in accordance with the requirements listed in 10 CFR 20.1906 [1], "Procedures for Receiving and Opening Packages".

Table 7.2-1 Operations during receipt of package from carrier

Step	*Description*	*Requirement*
K	**Surveys and inspections after receipt of the package.**	
K1	**Transfer of the package including transport papers.**	
K2	**Visual check of the package for proper condition, deformation, wear and corrosion. Check of type plates, labels tamper-indicating devices on the package.**	
K3 [1]	[redacted]	
K4 [1]	**Contamination measurement on the package.**	49 CFR 173.443
K5	**Dose rate measurement on the package.**	10 CFR 71.47
K6	**Visual inspection of the cask.**	
K6.1	Visual inspection of the outer surface coating of the cask.	
K6.2	Visual inspection of cask lid, blind flange and protection in installed condition, as far as accessible.	
K6.3	Visual inspection of the trunnions and the tilting studs in installed condition, as far as accessible.	
K6.4	Visual inspection of tilting studs and wear protection in installed condition, as far as accessible.	
K6.5	Visual inspection of the preservation on wear protection and of the hexagon screws.	
K6.6	Visual inspection of closure plate, hexagon head screws, sealing screws with valve and seal plug in installed condition, as far as accessible.	
K6.7	Visual inspection of the preservation of the closure plate, hexagon head screws and seal plug.	
K6.8	Leak-tightness test of the closure plate and the sealing screws.	
K7	**Preparation of the cask for interim storage.**	
K7.1	Tilting of the package by application of the tilting studs and the corresponding turning support.	
K7.2	Load attachment on the trunnions and vertical crane transfer of the cask to the desired storage.	
K7.3	Set up of CASTOR® geo69 storage configuration.	

Step	*Description*	*Requirement*
K8	**Interim storage of the cask in vertical orientation.**	10 CFR 72 [2]

[1] Contamination and dose rate measurement shall be performed as soon as practical after receipt of the package, but not later than 3 hours after the package is received at the licensee's facility. If the package is received outside normal working hours, the monitoring shall be performed not later than 3 hours from the beginning of the next working day.

7.2.2 Removal of Contents

The removal of contents from the canister in the FA storage pool may be performed via CLU System or directly from the CASTOR® geo69 DPC, depending on the crane capacity in the nuclear facility. Both cases are described in this subsection. Mandatory for the complete duration of unloading of a cask is that the validity of the Certificate of Compliance (CoC) is not exceeded.

The unloading in a FA storage pool requires the prior re-cooling of the canister and the loaded contents according to written and approved procedures to protect the loaded FAs from damage due to thermal shock. The owner is responsible for this procedure, which is not described in detail in this subsection.

7.2.2.1 Direct Removal of Contents

The initial condition is that the impact limiters, if present, are already dismantled, the loaded packaging has been accepted and is located in the service platform in the nuclear facility.

Table 7.2-2 Required steps for the unloading of contents directly from the DPC

Step	*Description*	*Requirement*
L	**Opening of the package.**	
L1	**Removal of the cask lid.**	
L1.1	Visual inspection of the threaded holes for the load attachment on top of the cask lid.	
L1.2	Remove hexagonal screws and hexagon head screws for sealing: - Removal of the three hexagon screws at marked positions (see numbering on the cask lid), - Visual inspection of the threaded holes in the cask body, as far as accessible, - Visual inspection of thread on the three guide bolts, - Installation of the three guide bolts in the corresponding threaded holes in the cask body, - Installation of the lid hanger on the cask lid, - Removal of the remaining hexagon screws.	
L1.3	Removal of the cask lid. The lifting pintle remains installed on the cask lid. Removal of the guide bolts.	

Step	*Description*	*Requirement*
L1.4	Visual inspection after removing the cask lid: - Cask lid as a whole, - Sealing groove for metal seal in the cask lid, - Sealing surface for metal seal on the cask body, - Hexagonal screws and hexagon head screws for sealing, - Threaded holes for hexagonal screws in cask body.	
L1.5	Visual inspection of sealing surface protection of cask lid fit for impurities and damage and install in lid fit.	
L2	**Removal of blind flange from cask lid.**	
L2.1	Removal of the cap screws.	
L2.2	Removal of blind flange via the LAP located in the centre.	
L2.3	Visual inspection after removing the blind flange: - Blind flange as a whole, - Sealing groove for metal gasket in the blind flange after removal of the metal gasket, - Sealing surface for metal gasket on the cask lid - Cap screws, - Threaded holes for cap screws in the cask lid.	
L3	**Removal of protection cap from cask lid.**	
L3.1	Removal of the cap screws.	
L3.2	Removal of protection cap via the two LAPs.	
L3.3	Visual inspection after removing the protection cap: - Protection cap as a whole, - Sealing groove for metal gasket in the protection cap, - Sealing surface for metal gasket on the cask lid, - Cap screws, - Threaded holes for cap screws in the cask lid.	
L4	**Disassembly of the retention ring.**	
L4.1	[redacted]	
L4.2	[redacted]	
M	**Unloading of the canister.**	
M1	**Preparation of the canister for re-cooling.**	
M1.1	Installation of the lifting pintle on the canister lid.	
M1.2	Removal of tightening plug and pressure nut from the canister lid.	
M1.3	Evacuation of canister cavity via quick connect.	
M1.4	Flushing of the canister cavity with helium at ambient pressure via quick connect for cooling the FAs.	
M1.5	[redacted]	
M1.6	[redacted]	
M2	**Preparations before unloading.**	

Step	*Description*	*Requirement*
M2.1	Load attachment on the trunnions of the cask. Transfer of the cask to the FA storage pool.	
M2.2	Partial lowering of the cask into the FA storage pool.	
M2.3	Filling of the canister cavity with pool water.	
M2.4	Removal of the dewatering lance.	
M2.6	Lowering of cask and canister into the FA storage pool.	
M2.5	Underwater removal of canister lid via the installed lifting pintle.	
M3	**Underwater unloading of the fuel assemblies.**	

7.2.2.2 Removal of Contents via CLU

Table 7.2-3 describes the steps to be performed at a minimum for an unloading of a cask via the CLU System. The initial condition is that the loaded packaging has been accepted, the loaded cask has been opened, the canister has been transhipped from the loaded DPC into the transfer cask (according to steps A – C in Table 7.1-1) and the loaded transfer cask is located in the service platform in the nuclear facility. The inner and outer water chambers of the transfer cask must be flooded with deionized water prior to canister transhipment.

Table 7.2-3 Required steps for the unloading of contents via CLU

Step	*Description*	*Requirement*
L	**Preparation of canister and transfer cask for unloading.**	
L1	**Preparation of the transfer cask.**	
L1.1	Inflate the annulus inflatable seal between bottom lid and bottom ring of the transfer cask.	
L1.2	Connection of the annulus between canister and transfer cask cavity wall to the deionized water service and flooding. The connection remains during the entire underwater loading of FAs.	
L2	**Preparation of the canister for re-cooling.**	
L2.1	Removal of tightening plug and pressure nut from the canister lid.	
L2.2	Evacuation of canister cavity via quick connect.	
L2.3	Flushing of the canister cavity with helium at ambient pressure via quick connect for cooling the FAs.	
L2.4	[redacted]	
L2.5	[redacted]	
M	**Unloading of the canister.**	
M1	**Preparations before unloading.**	

Step	*Description*	*Requirement*
M1.1	Load attachment on the trunnions of the transfer cask. Transfer of the loaded transfer cask to the FA storage pool.	
M1.2	Partial lowering of the transfer cask into the FA storage pool.	
M1.3	Start continuous flushing of annulus between canister and transfer cask cavity.	
M1.4	Filling of the canister cavity with pool water.	
M1.5	Removal of the dewatering lance.	
M1.6	Lowering of transfer cask and canister into the FA storage pool.	
M1.7	Disassembly of the crane traverse.	
M1.8	Removal of canister lid under water via the installed lid hanger.	
M2	**Unloading of the fuel assemblies under water.**	

List of References

[1] Title 10 CFR Part 20
Standards for Protection Against Radiation
U.S. Nuclear Regulatory Commission

[2] Title 10 CFR Part 72
Licensing Requirements for the Independent Storage of Spent Nuclear Fuel, High-Level Radioactive Waste, and Reactor-Related greater than Class C Waste
U.S. Nuclear Regulatory Commission

8.1 Acceptance Tests

	Name, Function	Date	Signature
Prepared	[redacted]		
Reviewed			

This section describes the acceptance tests performed before the first use of each CASTOR® geo69 transport packag. The described tests confirm that each packaging is fabricated in accordance with the drawings and specifications of chapter 1 of this SAR.

8.1.1 Visual Inspections and Measurements

The visual inspections of the packaging include a check of the manufacturing documentation for completeness and factual correctness, according the part lists and the corresponding drawings as listed in Section 1.3.

The visual inspections should verify that the package has been fabricated and assembled in accordance with these documents. The dimensions of all parts given in the manufacturing documentation shall be conform to the dimensions and tolerances specified in the drawings. Any occurring noncompliance with the part lists and drawings leads either to the further treatment of the part to correct its dimensions, or to the manufacturing of a new exemplar of that particular part. A verification that each part consists only of the materials specified in the part lists must be included in the manufacturing documentation. Furthermore, all components shall be visually tested for integrity and cleanliness. The package must be visibly marked in accordance with 10 CFR 71.85(c).

8.1.2 Weld Examinations

The examination of welds shall verify that the fabrication of the packaging and its components confirms with the drawings listed in Section 1.3. All weld examinations shall be performed according to written procedures. Weld examination of containment welds shall be performed in accordance with Division 3. The results shall be documented and become part of the quality documentation of the packaging. Weld metal defects detected by the methods specified in Subsection 8.1.2.1 shall be eliminated and repaired in accordance with Division 3, WB-4450. Personnel performing nondestructive examinations shall be qualified in accordance with Division 3, WB-5520.

Weld seams exist on the canister body and the [redacted] housing of the impact limiters. The nondestructive examination procedures applicable depend on the category of the weld seams. For the canister body, the welded joint categories according to Division 3, WB-3251 determine the required examination method and acceptance criteria. [redacted] Table 8.1-1 gives an overview on the required examinations of welds on the different parts of the packaging.

Table 8.1-1: Required examination of welds

Weld seam location	*Welded joint category*	*Code / standard*	*Required examination method*
Canister body	A, B, C	Div. 3, WB-3251	RT + PT
Impact limiters	[redacted]		VT + PT

8.1.2.1 Canister Body

When performing the NDE of welds in the canister body, the external and accessible internal weld surfaces and adjacent base material for at least [redacted] on each side of the weld shall be included in the examination.

8.1.2.1.1 Liquid Penetration Examination

PT shall be performed in accordance with Section V, Article 6 [6]. The acceptance criteria for penetration testing (PT) are specified in Division 3, WB-5352. The canister body shall be thoroughly cleaned in accordance with written and approved procedures after the examination procedure.

8.1.2.1.2 Radiographic testing

RT shall be performed in accordance with Section V, Article 2 [6], except that fluorescent screens are not permitted for film radiography, the geometric unsharpness shall not exceed the limits of Section V, Article 2, T-274.2, and the image quality indicators of Division 3, Table WB-5111-1 shall be used in lieu of those shown in Section V, Article 2, Table T-276. The acceptance criteria for RT are specified in Division 3, WB-5320. The digitization of radiographic film and radioscopic images shall meet the requirements of Section V, Article 2, Mandatory Appendix III.

8.1.2.2 Impact Limiter Housing

For the non-destructive examination of the weld seams in the impact limiter housing, the acceptance criteria of [redacted] Each weld shall be tested via VT and PT. VT shall be performed according to ISO 17637 [3] or another applicable standard. PT shall be performed according to ISO 3452-1 [4] or another applicable standard. Defects detected by the examinations shall be eliminated and repaired when necessary or the indication shall be reduced to an acceptable limit.

8.1.3 Structural and Pressure Tests

All test shall be performed according to written procedures and shall comply with the applicable cods and standards mentioned in the following respective subsections. The results shall be documented and become part of the quality documentation of the packaging.

8.1.3.1 Hydrostatic Tests

For the hydrostatic tests, the requirements of Division 3, WB-6200 are applicable. Hydrostatic tests shall be performed with a maximum internal overpressure of at least 1.5 times the design pressure, which is [redacted] in the cask (absolute pressure, helium atmosphere). The cask shall be tested with an internal test pressure of [redacted]. The external pressure of the canister is equal to the internal pressure of the cask. Since this pressure exceeds the internal design pressure in the canister, which is [redacted] (absolute pressure, helium atmosphere), the canister shall be pressure tested with a test pressure equal to 1.5 times the external design pressure, which equals [redacted]. The test pressure shall be maintained for at least ten minutes. The canister test pressure shall not be exceeded by more than 6 % during the test.

A deep water immersion test shall be considered for the cask according to IAEA Safety Standards [5]. A pressure test with an external gauge pressure of at least 2 MPa and a test period of not less than 1 h shall be considered to meet these conditions.

The test pressures for cask and canister are listed in Table 8.1-2.

Table 8.1-2: Test pressure for cask and canister for different load conditions

Containment	*Load condition*	*Absolute test pressure [MPa]*		*Test period [min]*
		Internal	*External*	
Cask	Hydrostatic test	[redacted]		10
	Deep Water Immersion Test	[redacted]		60
Canister	Hydrostatic test	[redacted]		10

After the test period time of the pneumatic tests is exceeded, the initiation of the examination for leakage starts. For the examination of leakage, the internal pressure is reduced to 0.75 times the test pressure. All joints, connections and regions of high stress are tested for leaks. Leak testing is performed in accordance with Section V, Article 10 [6] and ANSI N14.5 [7]. The maximum standard permissible leakage rate according to Section 8.1.4 shall not be exceeded. Otherwise, the containment material may be repaired in accordance with Division 3, WB-2500 or disposed of.

8.1.3.2 Structural Tests

Structural tests are performed on all lifting devices in terms of a static load test. The applied load depends on the maximum weight that will be attached to the LAP during operation of the package, multiplied with a certain load factor. The cask trunnions (Item 12) and the load attachment points on the canister lid (Item 3) are special lifting devices and thus tested with a load factor of three in order to fulfil the provisions of ANSI N14.6 [8]. All other lifting devices are tested with a load factor of 1.5. Furthermore, a hoist factor of 1.15 according to CMAA #70 applies to all lifting devices for slow crane operation. The loads for the static load tests are listed in Table 8.1-3.

Table 8.1-3: Static load tests

Lifting device (quantity)	*Load factor*	*Max. weight attached [Mg]*	*Load [kN]*
Cask trunnions (2)	3 x 1.15	[redacted]	
LAP on canister lid (12)	3 x 1.15	[redacted]	
Tilting studs (2)	1.5 x 1.15	[redacted]	
LAP on cask lid (6)	1.5 x 1.15	[redacted]	

The load tests shall be performed under the conditions specified in the following subsections. All load tests are performed at room temperature. The test load shall be applied for at least ten minutes. Bearing shells made of bronze must be placed between lifting lug and the trunnions or tilting studs as indicated in Figure 8.1-1.

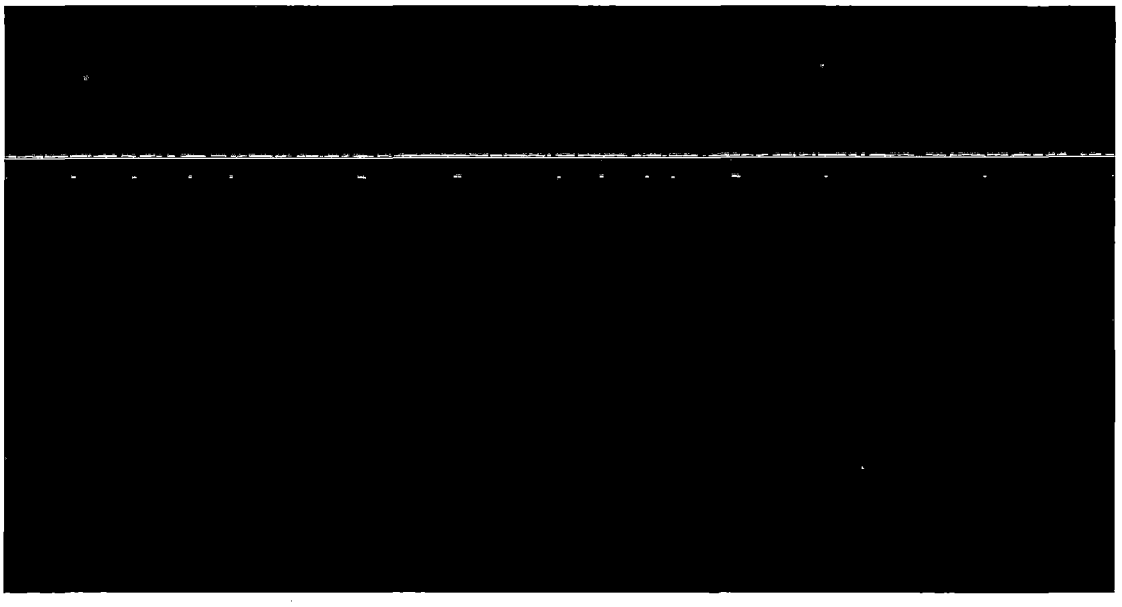

Figure 8.1-1 Geometry of load application on the trunnions / tilting studs of the package

8.1.3.2.1 Trunnions

The static test load must be distributed equally on the two trunnions. The direction of load application must be perpendicular to the axis of the trunnions. The following requirements must be met:

- Load-bearing width W ≥ 45 mm
- Mean lever arm L ≤ 67,5 mm
- Bearing shell radii R1 and R2 ≥ 3 mm
- Width of the lifting lug ≥ R1 + R2 + W
- Arc of contact between the bearing shell and the trunnion ≥ 60°

After the load test, a visual inspection and MT or PT must be performed on the installed trunnions, as far as accessible, to verify no distortion or cracking has occurred. MT or PT shall be performed in accordance with Section V, Article 7 or Article 6 [6], respectively, using the acceptance criteria specified in Division 3, WB-5342 or WB-5352. The trunnion deformation between the initial value prior to loading (null measurement) and after loading with the test load shall be determined via dial gauge (measuring accuracy ± 0.01 mm). A permanent trunnion deformation exceeding the measuring inaccuracy of the dial gauge is unacceptable. Otherwise, the deformed trunnions shall be replaced by new exemplars and the load test shall be repeated.

The cap screws that are exposed to the highest loading during the static lead test shall be removed and visually inspected after the test. Gauge testing of these screws and the corresponding threaded holes in the storage cask body shall be performed according to DIN ISO 1502 [9]. Defective cap screws shall be replaced with new exemplars. The tightening torque of all cap screws shall be checked after the load test.

8.1.3.2.2 Tilting Studs

The load test on the tilting studs has to be performed prior to the installation of the wear protection . The static test load must be distributed equally on the two tilting studs and must be applied perpendicular to the axis of the tilting studs. The following requirements apply:

- Load-bearing width W ≥ 30 mm
- Mean lever arm L ≥ 50 mm
- Bearing shell radii R1 and R2 ≥ 3 mm
- Arc of contact between the bearing shell and the tilting stud ≥ 45°

A visual inspection of the of the tilting studs as well as MT or PT of the whole shell surface of the tilting studs and in the area of the transition radius are performed after the test load is applied, to

verify no distortion or cracking has occurred. The deformation of the tilting studs due to the load shall be determined via dial gauge (measuring accuracy ± 0.01 mm). A permanent deformation of the tilting studs exceeding the measuring inaccuracy of the dial gauge is unacceptable. In case of a non-permitted deformation, the cask body shall be replaced by a new exemplar.

8.1.3.2.3 Cask Lid

The static load must be distributed equally on the [redacted] threaded holes by using the lifting pintle for the cask lid. The load must be applied perpendicular to the cask lid surface. The test screws must be screwed into the lid by hand until the minimum required screw-in depth is reached. A visual inspection and a gauge test according to DIN ISO 1502 [9] of the LAP must be performed before and after the load test. No adverse effects on the trueness to gauge of the threaded holes are permissible. The cask lid must be replaced by a new exemplar if the threaded holes do not pass the static load test.

8.1.3.2.4 Canister Lid

The static load must be distributed equally on the [redacted] threaded holes by using the lifting pintle for the canister lid. The load must be applied perpendicular to the canister lid surface. The test screws must be screwed into the lid by hand until the mini-mum required screw-in depth is reached. A visual inspection and a gauge test according to DIN ISO 1502 [9] of the LAP must be performed before and after the load test. No ad-verse effects on the trueness to gauge of the threaded holes are permissible. The canister lid must be replaced by a new exemplar if the threaded holes do not pass the static load test.

8.1.4 Leakage Tests

Leak tests apply for all metal gasket of the containment systems. They shall be performed according to Section V, Article 10 and ANSI N14.5 [7] and in accordance with written and approved procedures at any time after the containment boundary fabrication is complete (during assembly, dispatch after loading, etc.). The results shall be documented and become part of the quality documentation of the packaging.

The leak detector shall have a sensitivity of at least 10^{-10} Pa m³/s. The maximum standard permissible leakage rate is 10^{-8} Pa m³/s. A calibration of the leak detector is performed using a test leak before connecting the measuring setup to the test volume. Table 8.1-4 lists all metal gasket on which leakage test are to be performed.

Table 8.1-4: Seals with metal gaskets

Containment	*Sealing surface*	*Metal Gasket*	*Component*
Cask 1014-DPL-30934	Cask body (Item 2)	Item 69	Cask lid (Item 55)
	Cask lid (Item 55)	Item 44	Protection cap (Item 113)
	Cask lid (Item 55)	Item 71	Blind flange (Item 89)
Canister 1014-DPL-36855	Canister body (Item 2)	Item 16	Canister lid (Item 3)
	Canister lid (Item 3)	Item 13	Tightening plug (Item 10)

Leak testing is also performed on the elastomeric seals listed in Table 8.1-5. A less sensitive leak testing method can be used since these seals are not part of the containment.

Table 8.1-5: Elastomeric seals

Containment	*Seal*	*Component*	*Leak testing method*
Cask 1014-DPL-30934	Sealing ring (Item 47)	Closure plate (Item 7)	Gas pressure rise
	Bonded Seal (Item 49) O-ring (Item 184)	Wear protection (Item 183)	Bubble test

The leak tightness is considered proven when the calculated standard leakage rate is lower than the permissible one. In case of an unacceptable leakage rate the corresponding sealing barrier is depressurised and opened. The metal gasket or elastomeric seal is to be replaced, the sealing surface is checked for cleanliness and damage and necessary repairs are performed. After the new gasket/seal and the sealing surface are preserved the sealing is closed and a new leak test has to be performed.

8.1.5 Component and Material Tests

All test shall be performed according to written procedures and shall comply with the applicable cods and standards mentioned in the following respective subsections. The results shall be documented and become part of the quality documentation of the packaging.

8.1.5.1 Material Tests

The materials used for the containment must conform to the requirements of one of the specifications for material given in Section II [10], Part D, Table 2A, 2B, and 4. This requirement does not apply to seals and gaskets according to section Division 3, WB-2121(b). Table 8.1-6 gives an overview of the specified ferrous and nonferrous materials and the corresponding parts used in the

package. Table 8.1-6 also includes components that do not fulfil a containment function. The required tests originate from the material standard, which is included in Section II, Part A and B. Division 3 includes additional requirements for containment material. If not specified otherwise in Table 8.1-6, the required non-destructive examination shall be performed according to the applicable article in Section V[6].

Table 8.1-6: Specified materials

Spec. No.	*Type/Grade*	*UNS No.*	*Item No.*	*Parts list 1014-DPL-*	*Required material tests[1]*
[redacted]	[redacted]	[redacted]	21, 55	30934	Tensile Test, PT, UT
	[redacted]		2-5	36855	
[redacted]			13, 37 26	30934 36855	Tensile Test, Charpy Impact Test (only Item 13), VT[3], MT[4] or PT (only Item 13)
[redacted]			11	36855	Brinell Hardness, Rockwell C, Charpy Impact Test, VT[3], MT[4] or PT
[redacted]		[redacted]	7	30934	Tensile Test, Brinell Hardness or Rockwell B, UT[5]
	[redacted]		89, 113, 183	30934	
	[redacted]		30, 31	30984	
	[redacted]		2-2, 2-3, 2-4	36855	
	[redacted]		7	36855	
[redacted]	[redacted]		5, 9, 10 2	36855 30984	Tensile Test, Average Grain Size, UT, PT
		[redacted]	12	30934	Tensile Test, Brinell Hardness, Impact Toughness[2], UT, MT or PT
	[redacted]		4	36855	Tensile Test, Brinell Hardness (if annealed), Average Grain Size, UT, PT
[redacted]	B[redacted]		9, 62, 63 6	30934 36855	Tensile Test, Brinell Hardness, Charpy Impact Test (Item 62, 63), VT[3], MT[4] or PT (except Item 9)
[redacted]	[redacted]		8, 53	30934	Tensile Test, Bend Test
[redacted]			2	30934	Tensile Test, Microstructure, Rapid-load fracture toughness, UT, MT or PT
[redacted]	[redacted]		3	36855	Tensile Test, UT, PT
[redacted]		[redacted]	50 2, 3	30984 33604	Tensile Test, UT

[1]Analysis of chemical composition is mandatory for all specified materials

[2]Testing of impact toughness according to Subsection Division 3, WB-2300

[3]Visual examination in accordance with the requirements of ASTM F788 [11]

[4]Magnetic particle examination in accordance with the requirements of ASTM A275 [12]

[5]Straight beam or angle beam UT according to Subsection Division 3, WB-2531

The impact toughness testing, if not specified differently in Table 8.1-6, is conducted according to Subsection WB-2331.1 [1] to determine the reference temperature RT_{NDT} at which the ductile-to-brittle transition of the material occurs. This temperature is compared to the lowest service temperature (LST) of the material. Charpy impact tests are performed with three V-notched samples for each temperature. Fracture toughness tests consist of two test specimens, except for the ductile iron cask body, where a minimum of four samples is required. Ductile cast iron SA-874M is fracture toughness tested according to ASTM E1820 [13] at a temperature of −40 °C. Table 8.1-7 summarises the acceptance criteria for the required toughness tests. The trunnion material requires a minimum difference between the LST and the reference temperature. The screw material only requires a minimum lateral expansion of the Charpy impact tests. The ductile cast iron requires that the average fracture toughness of all samples minus three times the standard deviation is equal or bigger as 50 MPa $mm^{1/2}$.

Table 8.1-7: Acceptance criteria for toughness testing

Item No.	*Parts list*	*LST*	*Toughness acceptance criteria*
2	1014-DPL-30934	-40 °C	$K_{IC,R}$(average) – $3\sigma_{SD} \geq 50$ MPa $mm^{1/2}$
12	1014-DPL-30934	-40°C	LST – RT_{NDT} = 60.5 °C
13	1014-DPL-30934	-40 °C	Lateral expansion = 0.64 mm
62, 63	1014-DPL-30934	-40 °C	Lateral expansion = 0.64 mm
11	1014-DPL-36855	-40 °C	Lateral expansion = 0.64 mm

The package materials not listed in Table 8.1-6 do not conform to the requirements of one of the specifications for material given in Section II, Part D, Table 2A, 2B, and 4 of the ASME BPVC. These materials include gaskets, sealing rings, moderator material and the Al-B_4C-MMC used for the basket. These materials and their requirements are either specified by other standards, or they are tested individually for the use in the CASTOR® packages and their qualification is documented. Table 8.1-8 lists these materials.

Table 8.1-8: Materials not specified in the ASME BPVC

Material	*Type/Grade*	*Item No.*	*Parts list 1014-DPL-*
Al-B_4C-MMC	[redacted]	10 – 27	30984
UHMW-PE	[redacted]	4, 5, 54, 56	30934
Stainless steel	[redacted]	6, 31	30934
Silicone	VMQ	30[1] 14, 15[1], 17, 30[1], 74	30934 36855

Material	*Type/Grade*	*Item No.*	*Parts list 1014-DPL-*
Fluoroelastomer	FKM	47[1], 66[1], 94[1], 184[1]	30934
Metal gasket	Ag, stainless steel, Ni-alloy	44, 69, 71 13, 16	30934 36855
PU-foam	Polyurethane	90-30, 90-31, 90-32, 91-5 95-30, 95-31, 95-32	38772

[1]Non-safety-related items

8.1.5.1.1 Neutron absorber material tests

Information on acceptance tests and acceptance criteria relevant for the Aluminium-Boron Metal Matrix Composite (Al-B_4C-MMC) is provided in a material qualification report included in the Appendix 2-8 of Section 2.12. The acceptance tests ensure the required mechanical properties, thermal properties, and neutron attenuation performance of the material.

8.1.5.1.2 Moderator material tests

Information on the moderator material, [redacted] is provided in a material qualification report included in the Appendix 2-7 of Section 2.12. An elongation stress F 150/10 of [redacted] is required. Preparation of test specimens and determination of properties is performed in accordance with EN ISO 21304-2 [16]. After [redacted], each pressed plate is visually inspected for complete sintering, surface texture and optical inhomogeneity. The material must be free from bubbles, voids, foreign particles, cracks and other defects in accordance with EN ISO 15527 [17]. The density of the moderator material is measured in accordance with EN ISO 1183-1, method A [18] for each pressed plate after tempering. A density ≥ [redacted] is required. The coefficient of thermal expansion α is measured transversely in the direction of the sample diameter and lengthwise in the longitudinal direction of the sample for each pressed plate. For both directions α ≤ [redacted] is required at a test temperature of [redacted]. Dimensional checks are to be applied to the finished components.

8.1.5.1.3 Metal gasket material tests

Information on acceptance tests and acceptance criteria relevant for the components of the metal gaskets is provided in a material qualification report included in the Appendix 2-9 of Section 2.12. The acceptance tests ensure the required chemical composition, tensile properties and hardness of the material. The operational reliability of metal gaskets (required useful resiliency/spring back and leakage rate) is ensured via the tests.

8.1.5.1.4 Welding material tests

Welding consumables Type 316L in accordance with to [redacted] [19] and [redacted] in accordance with EN ISO 14174 [20] are used for the construction of the canister. The welding material is tested according to the applicable specification.

8.1.5.1.5 PU foam material tests

Information on the shock absorbing material used in the impact limiters, polyurethane foams [redacted] is provided in a material qualification report included in the Appendix 2-10 of Section 2.12. Density and compression strength of several samples from the centre of one PU foam plate are measured according to ASTM D-1622 [21] and ASTM D-1621 [22], respectively. The required acceptance criteria are shown in Table 8.1-9. Exclusion of significant damages impairing the proper function is ensured by spot-check inspection of the surface.

Table 8.1-9: Acceptance criteria for density and compression strength of the PU-foam used as shock absorber material in the impact limiters

[redacted]

8.1.5.2 Component Tests

After the acceptance of the materials, the components fabricated from these materials are examined visually to ensure integrity and cleanliness. The dimensions of the components are checked to ensure compliance with the dimensional requirements according to the manufacturing drawings and the parts lists.

8.1.5.2.1 Basket Calibre Test

The basket calibre test is used to simulate the loading of the canister with spent fuel in the nuclear facility. A replica of the intended fuel assembly is successively lowered into each chamber of the assembled basket to check if the fuel elements fit into the basket as requested. The calibre test is successfully completed when the replica fits into each chamber without hitting the chamber walls.

8.1.6 Shielding Tests

The performed dose rate calculations show that the dose rates calculated under conservative assumptions are always considerably below the regulatory dose rate limits for NCT and HAC. The

components and materials serving as radiation shield for neutron and/or gamma radiation are tested as described in Subection 8.1.5.1 to eliminate the possibility of defects, voids or streaming paths in the shielding, which could lead to a deviation from the calculated radiation profile and a local violation of a dose rate limit. Shielding materials are:

- Al-B_4C-MMC plates ([redacted]) in the basket (neutron absorber)
- [redacted] moderator rods and moderator plates (neutron moderator)
- Cask body (neutron and gamma absorber)
- Shielding elements (gamma absorber)
- Canister body and canister lid (gamma absorber)
- Cask lid, closure plate (neutron and gamma absorber)

Each shielding component is visually inspected to ensure homogeneity and the absence of cracks, voids, shrinkage holes and other defects in the material. The weld examination ensures the absence of such defects in the welded joints in the canister body. The chemical composition of the materials and their properties (see Subsection 8.1.5.1) ascertain that they exhibit the desired shielding properties used in the calculations.

8.1.7 Thermal Test

The thermal calculations performed provide reliable results in terms of three-dimensional temperature distribution and temperature time dependency in the package. The results indicate that the maximum temperatures during NCT and HAC (fire phase and cooling phase) are considerably below the limit values of each component. The materials used in the present CASTOR® geo69 design are applied in several other transport and storage casks with a comparable design since many years. Thereby GNS exhibits many years of experience in modelling and simulation of their thermal behavior. The material tests specified in Subsection 8.1.5.1 ensure that each material is manufactured in accordance with the applicable standard, which leads to reproducible thermal properties. The thermal properties of each material and the heat transfer between these materials determine the thermal behavior and heat dissipation in the package. Based on the established experience and the previous verification of the applied simulation models it is ensured by GNS that the simulations describe the actual thermal behavior of the package in use with adequate accuracy. Therefore, no thermal tests are designated for acceptance.

8.1.8 Miscellaneous Tests

No miscellaneous acceptance tests are intended for the CASTOR® geo69 packaging.

List of References

[2] ISO 10042 (2018)
Welding – Arc-welded joints in aluminium and its alloys – Quality levels for imperfections

[3] ISO 17637 (2016)
Non-destructive testing of welds – Visual testing of fusion-welded joints

[4] ISO 3452-1 (2014)
Non-destructive testing – Penetrant testing Part 1: General principles

[5] IAEA Safety Standards, No. SSR-6, Rev. 1
Regulations for the Safe Transport of Radioactive Material (2018 Edition)

[6] ASME Boiler and Pressure Vessel Code (2017)
Section V – Non-destructive Testing

[7] ANSI N14.5 (2014)
Radioactive Materials – Leakage Tests on Packages for Shipment

[8] ANSI N14.6 (1993)
Radioactive Materials – Special Lifting Devices for Shipping Containers Weighing 10000 Pounds (4500 kg) or More

[9] DIN ISO 1502:1996-12
Metrisches ISO-Gewinde allgemeiner Anwendung - Lehren und Lehrung

[10] ASME Boiler and Pressure Vessel Code (2017)
Section II – Materials

[11] ASTM F788 – 20
Standard Specification for Surface Discontinuities of Bolts, Screws, Studs, and Rivets, Inch and Metric Series

[12] ASTM A275 – 18
Standard Practice for Magnetic Particle Examination of Steel Forgings

[13] ASTM E1820 – 20b
Standard Test Method for Measurement of Fracture Toughness

[16] EN ISO 21304-2:2021
Plastics - Ultra-high-molecular-weight polyethylene (PE-UHMW) molding and extrusion materials
Part 2: Preparation of test specimens and determination of properties

[17] EN ISO 15527:2018
Plastics – Compression-molded sheets of polyethylene (PE-UHMW, PE-HD)
Requirements and test methods

[18] EN ISO 1183-1:2019
Plastics – Methods for determining the density of non-cellular plastics
Part 1: Immersion method, liquid pycnometer method and titration method

[19] ASME Boiler and Pressure Vessel Code (2017)
Section II – Materials Part C: Specifications for Welding Rods, Electrodes, and Filler Metals

[20] EN ISO 14174 (2019)
Welding consumables – Fluxes for submerged arc welding and electroslag welding

[21] ASTM D-1622
Standard Test Method For Apparent Density Of Rigid Cellular Plastics, Edition 2020

[22] ASTM D-1621
Standard Test Method For Compressive Properties Of Rigid Cellular Plastics, Edition 2016

8.2 Maintenance Program

	Name, Function	Date	Signature
Prepared	[redacted]		
Reviewed			

An ongoing maintenance program is defined and incorporated in the CASTOR® geo69 System Operations Manual that will be prepared and issued to each user prior to delivery and first use of the CASTOR® geo69 package. This document shall delineate the detailed inspections, testing, and parts replacement necessary to ensure continued radiological safety, proper handling, and containment performance of the CASTOR® geo69 Package in accordance with 10 CFR 71 regulations, conditions in the Certificate of Compliance (CoC), and the design requirements and criteria contained in this SAR.

All test shall be performed according to written and approved procedures and shall comply with the applicable codes and standards. The results shall be documented and become part of the quality documentation of the packaging. The maintenance program includes periodic inspection and testing procedures as well as replacement schedules to ensure the continuous capability of the package during its operation time. Periodic testing is required in the following intervals:

- Loaded package
    - Prior to transport after storage in an interim storage facility
- Empty package
    - After 15 transports or not later than after 3 years
    - After 60 transports or not lager than after 6 years

The testing procedures performed in the nuclear power plant on the loaded package prior to transport are described in the package operations. The testing procedure after 60 transports or 6 years includes additional tests on the cask, canister and basket compared to the testing procedure after 15 transports or 3 years. Each testing procedure includes the visual inspection of all components, coatings, sealing surfaces, threaded holes and screwing elements. In case of deformation, erosion or corrosion the corresponding component has either to be repaired or replaced.

8.2.1 Structural and Pressure Tests

8.2.1.1 Structural Tests

Periodic static load tests on the empty transport cask are performed on the LAP of the cask lid the canister lid and on the trunnions after 60 transports or 6 years at the latest. The load tests of the trunnions on the loaded package are performed prior to transport after interim storage and on the

empty package after 60 transports or 6 years. No periodic load test is performed on the tilting studs of the cask. The criteria to perform to pass the periodic load tests are as specified in Subsection 8.1.3.2. The load tests are accompanied by visual inspections and non-destructive examination according to Table 8.2-1, which is performed prior to and after the load tests.

A maximum number of lifting operations applies to all load attachment points after which the corresponding component is replaced. These numbers are specified acc. to Chapter 2 and the System Operations Manual.

8.2.1.2 Pressure Tests

No periodic pressure tests on the CASTOR® geo69 transport cask or canister following the initial acceptance tests (see Subsection 8.1.3.1) are required to verify continuing performance. Periodic LT is performed to verify continuing integrity and tightness of the containment boundaries.

8.2.2 Leakage Tests

All seals specified in Subsection 8.1.4 are leak tested at intervals of 15 transports or 3 years. Metal gaskets, sealing rings and the corresponding sealing surfaces shall be visually inspected. The metal gaskets and elastomeric sealing rings may be replaced with new exemplars in the course of the leak tests. The application of used metal gaskets and elastomeric seals is permitted as long as the required leak tightness is achieved. The test sensitivities and the equipment specified in Subsection 8.1.4 also apply to the periodic leak tests. Prior to transport leak testing is performed on the cask lid system, including the cast lid, protection cap and blind flange and on the canister lid system, including the canister lid and the tightening plug. The leak tightness of the wear protection is also tested prior to transport.

8.2.3 Component and Material Tests

Replaceable components that are important for handling and closure of the package are periodically tested and replaced, in necessary. Table 8.2-1 gives an overview of all components with a periodic test and replacement schedule. The periodic static load tests are not included in Table 8.2-1. Replaced components are documented in the cask logbook.

Table 8.2-1 Periodic tests and replacement schedules for components

Component	*Test method*	*Prior to transport*	*3 years*	*6 years*	*Replacement*
All metallic and elastomeric sealing rings	Visual inspection, leak testing	-	x	x	Automatic[7]
Trunnion	Visual inspection, MT or PT	x[1]	x[1]	x[2]	In case of cracks or when the maximum number of lifting operations is exceeded
Cap screw	Visual inspection, MT or PT, gauge test	x[3]	x[3]	x[4]	In case of cracks or improper deterioration
Hexagon screw	Visual inspection	x	x	x	In case of cracks or improper deterioration
Cask lid system screws	Visual inspection, MT or PT, gauge test	-	x	x	In case of cracks or improper deterioration
Canister closure system	Visual inspection, PT, gauge test	-	x	x	In case of cracks or improper deterioration
Quick connect and bonded seal	-	-	-	x	Automatic
Basket	Visual inspection, Calibre test	-	x[5]	x[6]	Replacement of individual parts
Shielding elements	Visual inspection	-	-	x	In case of visible cracks that are not repairable
Impact limiters	Visual inspection	-	x	-	In case of cracks or local deformation of the surface

0 Inspection of trunnions in installed condition
1 Inspection of trunnions after dismantlement (test range 100%)
2 Only the most highly stressed cap screws are dismantled and tested
3 All cap screws are dismantled and tested
4 Visual inspection and Calibre test are performed in the canister
5 Visual inspection and Calibre test are performed after removal of the basket from the canister
6 Automatic replacement at the discretion of the user

In cases where the calibre test is not passed successfully, a disassembly of the basket is necessary to find and replace any damaged parts. Sheets and segments are checked for deformation. After replacement of the damaged parts the basket is reassembled and the calibre test is repeated.

The moderator material fasteners are tested for tight fit after 15 transports or 3 years. The moderator material components do not have a fixed replacement schedule because no significant degeneration of the material occurs during package operation and storage as long as the components are properly fixed.

8.2.4 Thermal Tests

The periodic inspection and (in case of deterioration) replacement of components ensures that the thermal behaviour of each component and the heat dissipation in the package remains consistent

with the performed thermal calculations. Therefore, no periodic thermal tests are scheduled in the maintenance program.

8.2.5 Miscellaneous Tests

In addition to the periodic tests and replacement schedules listed in Table 8.2-1, the periodic testing of an empty CASTOR® geo69 after 15 transports or not later than after 3 years and after 60 transports or not later than after 6 years includes the following test steps:

- Visual inspection of the surface coating of the cask body
- Visual inspection of the surface and coating of the cask cavity wall and bottom
- Visual inspection of the surface of the canister cavity wall and bottom (with installed fuel basket, as far as visible)
- Visual inspection of parts of the cask and canister lid systems
- Visual inspection and gauge test of all threaded holes in the cask body for fastening the cask lid and the impact limiters
- Inspection of the nominal preload / tightening torque of all screws
- Visual inspection and thread gauging of the threaded holes for blind flange and protection cap in the cask lid
- Visual inspection and thread gauging of the threaded holes for the pressure nut in the canister lid
- Visual inspection and thread gauging of the LAP in cask lid and canister lid

Periodic testing of the impact limiters includes the following steps:

- Visual inspection of the removed penetration protection
- Visual inspection of casing of the impact limiters and of the surface coating of the coated parts
- Visual inspection and thread gauging of the cap screws and visual inspection of the washers

A complete list of all necessary test steps for the periodic testing of the packaging will be implemented in the CASTOR® geo69 System Operations Manual.

8.3 Appendix

	Name, Function	Date	Signature
Prepared	[redacted]		
Reviewed			

With intent no items.

7.5 Appendix

	Name, Function	Date	Signature
Prepared	[redacted]		
Reviewed			

With intent no items.